

AD A0 65829

DDC FILE COPY



CEEDO-TR-78-43

2  
R

# The Ozone Oxidation of Hydrazine Fuels

LEVEL II

USAMBRDL  
FT DETRICK  
FREDERICK, MARYLAND 21701

RAYMOND A SIERKA, Ph.D., P.E.  
WILLIAM F COWEN, Ph.D.

DDC  
RECEIVED  
MAR 16 1979  
A

SEPTEMBER 1978

FINAL REPORT FOR PERIOD JUNE 1978-SEPTEMBER 1978

Approved for public release; distribution unlimited

**CEEDO**

**CIVIL AND ENVIRONMENTAL  
ENGINEERING DEVELOPMENT OFFICE**

(AIR FORCE SYSTEMS COMMAND)

TYNDALL AIR FORCE BASE

FLORIDA 32403

79 03 16 026

UNCLASSIFIED

SECURITY CLASSIFICATION OF THIS PAGE (When Data Entered)

REPORT DOCUMENTATION PAGE		READ INSTRUCTIONS BEFORE COMPLETING FORM
1. REPORT NUMBER CEEDO-TR-78-43	2. GOVT ACCESSION NO. 9	3. RECIPIENT'S CATALOG NUMBER rept.
4. TITLE (and Subtitle) The Ozone Oxidation of Hydrazine Fuels.		5. TYPE OF REPORT & PERIOD COVERED Final Jun 1973 - Sep 1978
		6. PERFORMING ORG. REPORT NUMBER
7. AUTHOR(s) Dr Raymond A./Sierka Dr William F./Cowen		8. CONTRACT OR GRANT NUMBER(s) DTC-8-139
9. PERFORMING ORGANIZATION NAME AND ADDRESS USAMBRDL Ft Detrick, Frederick MD 21701		10. PROGRAM ELEMENT, PROJECT, TASK AREA & WORK UNIT NUMBERS 63723F 2103/W86 127W
11. CONTROLLING OFFICE NAME AND ADDRESS Det 1 AFESC (CEEDO)/ECW Tyndall AFB FL 32403		12. REPORT DATE September 1978
		13. NUMBER OF PAGES 116
14. MONITORING AGENCY NAME & ADDRESS (if different from Controlling Office) 12 117p.		15. SECURITY CLASS. (of this report) UNCLASSIFIED
		15a. DECLASSIFICATION/DOWNGRADING SCHEDULE
16. DISTRIBUTION STATEMENT (of this Report) Approved for public release, distribution unlimited		
17. DISTRIBUTION STATEMENT (of the abstract entered in Block 20, if different from Report)		
18. SUPPLEMENTARY NOTES Available in DDC		
19. KEY WORDS (Continue on reverse side if necessary and identify by block number) Ozone Hydrazine Monomethyl Hydrazine Unsymmetrical Dimethylhydrazine Ultraviolet Light Wastewater Treatment		
20. ABSTRACT (Continue on reverse side if necessary and identify by block number) This research centered on the treatment of aqueous solutions of hydrazine (H), monomethylhydrazine (MMH), and unsymmetrical dimethylhydrazine (UDMH) by ozone. A parametric study was conducted to evaluate the effect of solution concentration and pH, the two catalysts ultraviolet (UV) light and ultrasonics, reactor inlet ozone gas phase concentration and superficial gas velocity. The objectives of this research were (1) to establish the stoichiometry and kinetics of the ozone oxidation of H, MMH, and UDMH in aqueous solution; (2) to identify the partial oxidation products from the ozone oxidation of — Joseph		

DD FORM 1473 1 JAN 73

EDITION OF 1 NOV 65 IS OBSOLETE

UNCLASSIFIED

SECURITY CLASSIFICATION OF THIS PAGE (When Data Entered)

393 250

LB

UNCLASSIFIED

SECURITY CLASSIFICATION OF THIS PAGE(When Data Entered)

hydrazine fuels; (3) to accomplish toxicity testing of the ozone treated wastewaters with fathead minnows and Daphnia magna. The conclusions derived from this research were (1) increasing solution pH increases the rate of ozone oxidation of H, MMH, and UDMH; (2) increasing specie concentration increases required hydraulic detention times; (3) increasing ozone partial pressure decreases  $t_{1/2}$  values for H, MMH, and UDMH; (4) UV light acts as a catalyst and reduces  $t_{1/2}$  values for H, MMH, and UDMH; (5) the decomposition of MMH during oxygen or air sparging is dramatically enhanced by the presence of UV light; (6) ozonation does reduce the toxicity of the three compounds, but significant toxicity still exists in the reaction mixtures; (7) the ozonation of MMH and UDMH in alkaline solution results in several intermediate products which may present discharge problems as a result of organic loading or toxicity.

SEARCHED	INDEXED
SERIALIZED	FILED
APR 19 1968	
FBI - MEMPHIS	
A	

UNCLASSIFIED

## PREFACE

This report documents work performed during the period June 1978 through August 1978 under Project Order No. DTC-8-139. The work was conducted at the US Army Medical Bioengineering Research and Development Laboratory (USAMBRDL), Ft Detrick, Frederick, Maryland. The principal investigators were Dr Raymond A. Sierka, Professor Civil Engineering and Engineering Mechanics, University of Arizona, and Dr William F. Cowen, Research Chemist at USAMBRDL. The project monitor was Capt Gary McNutt, Civil and Environmental Engineering Development Office (CEEDO), Tyndall Air Force Base, Florida.

The authors wish to acknowledge the technical assistance of Mr John Kaefer, graduate student at the University of Arizona, and Ms Jillian Golden and Ms Iris Jones of USAMBRDL, in carrying out the chemical analyses of the engineering phase of this work.


Also acknowledged are Dr Mark Warner, SP Steven Broich, and SP Sally Diehl of USAMBRDL for the aquatic toxicity work, and 1Lt Joseph Zirrolli of CEEDO for the GC/MS identifications of partial oxidation products.


The assistance of Mr Mitchell Small, USAMBRDL Research Engineer, with the OMNITAB computer program at Ft Detrick, is gratefully acknowledged.

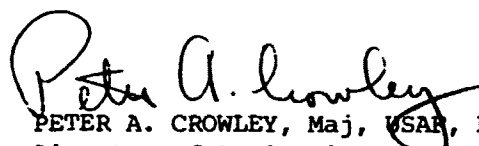
The authors wish to thank Mr William J. Cooper for his work in the initial coordination between the University of Arizona, USAMBRDL, and the US Air Force.

This report has been reviewed by the Information Office (OI) and is releasable to the National Technical Information Service (NTIS). At NTIS it will be available to the general public including foreign nations.

This technical report has been reviewed and is approved for publication.

  
GARY R. MCNUTT, Capt, USAF, BSC  
Project Officer

  
EMIL C. FREIN, Maj, USAF  
Chief, Environmental Engineering  
& Energy Research Division

  
PETER A. CROWLEY, Maj, USAF, BSC  
Director of Environics

  
JOSEPH S. PIZZUTO, Col, USAF, BSC  
Commander

## TABLE OF CONTENTS

PREFACE . . . . .	i
SECTION I . . . . .	1
INTRODUCTION . . . . .	1
SECTION II . . . . .	2
OBJECTIVES . . . . .	2
SECTION III . . . . .	2
MATERIALS AND METHODS . . . . .	2
1. Substrates . . . . .	2
2. Reactor Feed Gases . . . . .	3
3. Experimental Apparatus . . . . .	3
a. LMTOC . . . . .	3
b. OUR . . . . .	3
c. Ultrasonic System . . . . .	6
d. Ozonator . . . . .	7
4. Batch Preparation and Sampling . . . . .	7
5. Analytical Methods . . . . .	8
a. Ozone Reactors Process Data . . . . .	8
b. Characterization of Partial Ozonation Products . . . . .	9
c. Gas Chromatographic Surveys of Ozonated Waters Used for Aquatic Bioassay . . . . .	10
6. Kinetic Data Modeling . . . . .	11
SECTION IV . . . . .	12
1. Introduction . . . . .	12
2. Ozone Mass Transfer . . . . .	14
3. Hydrazine . . . . .	17
a. pH Effect . . . . .	17
b. Specie Concentration Effect . . . . .	21
c. Ozone Partial Pressure . . . . .	24
d. Superficial Gas Velocity Effect . . . . .	27
e. Catalysts . . . . .	29

f.	Characterization Run for Aquatic Toxicity Studies . . . . .	32
g.	Air Sparging of Hydrazine . . . . .	35
4.	Monomethylhydrazine . . . . .	35
a.	pH Effect . . . . .	35
b.	Specie Concentration Effect . . . . .	39
c.	Ozone Partial Pressure . . . . .	44
d.	Superficial Gas Velocity Effect . . . . .	44
e.	Catalysts . . . . .	47
f.	Characterization Run for Aquatic Toxicity . . . . .	49
g.	Oxygen Sparging of Monomethylhydrazine . . . . .	49
5.	Unsymmetrical Dimethylhydrazine . . . . .	53
a.	pH Effect . . . . .	53
b.	Specie Concentration Effect . . . . .	53
c.	Ozone Partial Pressure . . . . .	55
d.	Superficial Gas Velocity Effect . . . . .	58
e.	Catalysts . . . . .	58
f.	Characterization Run . . . . .	63
g.	Air Sparging of Unsymmetrical Dimethylhydrazine . . . . .	63
SECTION V . . . . .		66
CONCLUSIONS . . . . .		66
1.	pH Effect . . . . .	66
2.	Specie Concentration Effect . . . . .	66
3.	Ozone Partial Pressure . . . . .	66
4.	Superficial Gas Velocity Effect . . . . .	66
5.	Catalyst . . . . .	67
6.	Air Sparging of H <sub>2</sub> , MMH and UDMH . . . . .	67
REFERENCES . . . . .		68
APPENDIX A . . . . .		71
APPENDIX B . . . . .		78
APPENDIX C . . . . .		85
APPENDIX D . . . . .		104

## LIST OF TABLES

1. Design Characteristics and Construction Materials of the LMTOC Reactor . . . . .	5
---	---

## LIST OF FIGURES

1. Process Flow Diagram . . . . .	4
2. Dissolved Ozone Uptake ( $O_3/Air$ ) in Distilled Water at pH 9.1 Buffered with (0.01 M) Sodium Borate . . . . .	15
3. The Decomposition of Dissolved Ozone in Distilled Water at pH 9.1 Buffered with (0.01 M) Sodium Borate in the Presence of UV Light . . . . .	16
4. Dissolved Ozone Uptake ( $O_3/O_2$ ) in Distilled Water at pH 9.1 Buffered with (0.01 M) Sodium Borate . . . . .	18
5. The Decomposition of Dissolved Ozone in Distilled Water at pH 9.1 Buffered with (0.01 M) Sodium Borate in the Presence of UV Light . . . . .	19
6. The Effect of pH on the Ozone Oxidation of Hydrazine . . . . .	20
7. Nitrate-N Production During the Ozone Oxidation of Hydrazine at Two pH Levels . . . . .	22
8. The Effect of Initial Concentration on the Ozone Oxidation of Hydrazine . . . . .	23
9. The Oxidation of Hydrazine in High Concentration by Ozone . . . . .	25
10. The Effect of Inlet Ozone Concentration on Ozone Oxidation of Hydrazine . . . . .	26
11. The Effect of Superficial Gas Velocity on the Ozone Oxidation of Hydrazine . . . . .	28
12. The Effect of UV Light on the Ozone Oxidation of Hydrazine . . . . .	30
13. Nitrate-N Production During the Ozone Oxidation of Hydrazine in the Presence and Absence of UV Light . . . . .	31
14. The Effect of Ultrasonics on the Ozone Oxidation of Hydrazine . . . . .	33
15. The Change in Hydrazine and COD with Ozonation Time . . . . .	34

16.	Nitrate-N Production During the Ozone Oxidation of Hydrazine . . .	36
17.	The Effect of UV Light on the Decomposition of Hydrazine During Air Sparging . . . . .	37
18.	The Effect of pH on the Ozone Oxidation of MMH . . . . .	38
19.	Methanol Production from the Ozone Oxidation of MMH at Two pH Levels . . . . .	40
20.	The Effect of Initial Concentration on the Ozone Oxidation of MMH . . . . .	41
21.	Methanol Production from the Ozone Oxidation of MMH as a Function of Initial Specie Concentration . . . . .	43
22.	The Effect of Inlet Ozone Concentration on the Ozone Oxidation of MMH . . . . .	45
23.	The Effect of Superficial Gas Velocity on the Ozone Oxidation of MMH . . . . .	46
24.	The Effect of Ultraviolet Light on the Ozone Oxidation of MMH . .	48
25.	The Destruction of MMH and COD by Ozone Oxidation . . . . .	50
26.	The Change in Volatile Organic Carbon During the Ozone Oxidation of MMH . . . . .	51
27.	The Effect of Ultraviolet Light on the Oxygen Sparging of MMH . .	52
28.	The Effect of pH on the Ozone Oxidation of UDMH . . . . .	54
29.	The Effect of Initial Concentration on the Ozone Oxidation of UDMH . . . . .	56
30.	The Effect of Inlet Ozone Gas Concentration on the Ozone Oxidation of UDMH . . . . .	57
31.	The Effect of Superficial Gas Velocity on the Ozone Oxidation of UDMH . . . . .	59
32.	The Effect of Ultraviolet Light on the Ozone Oxidation of UDMH . .	60
33.	The Effect of Ultrasonics on the Ozone Oxidation of UDMH . . . . .	62
34.	The Destruction of UDMH and COD by Ozone Oxidation . . . . .	64
35.	The Effect of Ultraviolet Light on the Air Sparging of UDMH . . .	65



## SECTION I

### INTRODUCTION

The hydrazine family of fuels includes hydrazine (H), monomethylhydrazine (MMH) and unsymmetrical dimethylhydrazine (UDMH) as well as mixtures of the above.

The United States Air Force is responsible for the procurement, storage and transport of hydrazine fuels not only for its own systems, such as Titan II and III, Minuteman III, Bomarc and F-16, but also for NASA and the space shuttle program. During the course of these operations there is a potential for environmental degradation. For example, accidental spills could occur directly from tank trailers and tank cars or when transfer lines are connected or disconnected during loading and unloading. Since the transport container must be sampled at the site of production as well as the destination point, the problem of proper disposal of these materials and residual purged liquids must be carefully considered. Currently, aluminum tank cars are washed prior to their yearly hydrostatic test. These washings contain residual hydrazine fuels and therefore must be disposed of in an environmentally acceptable manner. Finally, the federal requirement that, per specie, a minimum fuel supply of 2 years be in storage increases the probability of accidental discharge merely from the increased number of handling operations.

Currently, the Civil and Environmental Engineering Development Office (CEEDO), of the US Air Force is engaged in chemical and biological research to develop treatment technologies for contaminated water generated at fuels production sites and/or spilled fuels.

This research centered on the treatment of aqueous solutions of H, MMH, and UDMH by ozone. A parametric study was conducted to evaluate the effect of solution concentration and pH, the two catalysts ultraviolet (UV) light and ultrasonics, reactor inlet ozone gas phase concentration and superficial

gas velocity. Additionally the effect of gas sparging (air or oxygen) in the presence and absence of UV light was evaluated.

## SECTION II

### OBJECTIVES

The objectives of this research were as follows:

(1) To establish the stoichiometry and kinetics of the ozone oxidation of H, MMH and UDMH in aqueous solution.

(2) To identify the partial oxidation products from the ozone oxidation of hydrazine fuels.

(3) To accomplish toxicity testing of the ozone treated wastewaters with fathead minnows and Daphnia magna.

## SECTION III

### MATERIALS AND METHODS

#### 1. SUBSTRATES

One pint samples each of H (Lot No. TKHAS 2), MMH (DRUM H-8642) and UDMH (TKLIS-1) were obtained from CEEDO. These fuels, which were stored at approximately 10°C in an explosion proof refrigerator in a locked storage area, served as the only materials from which all batches for pilot plant experimentation were prepared.

## 2. REACTOR FEED GASES

Ozone was produced from both air and oxygen. For runs when an ozone concentration of 13 mg/l air or less (approximately 1% ozone in air) was desired, air was the ozonator feed gas. Air was compressed in a Puregas Compressor Model 4 HCJ-12-M 400 X and passed through 1/4" I.D. stainless steel tubing to the ozonator at 15 psig. Tank oxygen, (extra-dry grade) was supplied to the ozonator in the same manner as the air. Oxygen feed gas permitted the production of higher concentrations of ozone (i.e., approximately 2% ozone in oxygen) than with air for the same electrical power input to the generator.

## 3. EXPERIMENTAL APPARATUS

The basic apparatus used for all experiments is presented in a process flow diagram shown in Figure 1.

All experiments were conducted in a semi-batch mode, that is, a constant liquid volume and a continuous supply of gas. Two reactors were employed in this work. The primary reactor was the Life Systems Modified Torricelli Ozone Contactor (LMTOC). Also an ozone-ultrasonic reactor (OUR), constructed from pyrex glass and fitted for an ultrasonic generator, was utilized.

### a. LMTOC

The basic design characteristics and construction materials of the LMTOC are listed in Table 1. More complete design and development information can be found in references (1) and (2).

### b. OUR

The OUR was a 6-inch internal diameter by 18.0-inch high reactor fabricated from pyrex glass pipe. The bottom closure plate was constructed

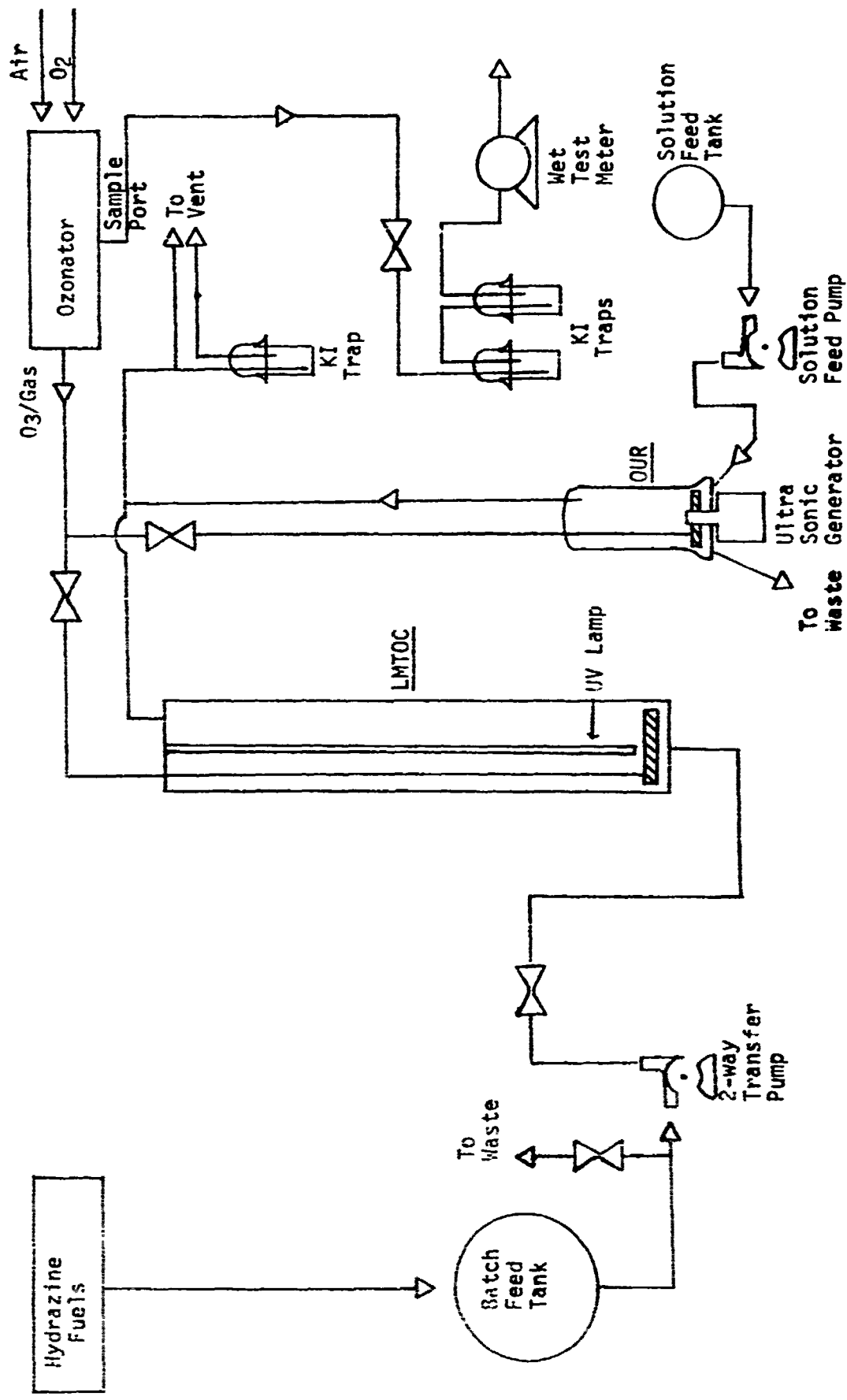


Figure 1. Process Flow Diagram

TABLE 1. DESIGN CHARACTERISTICS AND CONSTRUCTION MATERIALS OF THE LMTOC REACTOR

Characteristic	Descriptions
Column Volume	35.1; 1.2 ft <sup>3</sup>
Column Height	2.0 m; 6.5 ft <sup>3</sup>
Column Cross-Sectional Area	202.6 cm <sup>2</sup> ; 31.4 in <sup>2</sup>
Column Diameter	16.8 cm; 6.6 in
Sparger Surface Area	95.5 cm <sup>2</sup> ; 14.8 in <sup>2</sup>
Sparger Pore Size	5 micron average pore size; $1.97 \times 10^{-4}$ in
<u>Materials</u>	<u>Description</u>
Stainless Steel	Column (contactor) Contactor endplates Spargers Fittings
Teflon	Septums
Quartz	UV lamp housing

from 304 type stainless steel which served as the acceptor of the Biosonic IV ultrasonic system and was backed up with an aluminum plate. The bottom plate had two 0.25-inch diameter lines. One line was fitted with a stainless steel sampling valve, while on the other line, a one-way valve permitted fluid to be pumped into the reactor. The top cover plate on the reactor likewise was produced from 304 stainless steel and had two 0.25-inch diameter ports. One port was used for admitting the ozone/air or oxygen mixture through tygon tubing to the gas sparger located at the reactor bottom while the second port was used to permit residual gas to escape after it had been sparged through the reaction liquid. An identical gas sparger to the one used in the LMTOC was employed in this reactor.

The gas sparger was of a doughnut design with an outside diameter of 5.0 inches while the inside hole diameter was 1.25 inches. The Biosonic IV ultrasonic probe tip was inserted through the hole in the gas sparger and therefore sound waves flowed co-currently with the 5-micron size gas bubbles coming from the 316 stainless steel sparger.

### c. Ultrasonic System

For experiments involving the catalyst ultrasound, the Biosonic IV ultrasonic system was utilized. The unit had a lead zirconium titanate transducer which delivered up to 95% current efficiency at optimum performance. The unit had two ceramic discs in the transducer which provided a feedback from the probe to the generator and compensated for the required output assuring reproducibility in the reaction through constant power output. A power meter monitoring system was also used which indicated peak envelope power (PEP) delivered from the generator to the head in the tip. This unit reflected any changes in the process due to generator output, voltage input, increased temperature of the generator, out-gassing of the solution, and increased temperatures resulting from energy input from the transducer. The unit was theoretically capable of delivering up to 300 watts of acoustical power to the reaction liquid. Control as to the amount of acoustical power was accomplished by a dial in the front of the system. Energy utilization for this unit has been reported by Sierka (3).

#### d. Ozonator

A Grace ozonator Model LG-2-L2 was used to produce ozone from air or oxygen. The unit contained two corona cells and was designed to operate at gas pressures from atmospheric to 15 psig, with gas flows from 10 to 100 SCFH and an electrical power input from 0 to 200 watts per corona cell.

#### 4. BATCH PREPARATION AND SAMPLING

Solutions of H, MMH and UDMH were prepared from fuel grade material and distilled water in 36 l batches. Alkaline pH batches were buffered with sodium borate (0.01 M) while acidic batches were produced by adding concentrated hydrochloric acid (HCl) to the desired pH.

For all runs 30 liters of material were pumped to the LMTOC from the feed tank. During this transfer period of approximately 6 minutes, the reaction mass was air sparged to insure homogeneity. Prior to initiation of ozonation, a sample was extracted at the mid-depth point in the column. Throughout each run, at appropriate time intervals, samples were obtained at this sample tap for all analyses performed on liquids.

Five liters of solution were pumped to the OUR for each run through a one way valve. Liquid samples were obtained periodically from the reactor bottom through a stainless steel valve.

Ozone gas samples from the ozonator, the LMTOC and the OUR were passed through two potassium iodide (KI) traps in series. The first trap contained 300 ml of 2% KI while the second contained 100 ml of solution. Ozone gas samples were trapped exclusively in the 1st gas sampler, thus the second trap merely gave assurance that all of the ozone had been collected. Sample gas volumetric flow rates were measured with a wet test meter.

## 5. ANALYTICAL METHODS

### a. Ozone Reactors Process Data

Reactor temperature and pH were measured in small samples of water taken from the reactor as a function of time. Ozone in the gas phase entering and leaving the reactor was determined by trapping the ozone in gas washing bottles containing 2% KI solution, followed by thiosulfate titration as described in Standard Methods (4). Dissolved ozone was measured by the spectrophotometric method of Shechter (5), in water samples taken from the reactor and fixed immediately with neutral KI solution.

Hydrazine and monomethylhydrazine in the reactor were determined with an automated procedure based upon the colorimetric method of Watt and Chrisp (6). The Technicon II Autoanalyzer<sup>®</sup> module constructed for these analyses is shown in Appendix C. Standard curves were constructed in the range of 0-1.5 mg/l of H and 0-12 mg/l of MMH. Samples were diluted when necessary with glass distilled water using a Repipet<sup>®</sup> diluter. Replicate dilutions to 1/10 or 1/50 showed relative standard deviations of about 5-10% while recoveries of H and MMH spikes were 103-107%.

UDMH was determined by the colorimetric procedure of Pinkerton et al. (7), for the range of 0-60 mg/l. A Spectronic 700<sup>®</sup> spectrophotometer was used for this method and for the dissolved ozone in water determination. Recovery of a UDMH spike added to an ozonated sample water was 93% with a range of 92-93%.

MMH standards for chemical analysis were purchased from Aldrich Chemical Company and obtained from the US Air Force (same lots as used in ozonations). The latter source lot was assayed by titration, with potassium iodate to the iodine monochloride end point at ice bath temperature, with chloroform as the solvent layer for the initial iodine generation. UDMH was obtained from Aldrich and the US Air Force and was weighed into tared bottles for dilutions as standards. H was weighed out as the dihydrochloride salt and diluted to volume with HCl added as a preservative.



A complete listing of the ozone reactors process data can be found in Appendix A.

#### b. Characterization of Partial Ozonation Products

Total organic carbon (TOC) was measured on a Dohrman DC-50 carbon analyzer with a manually operated sample boat inlet system. A 30  $\mu$ l acidified sample was injected into the boat, which was then advanced to an evaporation heater at 110°C, where the volatile organic carbon (VOC) was measured and inorganic carbon removed via a porous polymer trap-backflush system. The boat was then advanced to the 850°C pyrolysis zone where the nonvolatile organic carbon was measured. The total area under the detected volatile and nonvolatile peaks was the TOC value. Tests with 100 mg/l MMH solutions indicated however, that the nonvolatile peak response was seriously reduced during repeated injections. Three sequential runs showed TOC values of 23.6, 19, and 17 units, for recoveries of 88, 70, and 63% of theoretical, respectively. This was possibly due to ammonia gas formed by reduction of the  $\text{NO}_x$  gas formed in the pyrolysis zone, as all gasses were passed over a nickel catalyst with hydrogen to form  $\text{CH}_4$  for final flame ionization detection on this instrument. Hence, TOC values from samples with high hydrazine concentrations were probably lower than the true values.

COD was measured by the procedure of Jirka and Carter (8) with Technicon II AutoAnalyzer<sup>®</sup> equipment.

Nitrate plus nitrite was determined by the automated cadmium reduction manifold of Technicon<sup>®</sup> (9), after the samples had been passed through a column of copper-chelex resin to remove the hydrazines, which were found to destroy the cadmium efficiency for reducing nitrate to nitrite. A 10 ml sample of hydrazine treated wastewater was passed through a 10 cm x 1/2-inch diameter column of 50-100 mesh Chelex-100 resin (Bio-rad<sup>®</sup>) in the copper-ammonia form. The sample was washed from the column with 10 ml of water and the eluted liquids were collected and diluted to 50 ml for nitrate plus

nitrite analysis. Tests with a 138 mg/l H solution demonstrated complete removal of H. No loss of nitrate-N in the copper-chelex column was seen in a test where a 114 mg/l MMH solution was spiked with nitrate-N at the 2 mg/l level. Because nitrite cannot exist in the presence of ozone, the results of the nitrate plus nitrite analysis are expressed as nitrate-N

Methanol was analyzed by direct aqueous injection gas chromatography with a 6' x 2 mm ID glass column packed with Tenax GC<sup>®</sup>, 60/80 mesh. Helium carrier gas flow was 23 cc/min and the column temperature was 50°C (2 min), 20°C/min to 100°C (1 min). The flame ionization detector on the Hewlett-Packard 5750 gas chromatograph was set on range 10 x 1 attenuation. Peak area data in the range of 0-100 mg/l methanol were collected with an AutoLab<sup>®</sup> System IV integrator. All injections were 2 µl volume; about 5 mg/l was the detection limit for methanol.

Ultraviolet (UV) spectra of high concentration, ozonated UDMH solutions ( $C_0$  approximately 5600 mg/l), pH 9.1, were run on a Beckman Acta CV<sup>®</sup> spectrophotometer between 200 and 400 nm with a 1 cm cell, after dilution of all samples by 1/20 with water. All spectra were scanned with distilled water in the reference cell in double-beam mode.

A fresh UDMH solution was prepared in borate buffer at the same approximate molarity (0.01 M) as that used in the ozonation tests. A UDMH solution of concentration 3,161 mg/l was diluted to 1/20 for UV analysis as a zero time UDMH reference solution.

#### c. Gas Chromatographic Surveys of Ozonated Waters Used for Aquatic Bioassay

Three ozonation runs, with H, MMH, and UDMH, were made to furnish waters for aquatic toxicity studies. The results of these assays are given in Appendix B. For each run, COD, hydrazine species, and TOC (for UDMH and MMH) were run. In addition, methanol data were collected for UDMH and MMH

runs and direct aqueous injection gas chromatography was used with a flame ionization detector and a nitrogen-specific Hall electrolytic conductivity detector (Tracor Model 700) to locate end products of the MMH and UDMH ozonations. The columns used were two 6' x 2 mm ID glass columns packed with 60/80 mesh Tenax GC<sup>®</sup> and operated isothermally at 100°C and 150°C, with a carrier helium flow of 22 cc/min. The Hall detector conductivity solvent was 15% V/V isopropanol water at a 0.7 cc/min recirculation rate.

The results of these chromatographic studies are given in Appendix C.

## 6. KINETIC DATA MODELING

All reported trial data were analyzed to determine rate constants for zeroth-, first- and second-order reaction with respect to the hydrazine species involved. In addition, UDMH runs were analyzed for the half-order reaction rate constant. First order fit procedures were performed on transformed data as provided in the GMNITAB data processing package (10). For first-order reactions, the transformation is:

$$\ln [C(\text{time} = 0)/C(t)] = kt$$

The rate constants and derived "half-life" times are presented in Appendix D. Also presented in Appendix D is the ratio

$$F \text{ Ratio} = \frac{(n-1) \text{ sum of squares removed by fit}}{\text{Residual sum of squares}}$$

and  $n$ , the number of data points in each trial.

## SECTION IV

### RESULTS AND DISCUSSION

#### 1. INTRODUCTION

The parameters studied in this research included solution pH and concentration, reactor ozone partial pressure and superficial gas velocity and the catalysts UV light and ultrasound. The rationale for each parameter choice and level is given below.

The solution characteristics of pH and specie concentration are related not only from the standpoint of chemical kinetics and reaction oxidation pathway but also in terms of ozone mass transfer. In the former case, the pH of the solution greatly affects the rate of oxidation of hydrazine fuels and their partial oxidation products. Methanol is one such product of MMH and UDMH oxidation with ozone. Gollan *et al.* (11) have shown with methanol that the oxidation rate is accelerated at alkaline pH. Solution pH also dictates at what rate dissolved ozone in solution will auto-decompose and therefore the steady state dissolved ozone residual level achievable. Since ozone decomposition leads to oxygen radical production, again pH is expected to play a major role in the ozone oxidation of hydrazine fuels. For this work, two pH levels were investigated - highly acidic (pH - 2.6 to 3.8) and alkaline (pH - 9.1).

The concentration of reactant is important from the standpoint of ozone mass transfer requirements. It is expected that hydrazine fuels concentration ranging between 100 and 1000 mg/l would be found in the environment under the conditions of accidental discharge and therefore this range was chosen for study. For H only, one run at approximately 5,500 mg/l was performed specifically at the request of the US Air Force.

Superficial gas velocity (SGV) at a fixed ozone partial pressure dictates the mass flow rate (mg/time) of ozone to the reactor. Also, SGV is related

to the degree of mixing in a gas sparged reactor. It has been shown by McCarthy *et al.*, (12) that at a 20 SCFM gas flow rate, the LMTOC behaves essentially as a completely stirred tank reactor. In order to ensure that mixing would not limit the reaction rate, all experiments were carried out at either 20, 30, or 40 SCFH. For the vast majority of experiments the 30 SCFH condition prevailed.

Inlet ozone gas concentration to the reactor is related to ozone mass transfer and to the maximum dissolved ozone concentration that can be achieved at fixed reactor operating conditions. Commercially available ozonators operate with an air feed and produce consistently no more than 1% by weight ozone in air. However, when ozone is produced within the same unit with an oxygen feed gas, a 2% by weight ozone gas concentration can be expected. Since the Air Force would most likely utilize air to produce ozone in its projected field treatment sites, the major portions of the experiment were performed at between 11.0 and 13.0 mg O<sub>3</sub>/l air (approximately 1.0% ozone). The range of ozone concentrations studied were approximately 4.0 to 30.0 mg O<sub>3</sub>/l gas.

Ozone partial pressure also affects oxidation rates. This in turn can be related to reactor hydraulic retention time which is directly related to system capital costs and operational costs (i.e., ozone production) and therefore by studying this parameter an indication of the tradeoff between these two cost centers is possible.

Two catalysts (UV light and ultrasound) were chosen for study in this research. UV light is a catalyst which is reliable, effective when used in conjunction with ozone, and it is essentially immune to the catalyst poisoning which would occur with the traditional metal catalysts. As previously mentioned, UV also accelerates the decomposition of ozone. Ultrasound has also exhibited catalytic effects in the ozone oxidation of organics principally because the sound energy enhances the rate of ozone decomposition to free radicals (3). Sound waves have another benefit, which is the enhancement of gas mass transfer. This is one advantage which UV light cannot duplicate.

Since knowledge of mass transfer is crucial to the correct interpretation of kinetic data, ozone uptake and decomposition studies were conducted in distilled water at pH 9.1 in the presence and absence of UV light. Measurement of inlet ozone gas and reactor off-gas conditions yielded information on the decomposition of ozone, while dissolved ozone measurements gave indication of the LMTOC's mass transfer characteristics as well as the ability of UV light to decompose ozone.

Finally, gas sparging at 30 SCFH with air and/or oxygen was studied to ascertain if this less costly alternative to ozone oxidation would be feasible. These experiments also compared the effect of UV light and ultrasound on this process.

## 2. OZONE MASS TRANSFER

The mass transfer of ozone from the gaseous to the liquid phase was studied in the LMTOC. Using 30 l of distilled water, buffered with 0.01 M sodium borate and an ozone in air gas input flow rate of 30 SCFH, the increase in dissolved ozone was measured as a function of time. These data are plotted in Figure 2. When steady state was achieved the ozone in and out of the LMTOC was measured and found to be 11.2 mg  $O_3/l$  (air) and 8.9 mg  $O_3/l$  (air), respectively.

While continuing to maintain these gas flow conditions, the UV light was turned on and the change in dissolved ozone monitored with time. These data are plotted in Figure 3. Again, measuring the ozone content of the LMTOC off-gas it was found that only 2.5 mg  $O_3/l$  (air) was present.

Since some oxidation runs with H<sub>2</sub>, MMH and UDMH were made with ozone produced from a pure oxygen feed gas, the following mass transfer experiment was performed. For this run 24.2 mg  $O_3/l$   $O_2$  was passed through 30 l of distilled water maintained at pH 9.1 with sodium borate (0.01 M). At steady state the LMTOC off-gas concentration was 21.0 mg  $O_3/l$   $O_2$ . The ozone uptake

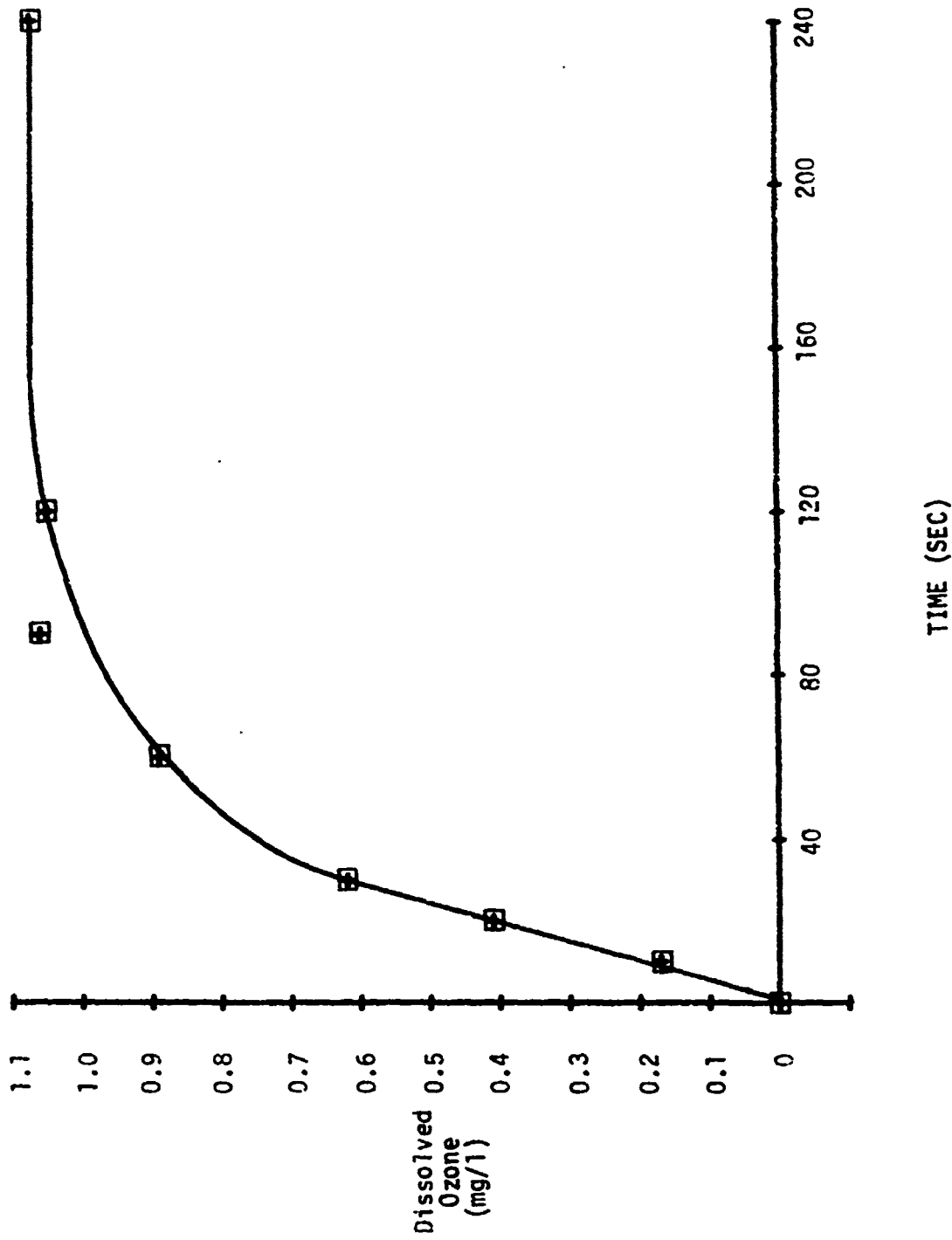


Figure 2. Dissolved Ozone Uptake ( $O_3$ /Air) in Distilled Water at pH 9.1 Buffered with (0.01M) Sodium Borate

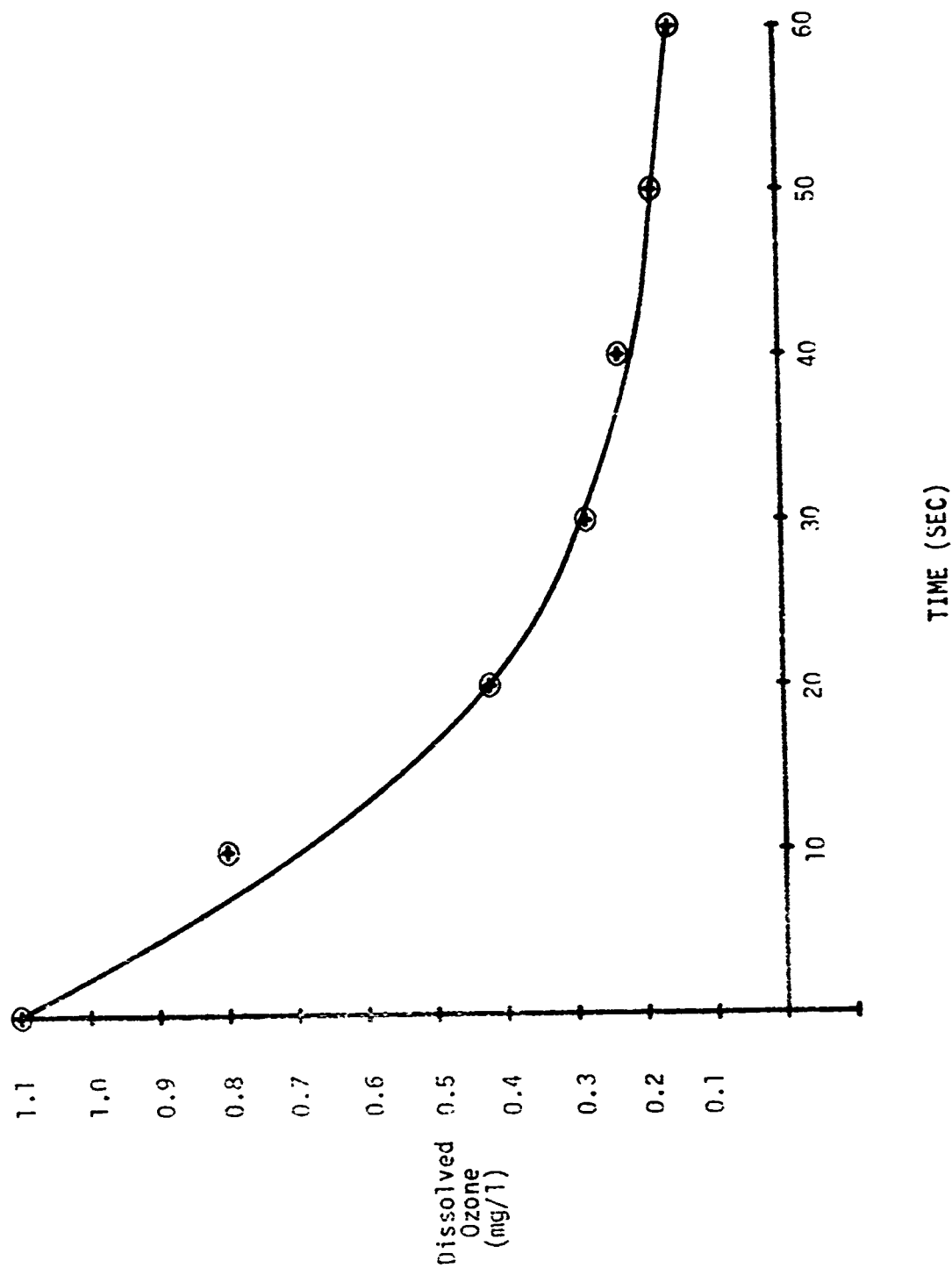


Figure 3. The Decomposition of Dissolved Ozone in Distilled Water at pH 9.1 Buffered with (0.01 M) Sodium Borate in the presence of UV Light



curve is given in Figure 4. When steady state was achieved, simultaneously the gas flow to the reactor was stopped and the UV light turned on. The decay in dissolved ozone is shown in Figure 5.

These data show the effect that an increase in ozone partial pressure has on the steady state dissolved ozone level and the positive effect that UV light has on the autodecomposition of ozone in solution. The latter is responsible for the net production of free radicals for substrate oxidation. Chang (13) has measured the decomposition of dissolved ozone and found a first order rate constant of  $0.01006 \text{ sec}^{-1}$  and a  $t_{1/2}$  of 68.9 seconds at a pH of 9.0 buffered with 0.1 M sodium borate and a temperature of 25°C. For this study, with the UV light on, the first order rate constant was  $0.077 \text{ sec}^{-1}$  and the  $t_{1/2}$  was 9 sec. Thus it can be seen that with UV light the decomposition of dissolved ozone is substantially increased.

### 3. HYDRAZINE

#### a. pH Effect

Two oxidation runs were performed at solution pH values of 3.1 and 9.1 and the results shown in Figure 6. For the high pH run (R-44) all of the H was destroyed with 45 minutes of ozonation while at the low pH (R-56) condition 35% of the initial amount of H present was oxidized.

The increased reaction rate at high pH is probably principally due to the increased auto-decomposition of ozone to oxygen free radicals. Also, at high pH values the free base form of H ( $\text{NH}_2\text{-NH}_2$ ) would predominate over the protonated form, and some of the rate enhancement may be due to the greater reactivity expected of the free base form.

Using the zero order kinetic model, the half-life  $t_{1/2}$  (min) and reaction velocity constants  $k$  (mg/l-min) are predicted to be 20.7 and 3.35, respectively for the pH 9.1 run; and 89.8 and 0.84 for the pH 3.1 run.

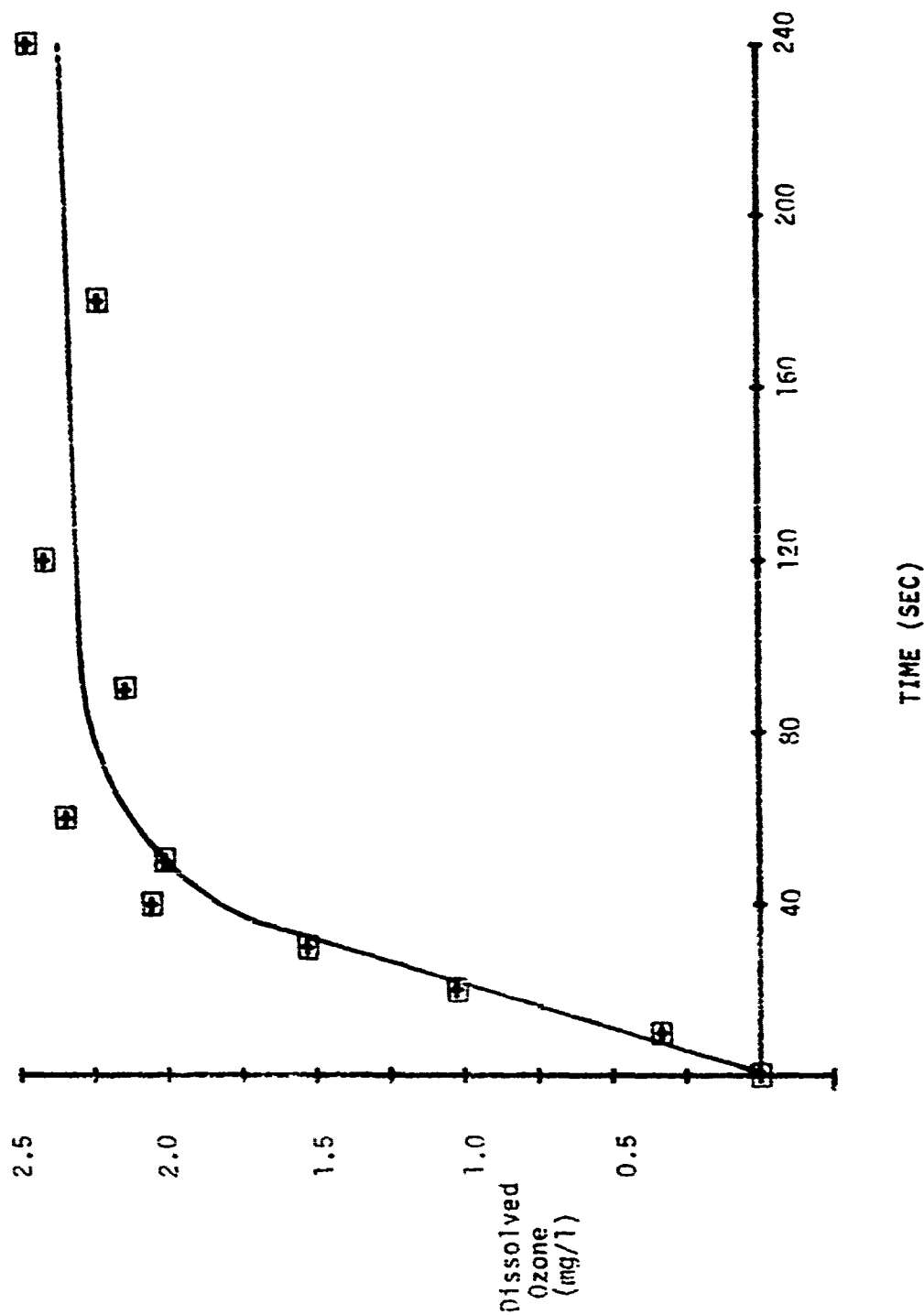


Figure 4. Dissolved Ozone Uptake ( $O_3/O_2$ ) in Distilled Water at pH 9.1 Buffered with (0.01M) Sodium Borate

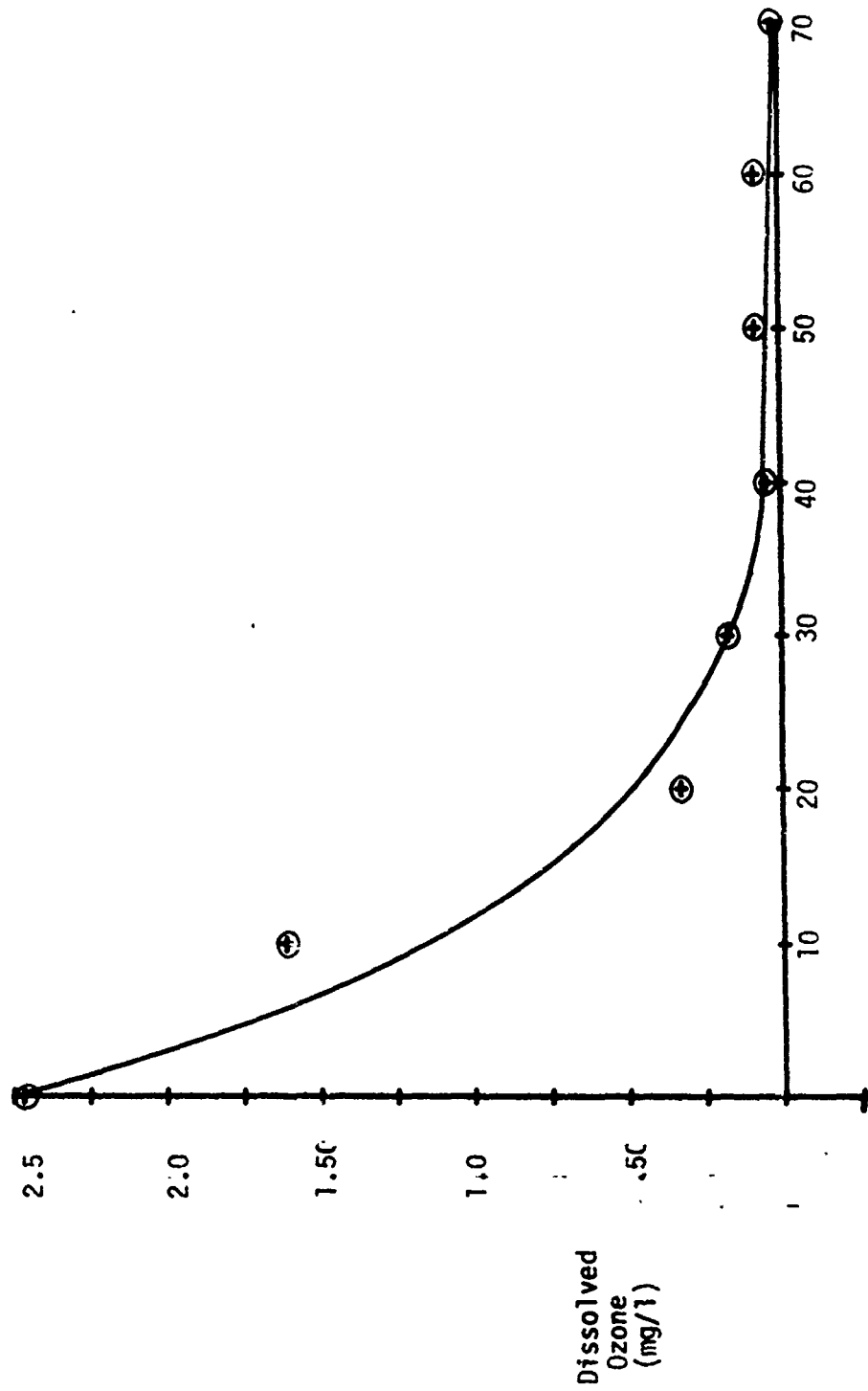
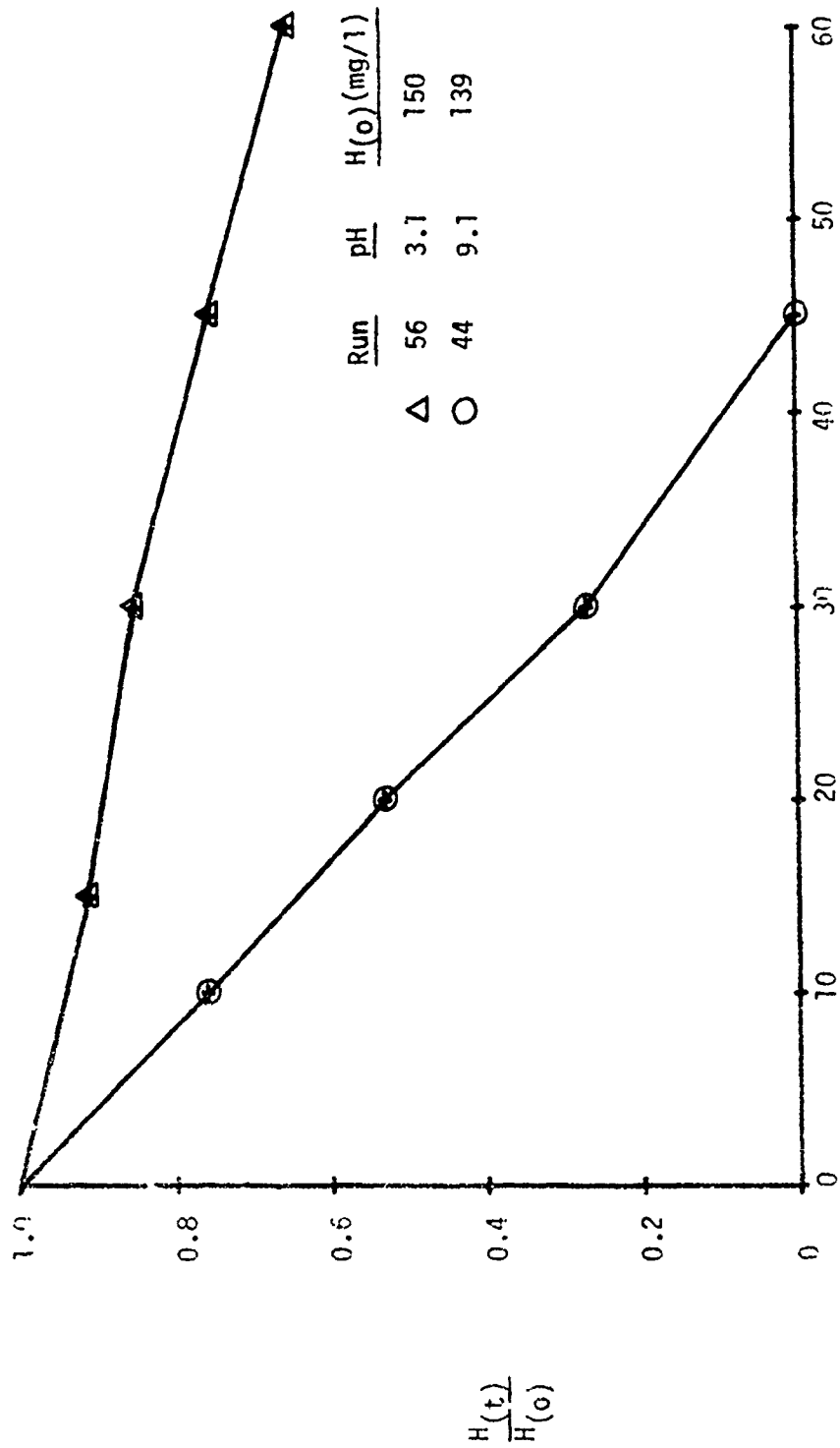


Figure 5. The Decomposition of Dissolved Ozone in Distilled Water at pH 9.1 Buffered with (0.01M) Sodium Borate in the Presence of UV Light



REACTION TIME (MIN)

Figure 6. The Effect of pH on the Ozone Oxidation of Hydrazine

At the end of each run, the reactor off-gas was analyzed and found to contain 2.81 mg  $O_3$ /l of air and 2.19 mg  $O_3$ /l air for R-44 and R-56, respectively. As it was demonstrated in section 2 during the ozone mass transfer experiments conducted with distilled water with the UV light on, buffered with 0.01 M sodium borate to a pH of 9.1, approximately 22.3% of the inlet ozone gas would exit the LMTOC at steady-state conditions. Near the termination time of R-44 the reactor-off gas contained 25.6% ozone which closely approximates the above findings. This was expected since all of the H had been oxidized to the principal end products nitrogen and water, thus steady state with respect to ozone had been achieved.

Under acidic conditions (R-56) the reactor off-gas should have contained considerably more ozone than 16.9% since the half-life of dissolved ozone is increased as pH decreases (14). However, it should be noted that 65% of the initial H concentration remained and therefore presented an ozone demand which kept the ozone off-gas concentration low.

In R-44 and R-56 the mg H oxidized/mg  $O_3$  applied was 0.61 and 0.15, respectively over the first 45 minutes of ozonation.

The effect of solution pH on nitrate production is shown in Figure 7. After 60 minutes of ozonation, the nitrate concentration for R-44 was 3.8 mg/l. However, for R-56 a total of 7.8 mg/l was produced. This response was indicative that different ozone oxidation reaction pathways were operative with the different pH levels in the reaction mass.

#### b. Specie Concentration Effect

Increasing initial H concentration in a reactor with fixed inlet gas condition leads to increased hydraulic detention times to reach the desired specie reduction level. This can be observed in Figure 8.

Assuming the zero order model, k (mg/lmin) values for the low (139 mg/l), medium (432 mg/l) and high (785 mg/l) H concentration runs

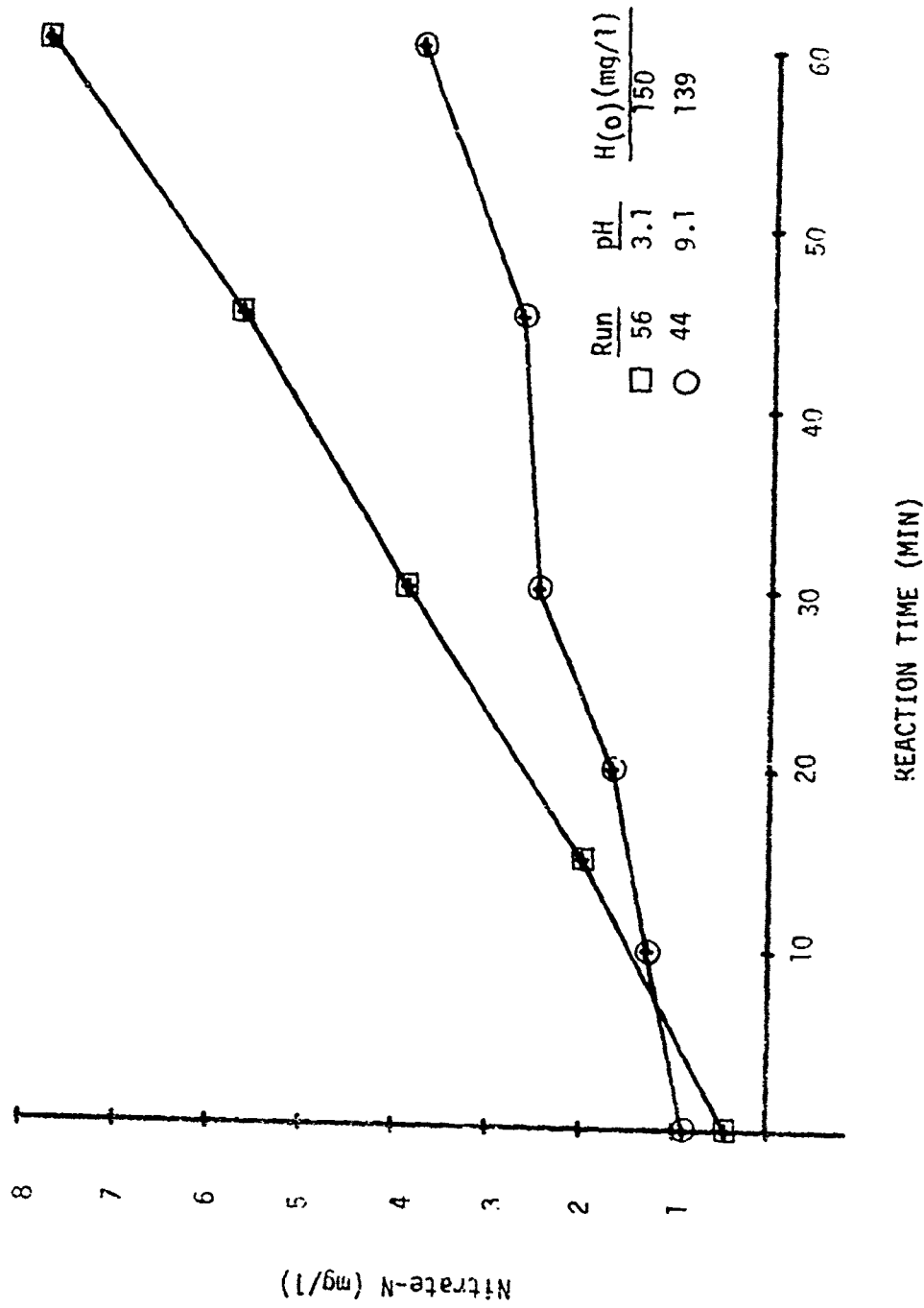


Figure 7. Nitrate-N Production During the Ozone Oxidation of Hydrazine at Two pH Levels.

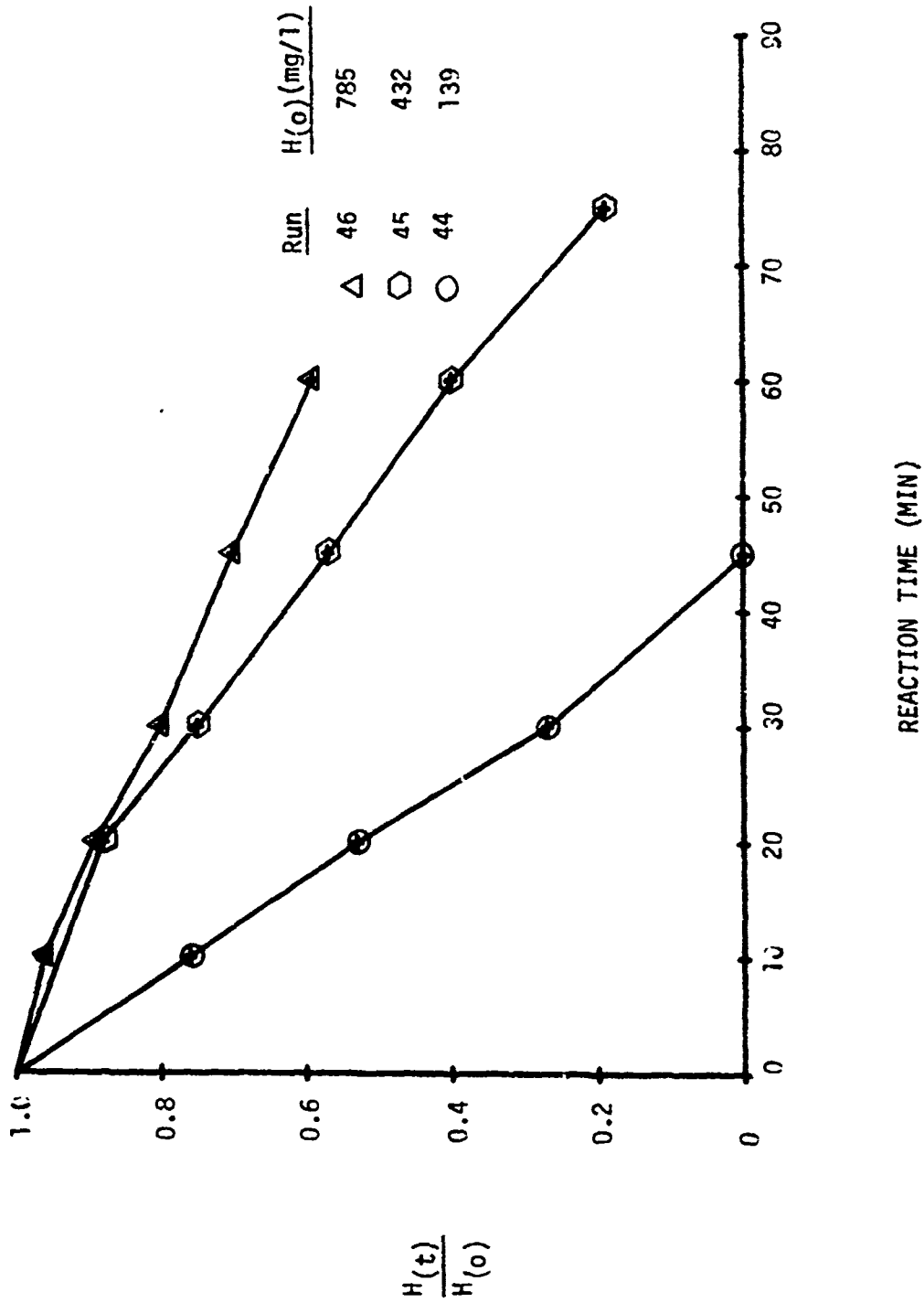


Figure 8. The Effect of Initial Concentration on the Ozone Oxidation of Hydrazine

(R-44, 45, 46) were 3.35, 4.27 and 5.26, respectively while the  $t_{1/2}$  (min) values were 20.7, 50.6 and 74.5, respectively.

Employing the above kinetic constants and assuming that all of the H would be destroyed, the ratio of mg H oxidized/mg  $O_3$  applied was 0.66, 0.72 and 0.95. The difference in these values is postulated to be the result of different ozone inlet concentrations, 10.8, 12.6, and 13.0 mg  $O_3$ /l. Even though it was attempted to achieve exactly the same ozonator outlet conditions the variability of the system did not permit complete control.

One run (R-57) at a concentration of 5,500 mg/l was performed at the contractors request. The H solution for R-57 was pumped to the LMTOC and remained there with the UV light turned on for a period of 30 minutes. Samples were analyzed at 15 minute intervals and showed no reduction in H. After 30 minutes of exposure to UV light, ozonation was begun. The results of this ozonation are depicted in Figure 9. Basically this run shows that after an initial ozonation period of 15 minutes the rate of H destruction followed zero order kinetics.

### c. Ozone Partial Pressure

The effect of increasing the partial pressure of ozone to the LMTOC was studied in three experimental runs. These runs (R-49, 44 and 50) were conducted with ozone inlet concentrations of 4.42, 10.82 and 29.85 mg/l (gas). Inlet H concentrations and reactor conditions (i.e., pH and UV light) were virtually constant. Likewise, superficial gas velocity was maintained at 30 SCFii.

The results of these runs are graphed in Figure 10, from which it can be observed that reaction rates increase with increased ozone partial pressure. A zero order kinetic model yielded  $k$  (mg/l-min) values of 2.71, 3.35 and 7.74 and  $t_{1/2}$  (min) values of 25.5, 20.7 and 8.1, respectively for the low, medium and high ozone concentration runs.



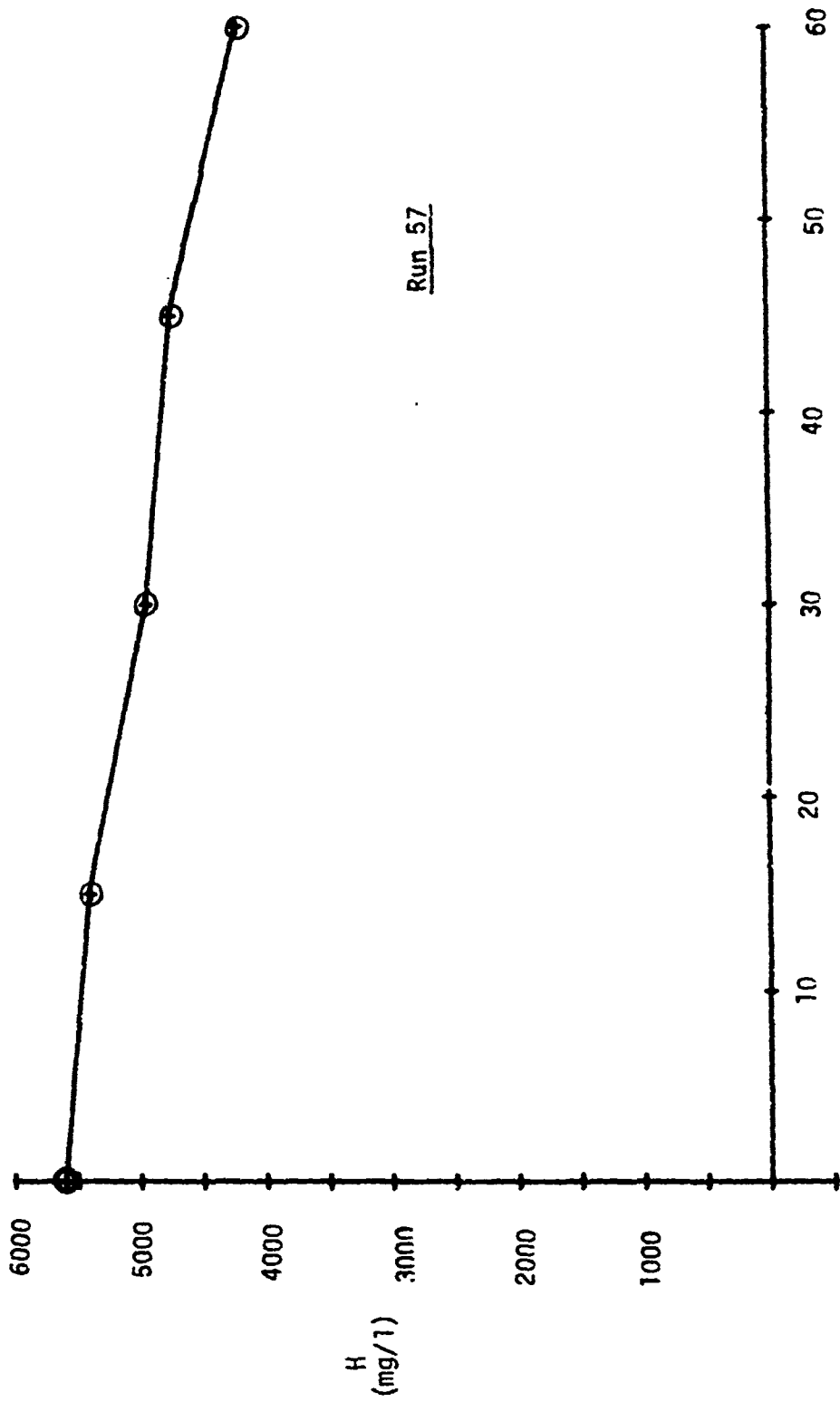
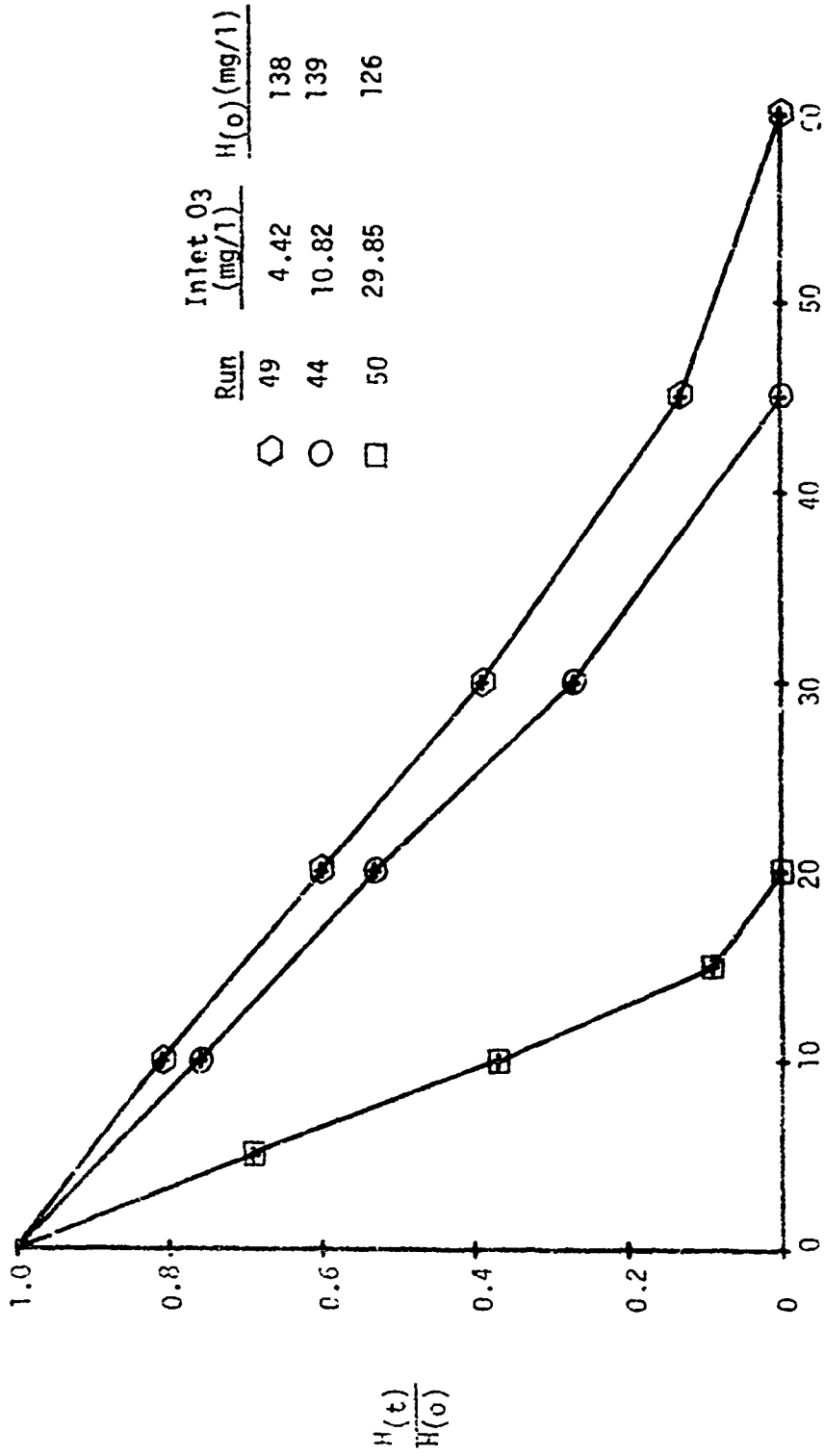


Figure 9. The Oxidation of Hydrazine in High Concentration by Ozone



REACTION TIME (MIN)

Figure 10. The Effect of Inlet Ozone Concentration on Ozone Oxidation of Hydrazine

Using the data it was calculated that 1.3, 0.66 and 0.55 mg H were oxidized per mg of ozone applied for R-49, R-44 and R-50, respectively.

These results were expected since the autodecomposition of dissolved ozone follows first order kinetics (13) and therefore as the ozone partial pressure increased, the amount of ozone decomposing likewise increased and this led to the self extinguishment of ozone free radicals before they could react with H. It should be recalled that the ozone admitted to the LMTOC is used up by two separate reactions. The first is in the oxidation of H and the second in ozone auto-decomposition. Since the latter reaction is first order;

$$\frac{dO_3}{dt} = k' \text{ (dissolved ozone)}$$

as the ozone partial pressure is increased, the decomposition of ozone becomes more important in terms of overall usage.

#### d. Superficial Gas Velocity Effect

Yoshida and Akita (15) have demonstrated that an SGV of 0.661 cm/sec is required to have liquid back mixed conditions in a gas sparged reactor. In this research the effect of SGV was studied by changing the gas flow rate in the LMTOC from 20 through 40 SCFH (0.90 to 1.8 cm/sec) which is well above the criterion for back mixing. The change in H concentration with ozonation time was then measured. These results are presented in Figure 11.

Since the inlet gas phase ozone concentration, pH and H concentration were essentially constant, the differences in rate were simply related to the mass of ozone admitted to the reactor. At 20, 30 and 40 SCFH (R-52, R-44, R-53) the k (mg/l-min) values were 2.74, 3.35 and 4.33, respectively while  $t_{1/2}$  (min) values were 25.2, 20.7 and 15.8, respectively assuming the zero order model.

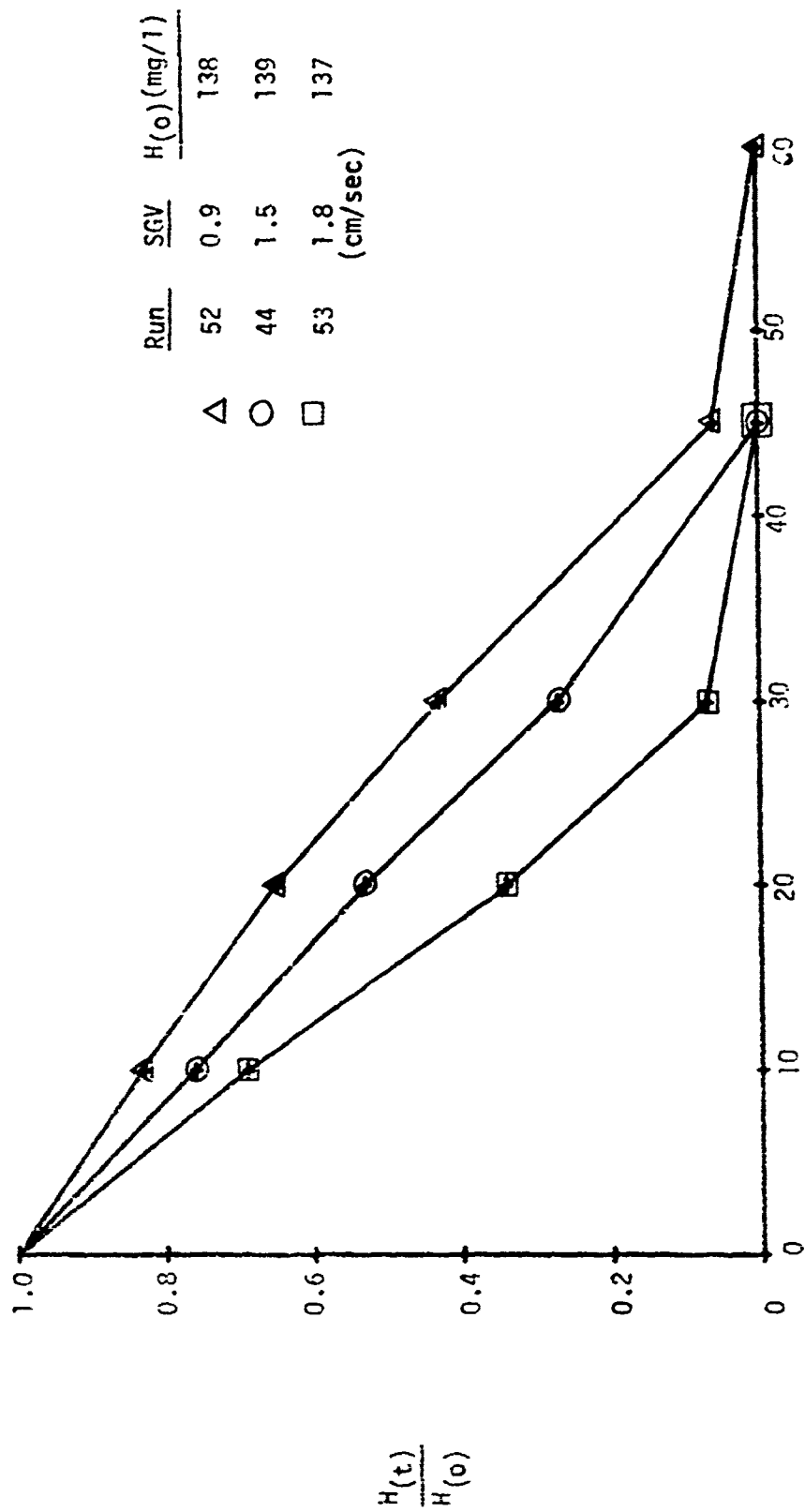


Figure 11. The Effect of Superficial Gas Velocity on the Ozone Oxidation of Hydrazine

Using the above kinetic data and ozone concentration and flow rate the average amount of ozone calculated to have been used to achieve zero H concentration was 5,885 mg  $O_3$  with a standard deviation of 379 mg/l mg  $O_3$ . In terms of mg H oxidized/mg  $O_3$  applied the values were 0.79, 0.66 and 0.71 for the 20, 30 and 40 SCFH runs. The difference in stoichiometry can be explained in terms of the lack of perfect fit in the kinetic model and the differences in inlet ozone gas concentration (9.74 to 11.0 mg  $O_3$ /l).

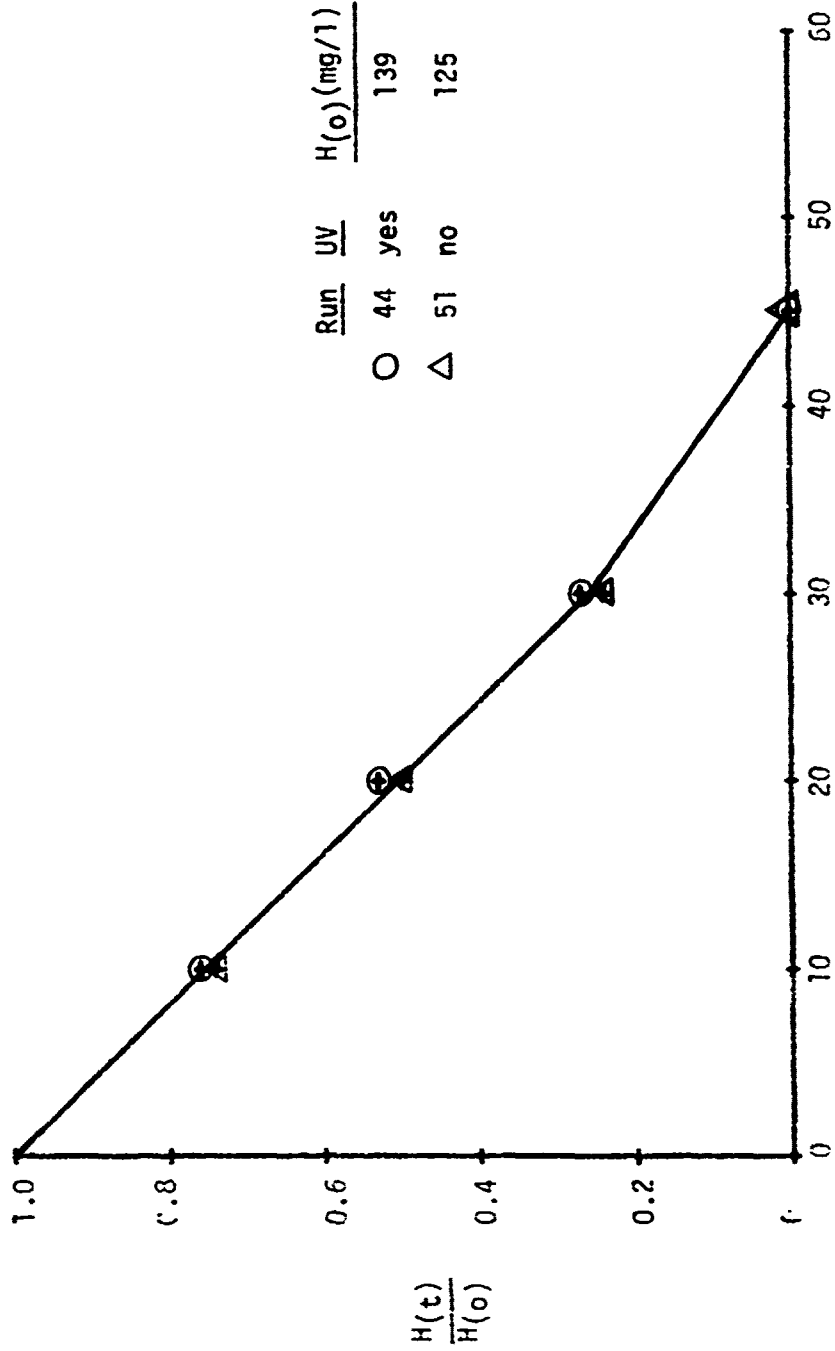
#### e. Catalysts

The effect of the catalysts UV light and ultrasound were investigated in the LMTOC and OUR, respectively.

The presence or absence of UV light in the LMTOC basically made little difference on the ozone oxidation of H, at least for the reactor conditions employed in R-51 and R-40. This can be seen in Figure 12 and in the zero order kinetic model data. For example the k (mg/l-min) values for R-51 (without UV light) and R-44 (with UV light) was 2.94 and 3.35 while the  $t_{1/2}$  (min) were 21.3 and 20.7 respectively. However, the mg H oxidized/mg  $O_3$  applied was calculated to be 0.56 and 0.66 for R-51 and R-44 respectively; pointing out that the UV light was beneficial from this standpoint.

In terms of ozone utilized in the LMTOC there was a large difference. Immediately preceding the termination of R-51, 77.7% of the entering ozone gas left the LMTOC unreacted. In R-44, 25.9% of the ozone entering, left the reactor. Since no H remained at the time of these measurements, the difference in off gas concentration was simply due to the decomposition effect of UV light. This has implication in multi-stage reactors where off gas per stage are often recycled to downstream stages.

Nitrate production in the LMTOC was also monitored and is shown in Figure 13 as a function of ozonation time for R-51 and R-44. These data showed that with UV light in the LMTOC less nitrate was produced than when UV light was not employed.



REACTION TIME (MIN)

Figure 12. The Effect of UV Light on the Ozone Oxidation of Hydrazine

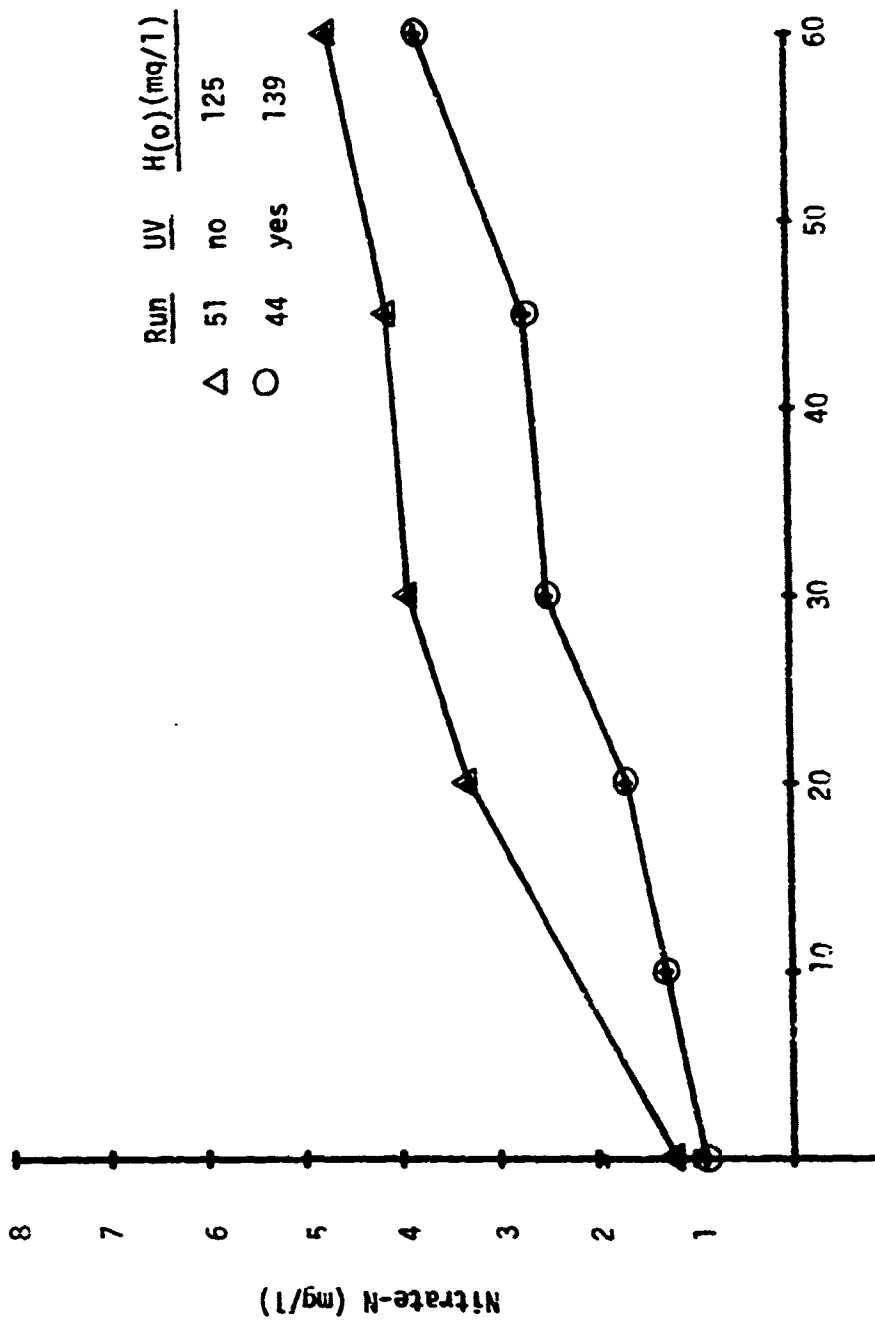


Figure 13. Nitrate-N Production During the Ozone Oxidation of Hydrazine in the Presence and Absence of UV Light

Ultrasound as a catalyst was investigated in the OUR. Two runs, one (R-47) with ultrasound and one (R-48) without ultrasound were made to evaluate the effect of sound waves. These data are depicted in Figure 14.

During both runs the full production capability of the ozonator was passed through the OUR which contained only 5 liters of solution compared with the 30 liters in the LMTOC. This mass and volume of ozone in the OUR produced a very large excess of ozone. Actually, within 1 minute of reaction, ozone was detected in the reactor off-gasses for both runs. Also, in the headspace of the OUR a white dense gas formed indicating a saturated ozone condition.

The  $k$  (mg/l-min) values for R-47 and R-48, assuming a zero order model were 21.1 and 24.6, respectively, while the  $t_{1/2}$  (min) values were 16.7 and 14.8. On a mg H oxidized/mg  $O_3$  applied basis, the run with ultrasound produced a ratio of 0.82, while for the run without ultrasound, the value was 0.67.

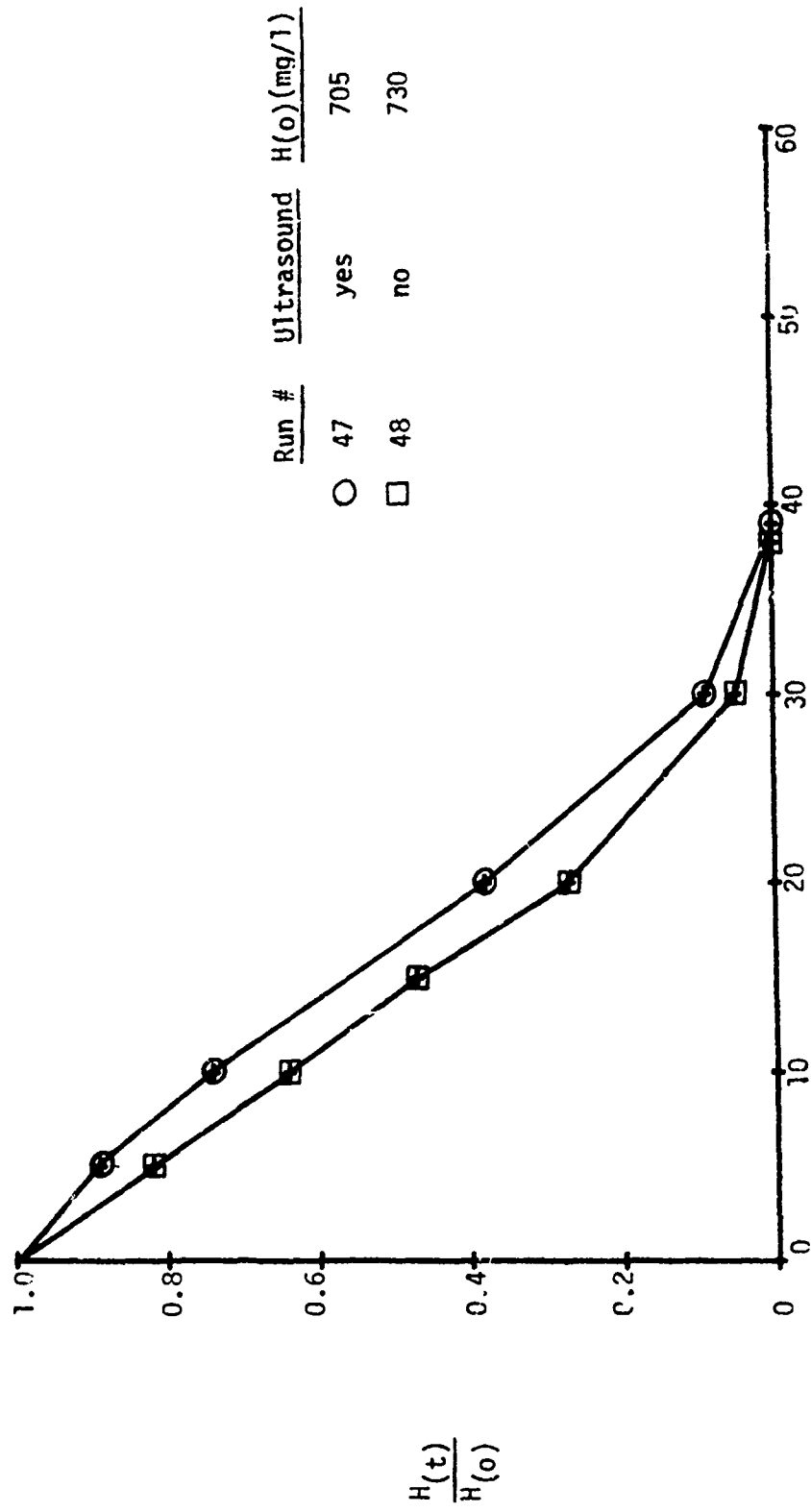
#### f. Characterization Run for Aquatic Toxicity Studies

After completing the parametric study on H, a run (R-70) was made to produce an effluent for aquatic toxicity studies with fathead minnows and Daphnia magna. The results of these tests are given in Appendix B.

The objective of this run was to ozonate an aqueous solution of H until the specie disappeared regardless of partial oxidation products. For R-70 this required 45 minutes of ozonation.

The results of this run, in terms of COD, and H disappearance as a function of ozonation time are presented in Figure 15. Basically the data show that the COD/H ratio averaged 1.029 with a standard deviation of 0.258 throughout the run. Since the COD/H ratio theoretically is 1.00 if  $H_2$  and water are the only reaction products (see Equation 1, below) the above





REACTION TIME (MIN)

Figure 14. The Effect of Ultrasonics on the Ozone Oxidation of Hydrazine

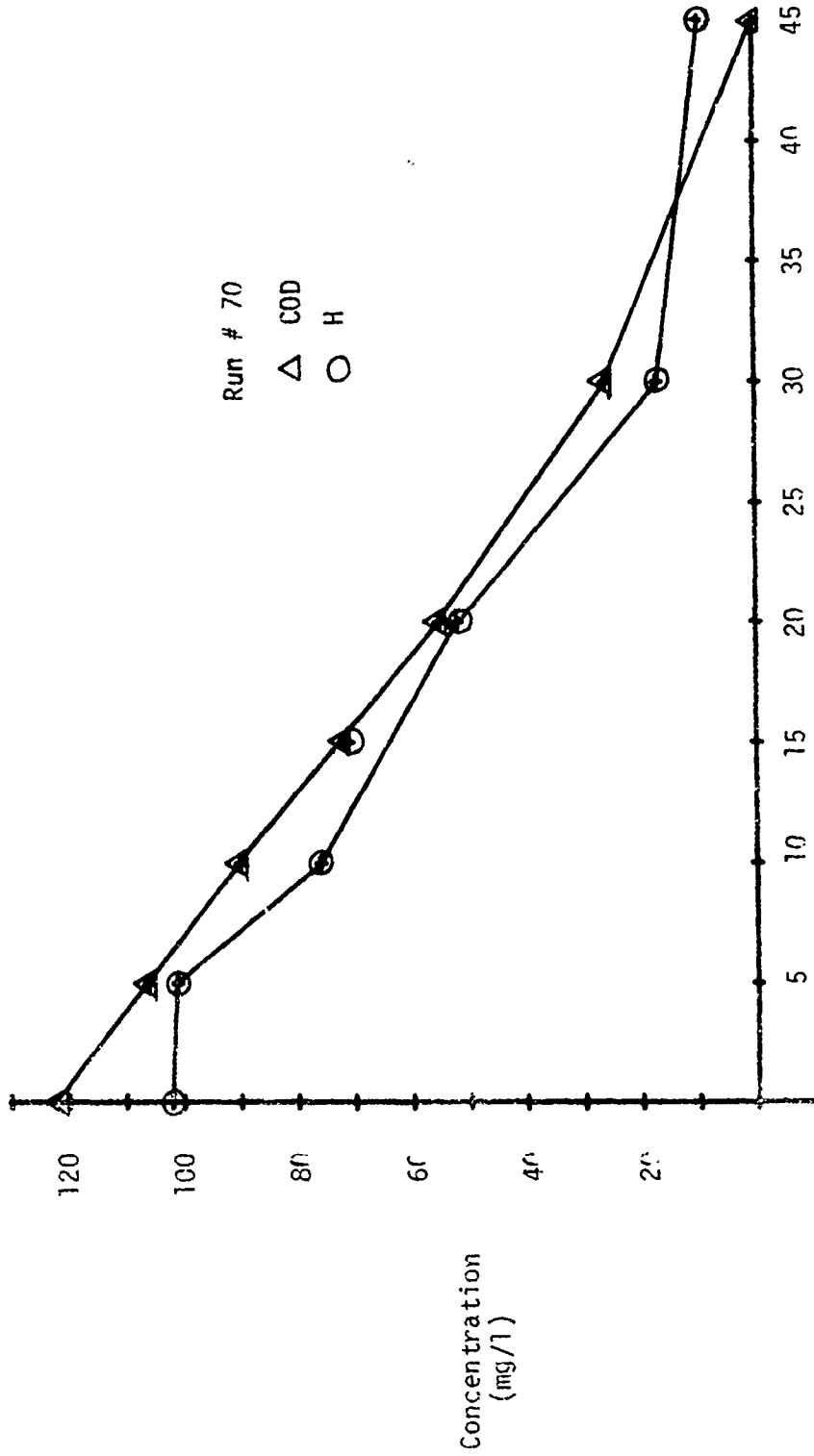


Figure 15. The Change in Hydrazine and COD with Ozonation Time

higher value is partially explained by the nitrate formation observed throughout the run. Nitrate-N rose from 0 to 2.49 mg/l over the 45 minutes ozonation time as shown in Figure 16.

#### g. Air Sparging of Hydrazine

R-54 and R-55 were performed to evaluate the effect of air sparging (30 SCFH) in the presence and absence of UV light, respectively. The results of these runs can be seen in Figure 17. These data showed that 35% of the initial H concentration was removed in 60 min when UV light was present during air sparging, yet when the experiment was repeated in the absence of UV light, only 19% of the specie was removed during the same time period.

Careful examination of Figure 17 indicates that while the run without UV (R-55) yielded a regular decrease in H concentration with time, in R-54 it appeared that two different rates corresponding to the 0-15 min and 15-60 min time segments were present. This could indicate that some finite time period is required before the total contents of the LMTOC were activated by UV light and a new removal mechanism became dominant.

Bowen and Birley (16) in their experiments indicate the main reaction between H and oxygen would indicate the following stoichiometry;



#### 4. MONOMETHYLHYDRAZINE

##### a. pH

The effect of solution pH on the ozone oxidation of MMH is depicted in Figure 18. R-17 was buffered to pH 9.1 with (0.01 M) sodium borate and R-18 was run with an initial pH of 2.57, produced by the addition of concentrated HCl.

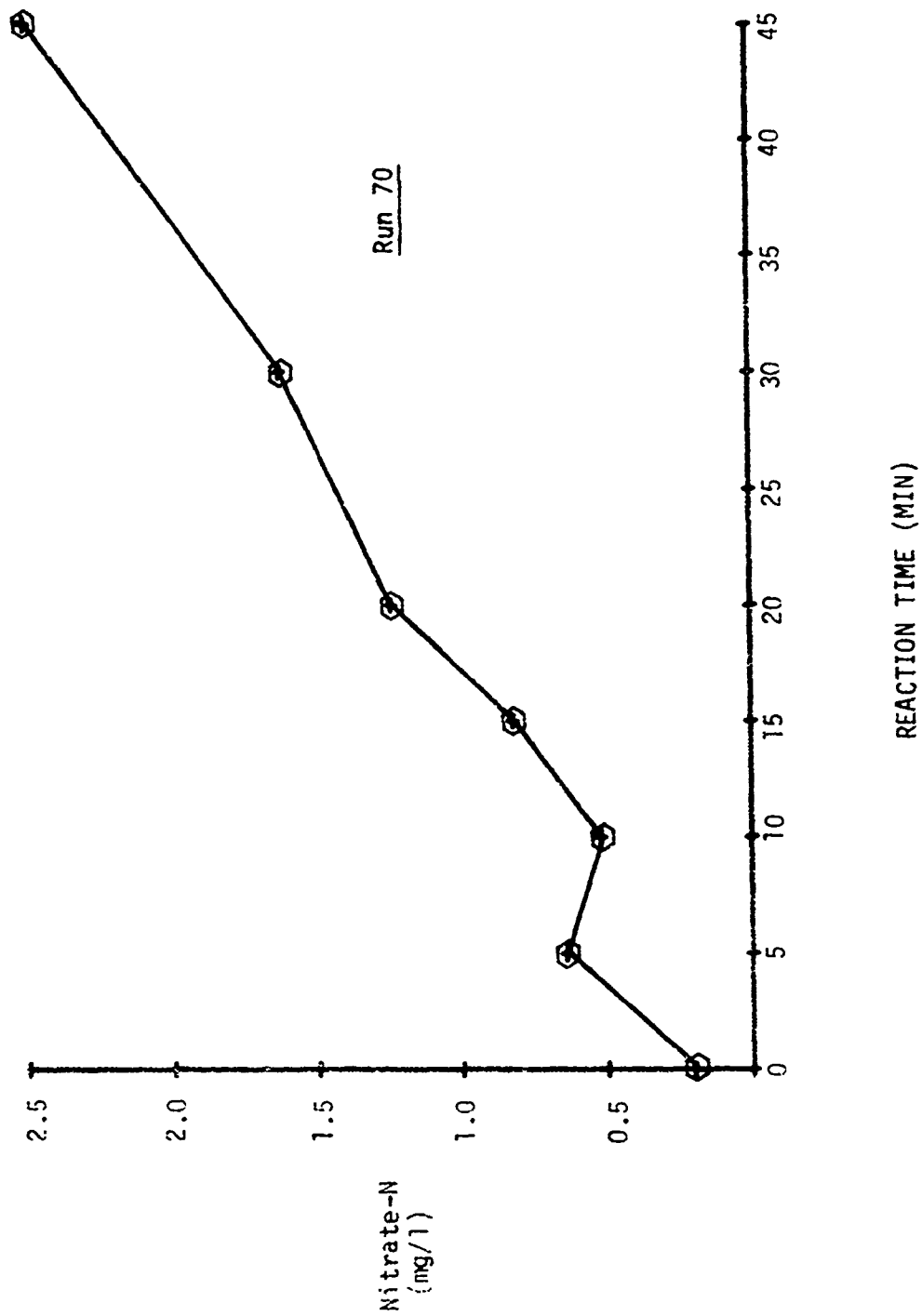


Figure 16. Nitrate-N Production During the Ozone Oxidation of Hydrazine

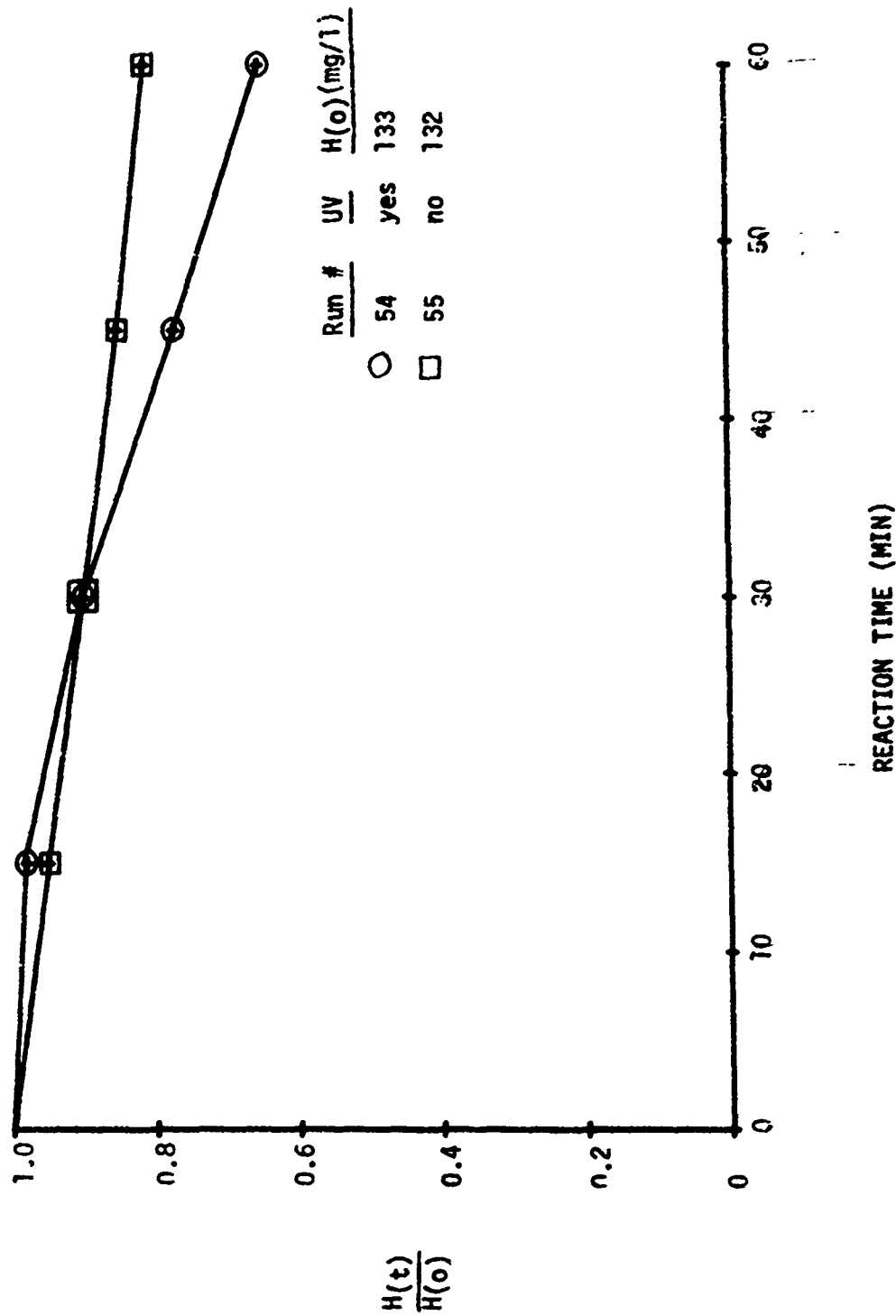


Figure 17. The Effect of UV Light on the Decomposition of Hydrazine During Air Sparging

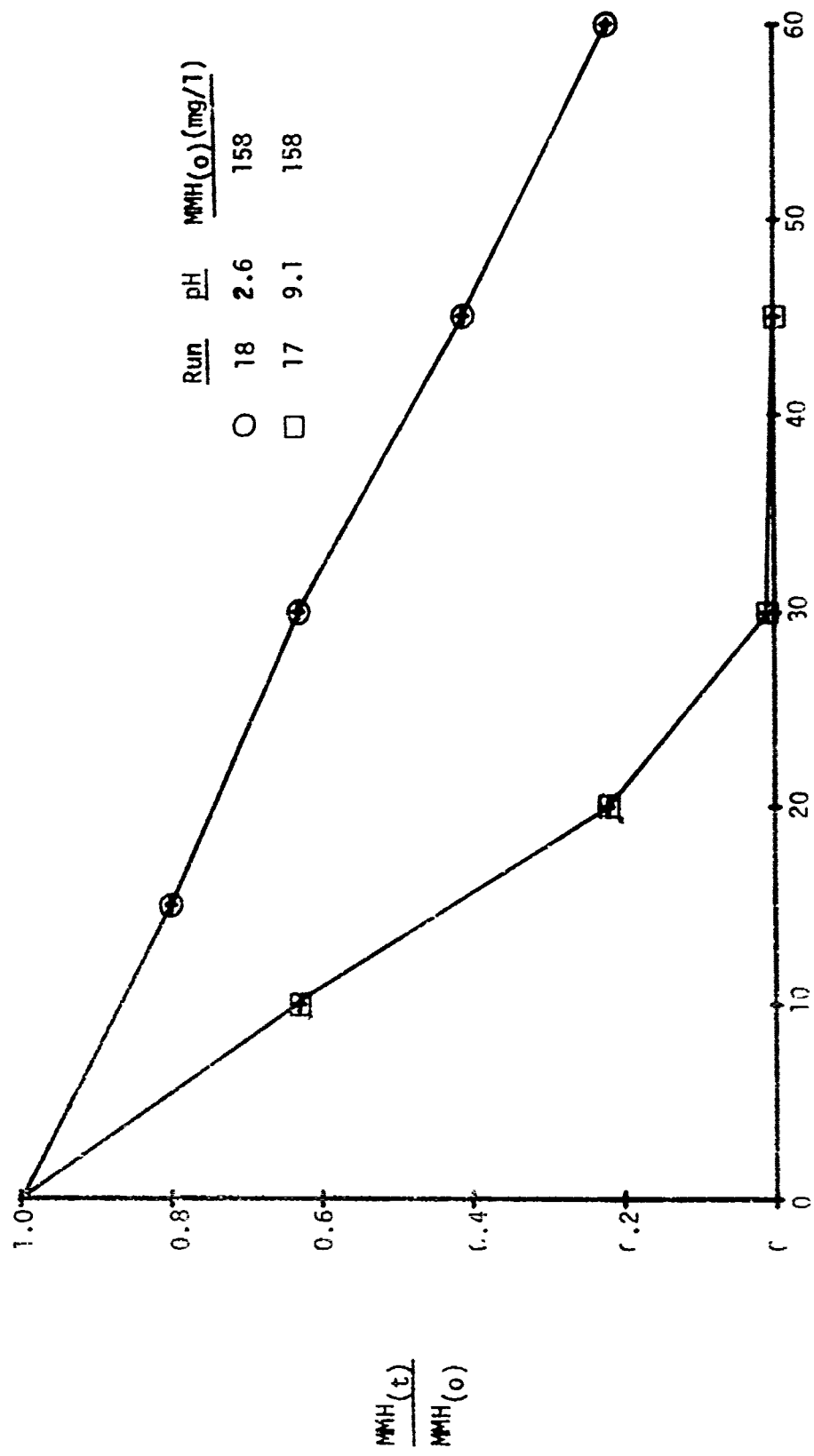


Figure 18. The Effect of pH on the Ozone Oxidation of MMH

From the graph it can be seen that as solution pH decreased, the rate of oxidation decreased. If zero order kinetics are assumed, the  $k$  (mg/l-min) values for R-17 and R-18 are 2.9 and 2.1 while  $t_{1/2}$  (min) values were 20.8 and 38.4, respectively.

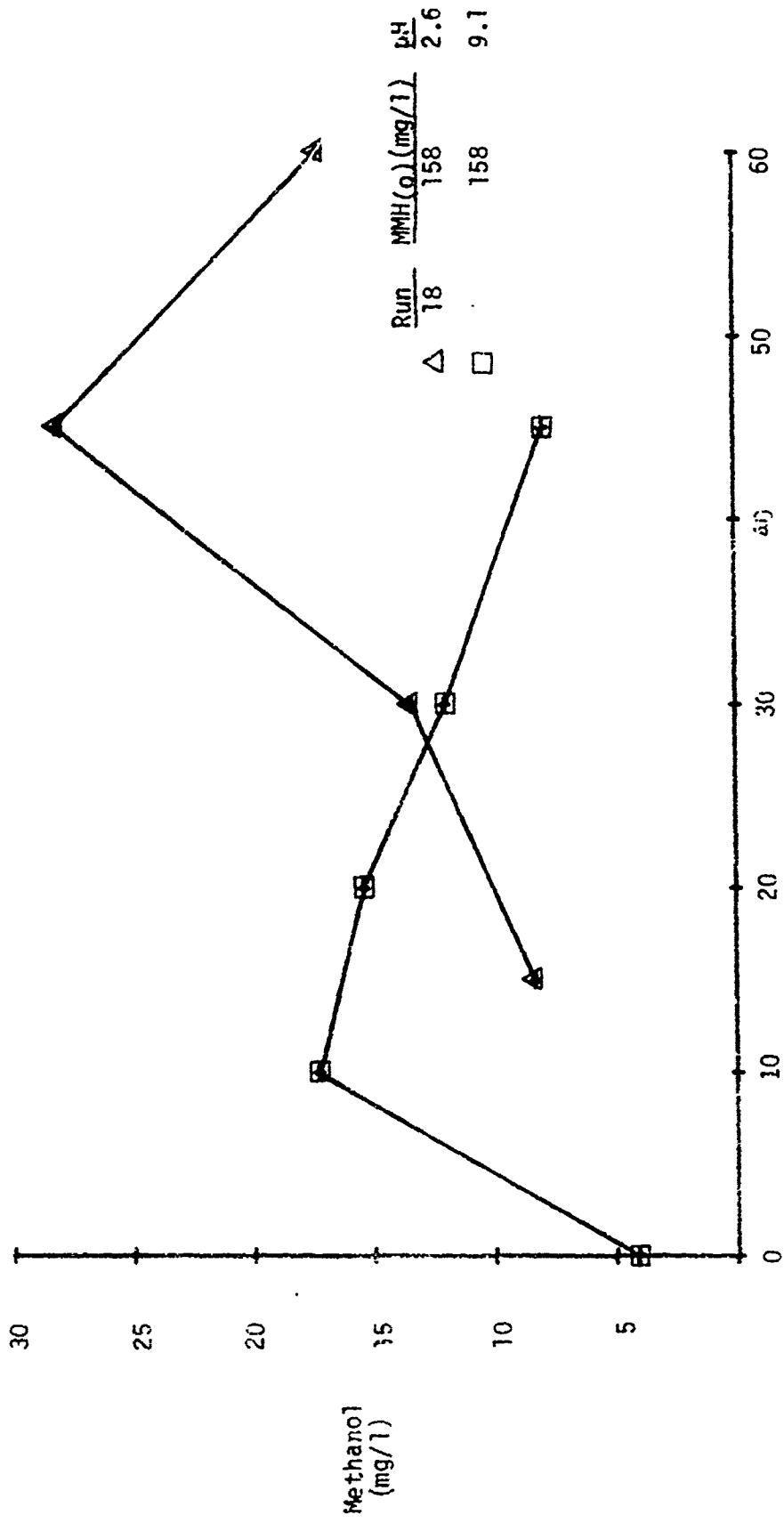
In Figure 19 are plotted the methanol concentrations found in these experiments versus time. When the solution pH was 9.1 the maximum observed concentration was 17.3 mg/l after 10 minutes of ozonation. From 10 through 45 minutes the methanol concentration decreased to 7.9 mg/l and at that time only 0.5 mg/l of MMH remained in solution. During R-18 the methanol concentration reached an observed maximum of 28.1 mg/l after 45 minutes of reaction time, then decreased to 17.2 mg/l over the next 15 minutes of ozonation. The fact that the observed peak production of methanol occurs at a later reaction time for the low pH (2.6) run than the high (9.1) pH run was expected based on the results plotted in Figure 18. Also Gollan et al. (11) have shown that methanol oxidation rates with ozone are enhanced at alkaline pH's. The difference in the peak concentrations of methanol could simply be due to the fact that in R-17 the maximum concentration occurred prior to the 10 minute reaction time sample.

Examination of the reactor off-gas data taken at the end of the run shows that with R-18, 16% of the inlet ozone left the LMTOC while for R-17 this value was only 4.5%. This phenomena, as previously discussed, is the result of ozone decomposition rate changes with pH.

#### b. Specie Concentration Effect

The initial concentration of MMH was 158, 505 and 1171 mg/l in R-17, R-14 and R-2. Maintaining reactor and ozonator conditions relatively constant for these runs, the disappearance of MMH was followed with ozonation time. The data for these runs is graphed in Figure 20.

For R-2, as seen in Figure 20, the reaction appears to proceed through three distinct stages. In the first stage, corresponding to the first 30 minutes of ozonation, the reaction is evidently severely ozone mass



REACTION TIME (MIN)

Figure 19. Methanol Production From the Ozone Oxidation of MMH at Two pH Levels



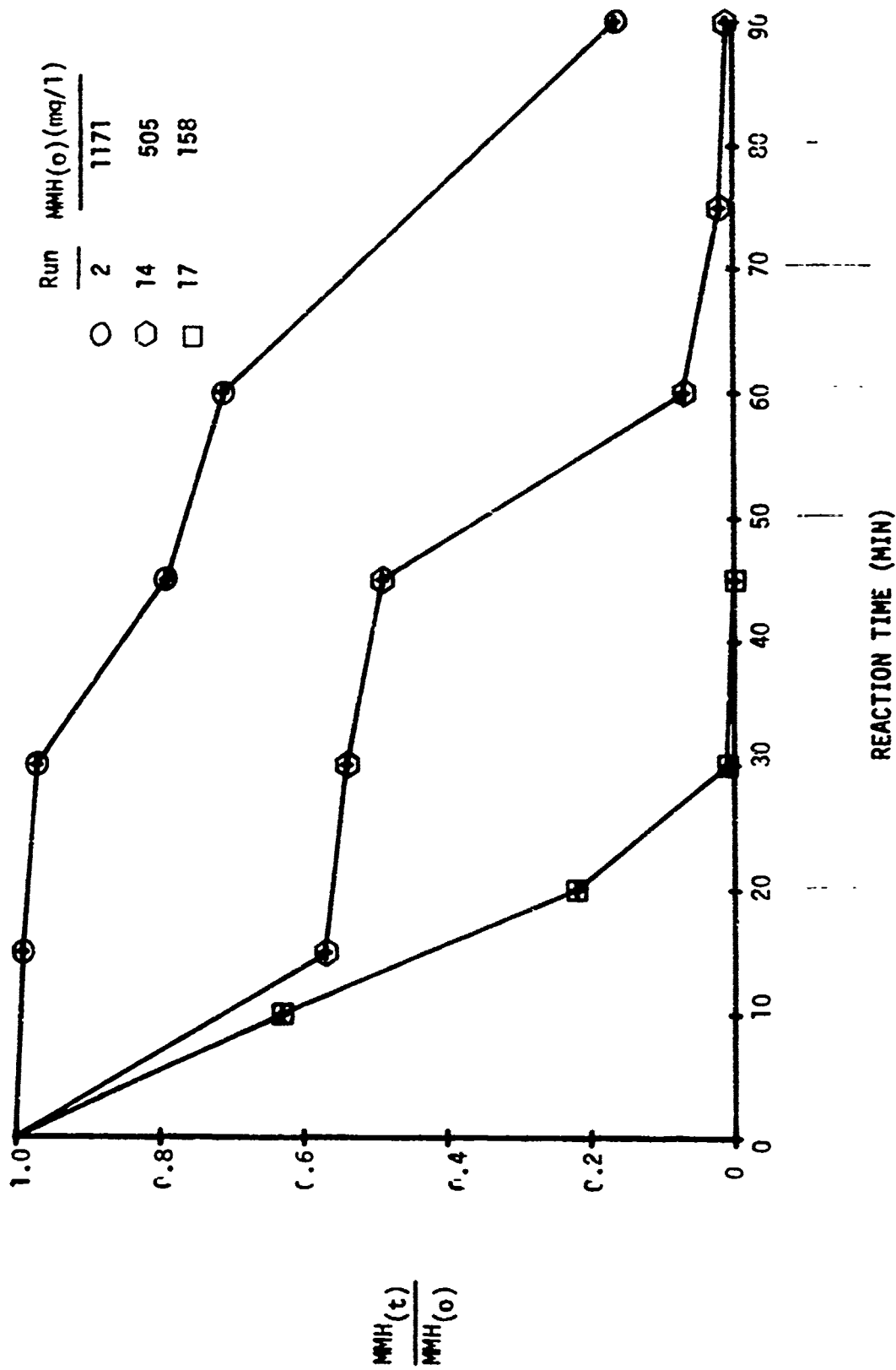


Figure 20. The Effect of Initial Concentration on the Ozone Oxidation of MMH

transfer limited. Stage two occurs from 30 to 60 minutes, and in this time period the LMTOC was approaching saturation at the prevailing operating conditions. Finally, in stage three the system appears to be operating under reaction rate conditions. The data from R-14 indicates the same responses, however, the time period for phase I is reduced. This was expected since the initial mass of MMH present was substantially reduced. Finally, in R-17 with the further reduction in MMH concentration the mass transfer limitations that existed previously were not present and this is reflected in the shape of the curve in Figure 20. These data received computer analysis according to the zero, first, and second order kinetics and are reported in Appendix D. Ignoring the limitations of mass transfer and applying the zero order kinetic model to the changes in MMH with ozonation time, the  $k$  (mg/l-min) values were 2.9, 6.5, and 6.4, and  $t_{1/2}$  (min) values were 20.8, 39.1, and 76.5 for R-17, R-14, and R-2, respectively.

Figure 21 is a plot of the methanol concentration as a function of ozonation time. It is evident from Figure 21 that the extent of methanol production is related to the concentration of MMH remaining in solution and ozonation time. It can be noted that at time zero, the methanol concentration is not zero. This is due to the manner in which the batch was charged into the reactor. While pumping the MMH from the solution feed tank (Figure 1) the reactor contents were air sparged. Since this procedure required approximately 8 minutes, a portion of the MMH was converted to methanol. Thus, as the initial concentration of MMH increased the alcohol production prior to the commencement of ozonation likewise increased. Finally, it should be noted that traces of methanol were found by gas chromatographic analyses of the original feedstock.

Methanol is oxidized by ozone at pH 9.1 in the presence of UV light, acting as a catalyst, to carbon dioxide and water by the following routes according to Chian (17).

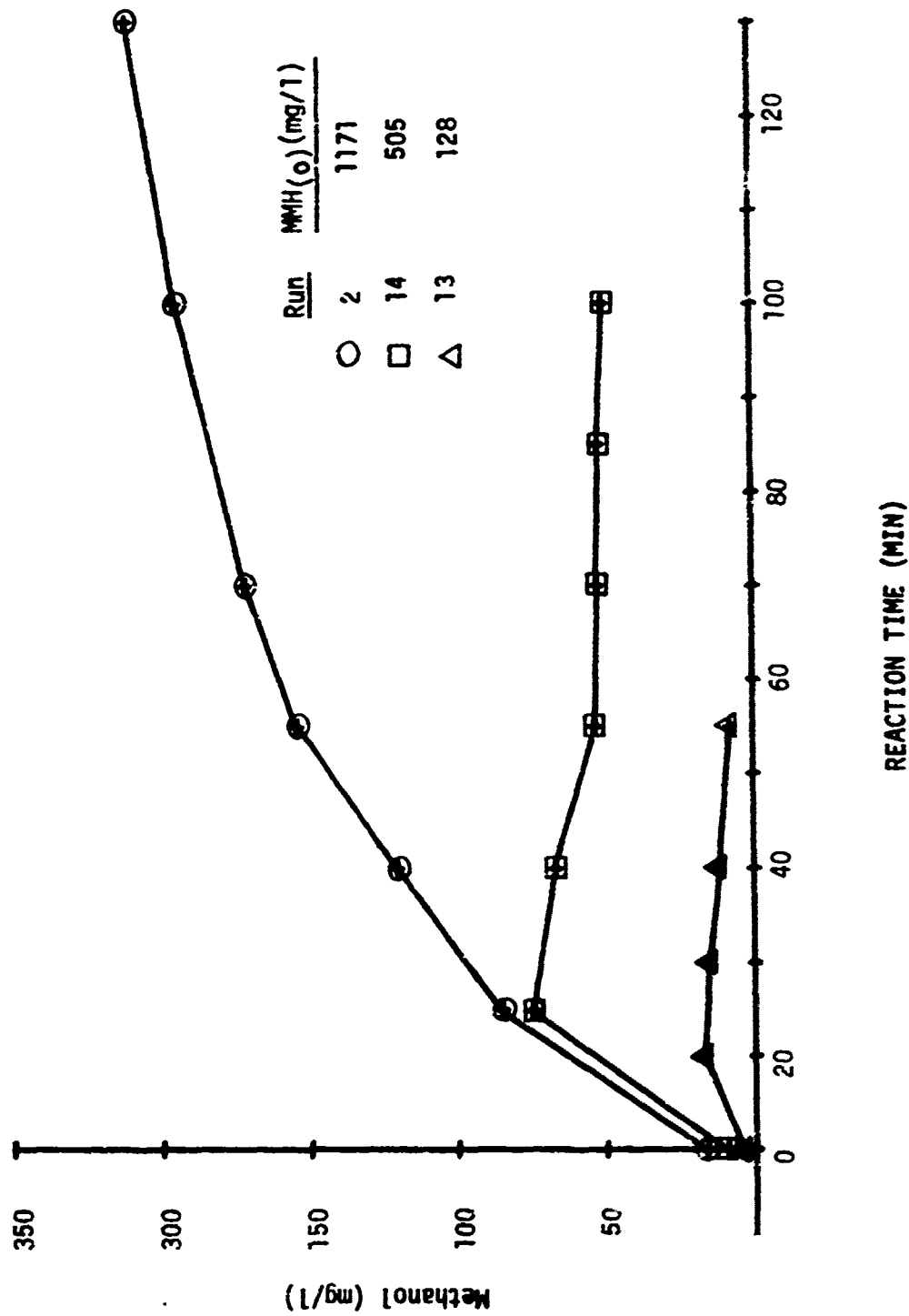
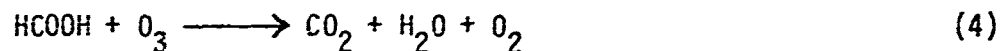
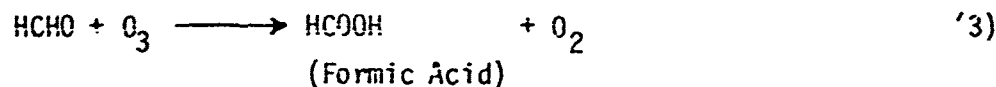
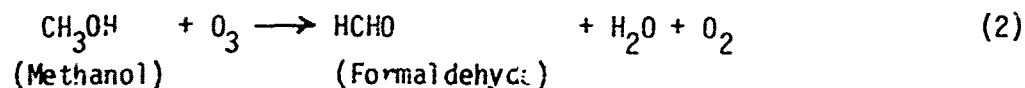


Figure 21. Methanol Production from the Ozone Oxidation of MMH as a Function of Initial Specie Concentration

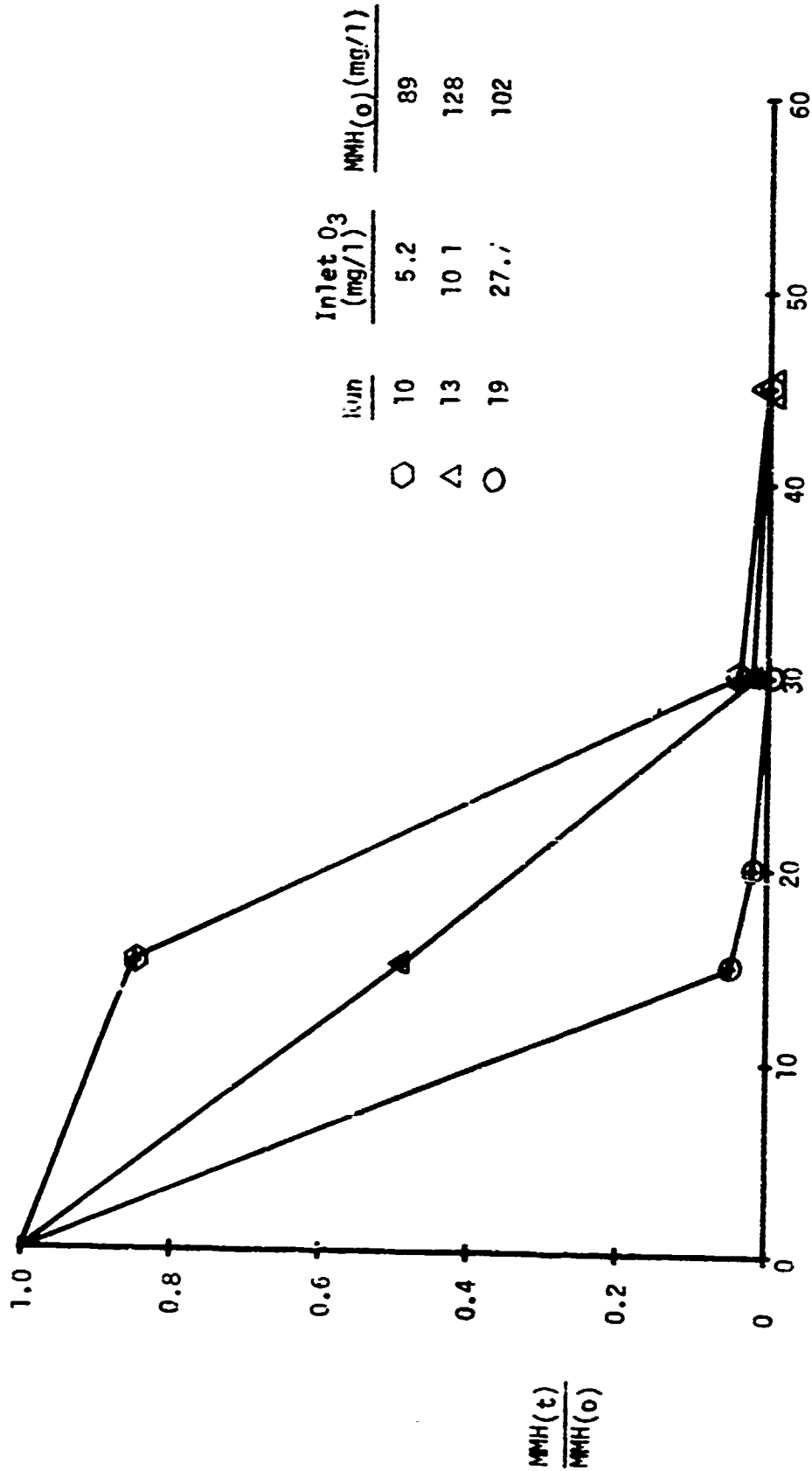


The fact that MMH was partially and not fully oxidized requires that consideration be given to extension of ozonation time after all MMH disappears. Methanol is relatively difficult to oxidize and unless a high pH and UV light is present within the reactor, the effluent would have an oxygen demand as measured by COD or biochemical oxygen demand (BOD). Thus, before this partially treated wastewater can be released to the environment, this problem must be resolved.

#### c. Ozone Partial Pressure

Three experiments R-10, R-13, R-19 were carried out with reactor inlet ozone concentrations of 5.2, 10.1 and 27.7 mg O<sub>3</sub>/l gas with all other reactor conditions virtually constant.

The data for these runs are plotted in Figure 22 and shows that MMH disappears rather readily for all runs regardless of ozone partial pressure conditions in the LMTOC, however, for R-10 the run is ozone mass transfer controlled for the first 15 minutes of reaction. The ease of MMH partial oxidation is predictable from the molecular properties of MMH, but as previously pointed out, methanol is produced as a reaction product and must be considered in reactor system design. In essence, the stoichiometry is more complicated than it would appear from the MMH oxidation data and kinetics. Information on the kinetics of MMH oxidation can be found in Appendix D. Employing the zero order model, the k values (mg/l-min) of 0.93, 3.33, and 5.20, and t<sub>1/2</sub> (min) values of 47.7, 19.8, and 9.8 were calculated for R-10, R-13 and R-19, respectively.



Run	Inlet O <sub>3</sub> (mg/l)	MMH(0) (mg/l)
10	5.2	89
13	10.1	128
19	27.7	102

REACTION TIME (MIN)

Figure 22. The Effect of Inlet Ozone Concentration on the Ozone Oxidation of MMH

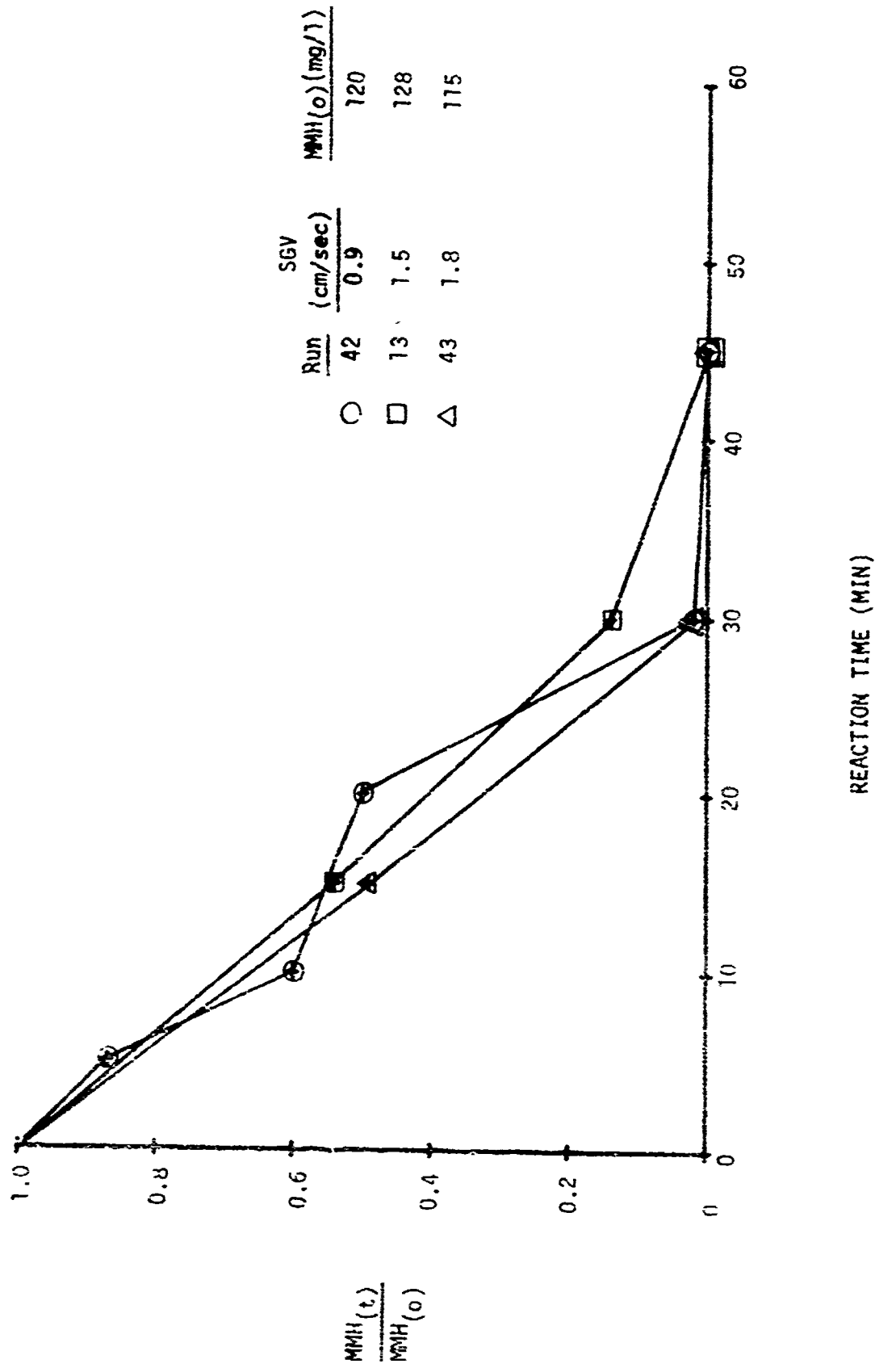


Figure 23. The Effect of Superficial Gas Velocity on the Ozone Oxidation of MMH

#### d. Superficial Gas Velocity Effect

To ascertain the effect of SGV on the ozone oxidation of MMH, three runs were performed at 20, 30 and 40 SCFH which corresponds to SGV values of 0.9, 1.5 and 1.8 cm/sec, respectively. The results of these runs (R-42, R-13 and R-43) are given in Figure 23.

The zero order kinetic model was applied to calculate the time required for complete destruction of MMH and together with the ozone mass flow rate data the ratio of mg H oxidized/mg  $O_3$  applied was calculated. For R-42, R-13 and R-43 the numerical values were 0.73, 0.70 and 0.51, respectively. While the first two values agree, the value obtained for R-43 is somewhat lower. This could be explained by the fact that the inlet ozone concentration was approximately 8% to 12% lower than in R-42 and R-13. The  $k_0$  values were 2.4, 3.3, and 3.0 mg/l-min and  $t_{1/2}$  values were 24.7, 19.2, and 19.3 min for runs R-42, R-13, and R-43, respectively.

#### e. Catalysts

The effect of the catalyst UV light and ultrasound were investigated in the LMTOC and OUR, respectively.

R-13 was performed with the UV light on in the LMTOC while in R-15 UV light was not employed. Figure 24 is a plot of the data from these runs and it shows the positive effect of UV as a catalyst. The zero order model predicts  $t_{1/2}$  (min) values of 19.2 and 26.2 and  $k$  (mg/l-min) constants of 3.33 and 2.27 for R-13 and R-15, respectively. The additional benefit of UV in the treatment of MMH is the enhanced oxidation rate for methanol. For example, in R-15 after 60 minutes of ozonation there still remained 11.6 mg/l of methanol while for R-13 only 5.2 mg/l was present in the LMTOC.

The reaction off-gas, measured near the end of the runs, contained 27.8% and 16.7% ozone for R-15 and R-13. This discrepancy is due to the presence and absence of UV light and the enhanced decomposition of dissolved ozone.

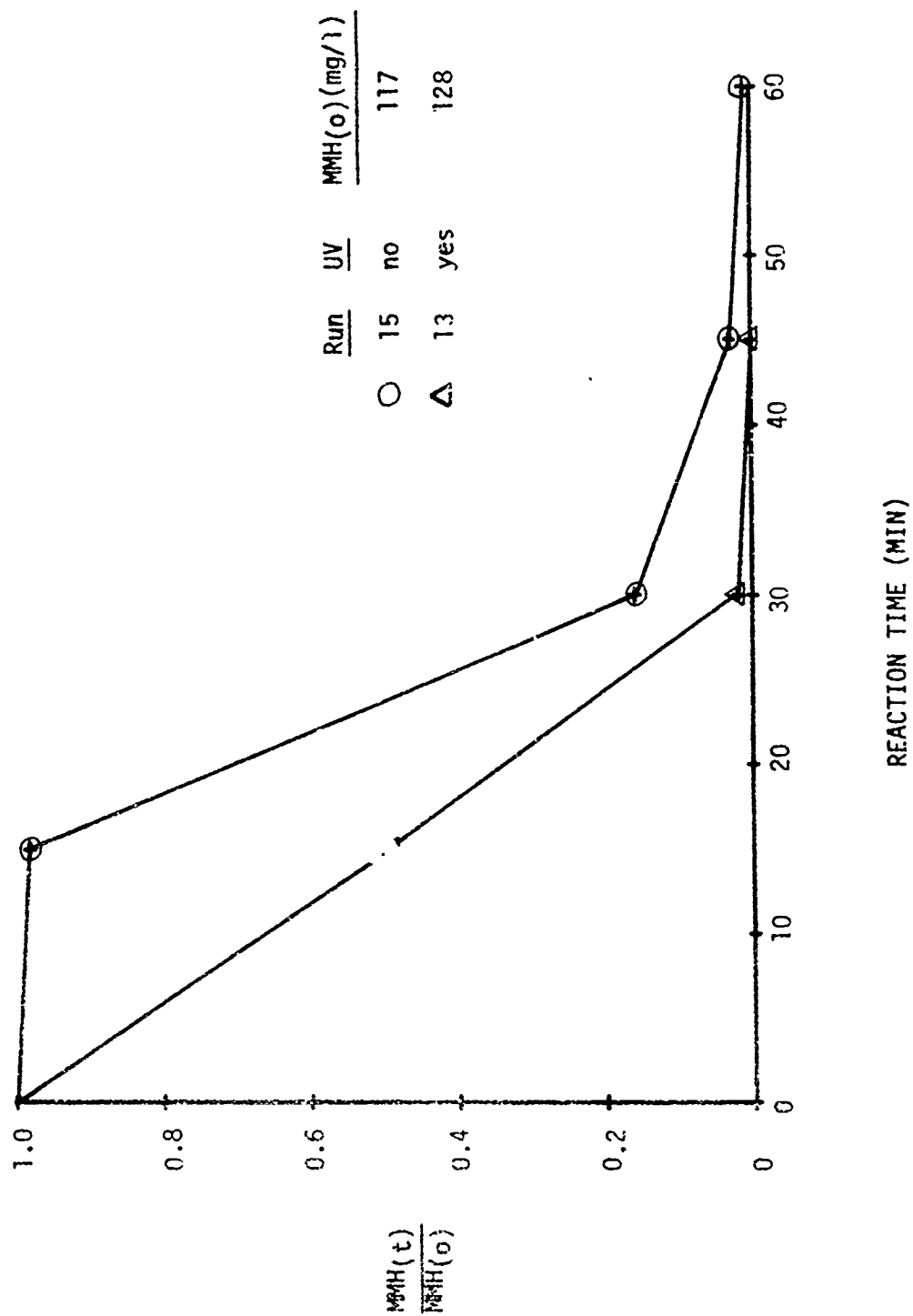


Figure 24. The Effect of Ultraviolet Light on the Ozone Oxidation of MMH



#### f. Characterization Run for Aquatic Toxicity

R-43 was performed to produce a large sample for aquatic toxicity studies. The criteria for run termination was total specie (MMH) disappearance, which occurred after 60 minutes of ozonation.

Plotted in Figure 25 is the change in MMH and COD with ozonation time. It should be noted that approximately 98% of the MMH was destroyed after 30 minutes of ozonation and up to that time the COD destruction rate was constant. From 30 to 60 minutes, the COD destruction rate was reduced. This is due to the changing nature of the reaction-produced organics undergoing ozone oxidation.

The change in methanol and VOC concentration for R-43 is plotted in Figure 26. The data indicated that methanol production is maximized after 15 minutes of ozonation. Since the oxidation of methanol by ozone proceeds more slowly than MMH, the reduced COD destruction rate, from 30 to 60 minutes, is due to the presence of this alcohol.

During the course of this run nitrate concentration increased in the reactor to 2.5 mg/l after 60 minutes of batch ozonation.

#### g. Oxygen Sparging of Monomethylhydrazine

Oxygen sparging of aqueous MMH solutions were performed in the presence (R-21) and absence of UV light (R-24) and the results of the runs are presented in Figure 27.

The  $t_{1/2}$  estimated from Figure 27 is 20 minutes for the run with UV while in R-24 virtually no reduction of MMH occurred. These findings were substantiated in R-25 when air was substituted for pure oxygen and the experiment duplicated, with the end results being identical to R-21. One air sparging run, in the absence of ultrasound, was performed in the OUR (R-26) and 13% of the MMH was removed. This increased removal was probably

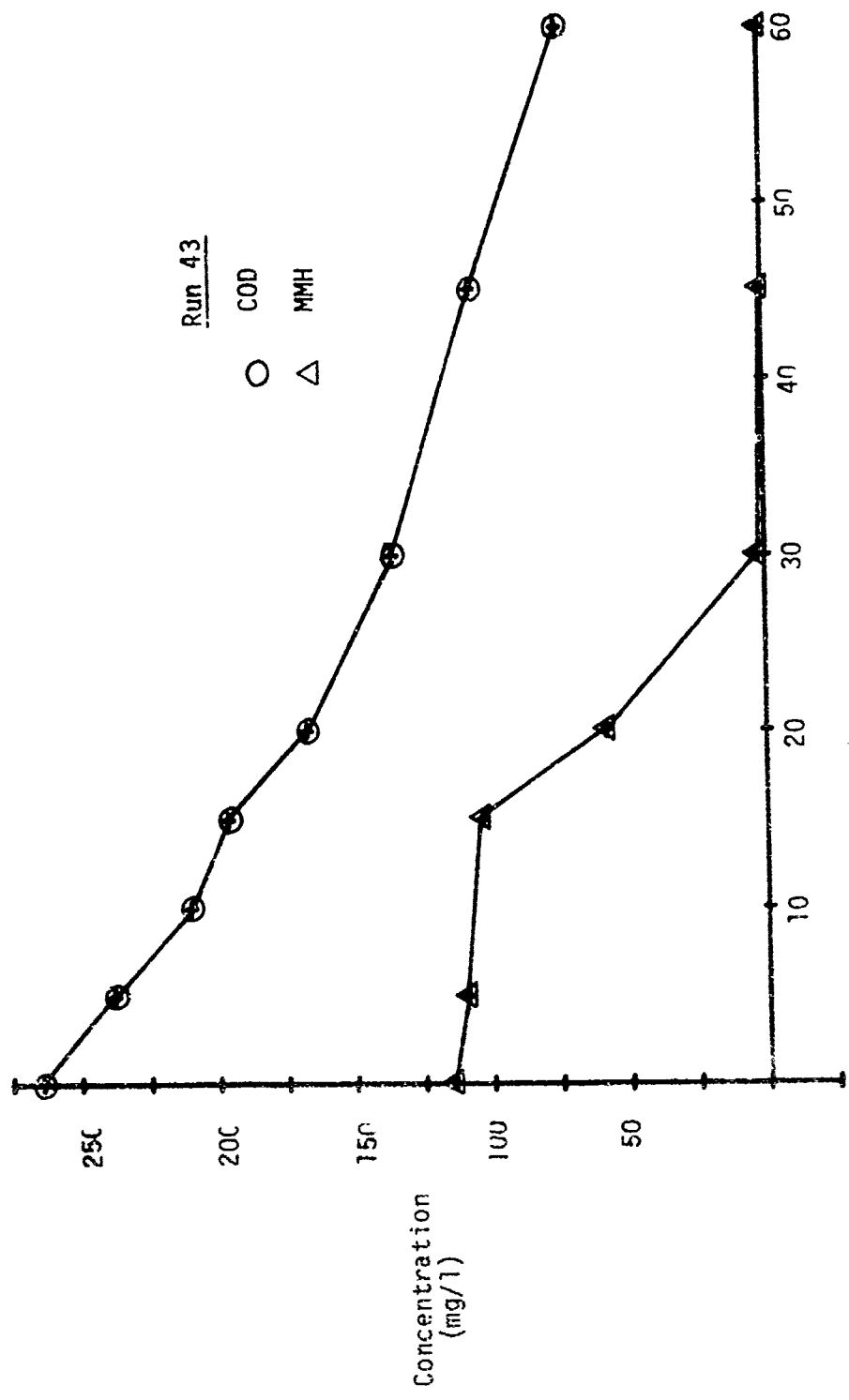


Figure 25. The Destruction of MMH and COD by Ozone Oxidation

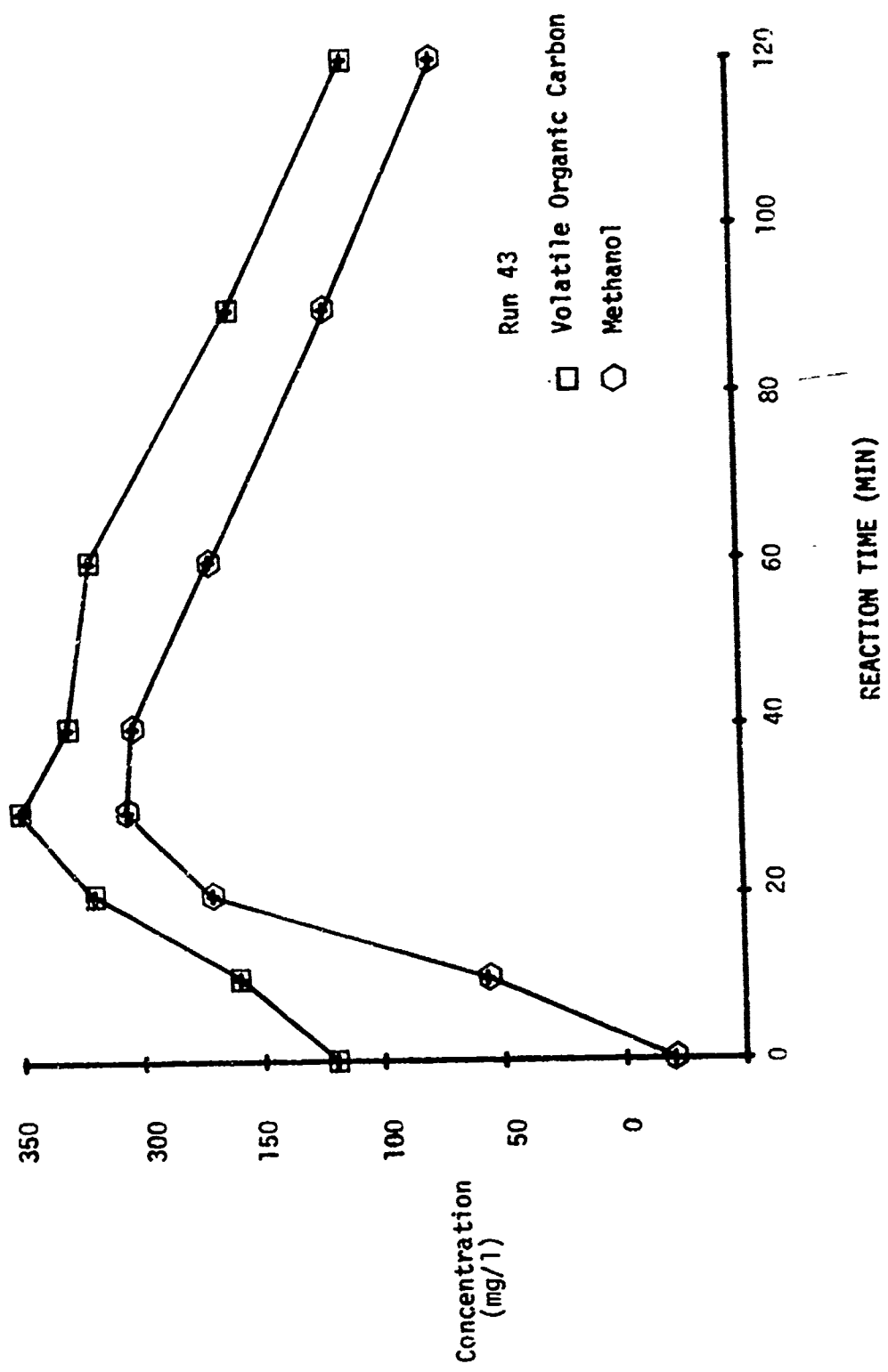
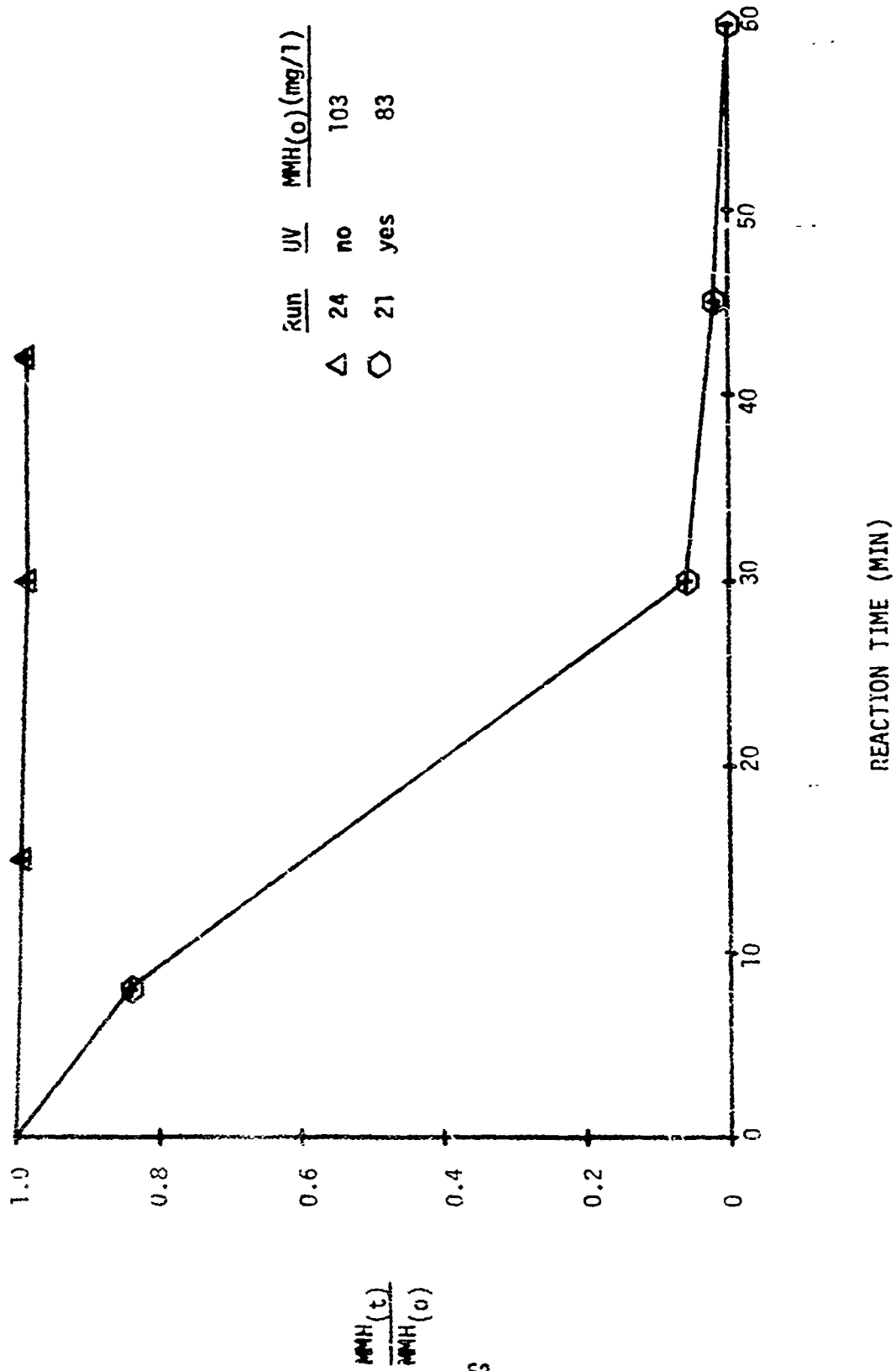


Figure 26. The Change in Volatile Organic Carbon During the Ozone Oxidation of MMH



$\bar{x}_{run}$	UV	$\frac{MMH(o)}{(mg/l)}$
24	no	103
21	yes	83

Figure 27. The Effect of Ultraviolet Light on the Oxygen Sparging of MMH

The  $t_{1/2}$  estimated from Figure 27 is 20 minutes for the run with UV while in R-24 virtually no reduction of MMH occurred. These findings were substantiated in R-25 when air was substituted for pure oxygen and the experiment duplicated, with the end results being identical to R-21. One air sparging run, in the absence of ultrasound, was performed in the OUR (R-26) and 13% of the MMH was removed. This increased removal was probably due to the increased volume of air passed through the OUR and a higher overall mass transfer coefficient ( $K_L a$ ).

## 5. UNSYMMETRICAL DIMETHYLHYDRAZINE

### a. pH Effect

Two runs (R-39 and R-29) were performed at an acidic pH (3.8) and an alkaline pH (9.1) respectively, and the conversion of UDMH monitored with ozonation time. These data are plotted in Figure 28.

In R-29 all of the UDMH had been oxidized within 60 minutes yet 36% of the UDMH remained in solution in R-39 at that time.

The data from all UDMH runs were analyzed by computer modeling for zero, first, second, and half-order kinetics and are reported in Appendix D. It has been shown (18) that the oxidation reaction between UDMH and oxygen follows half-order reaction kinetics. Further, it has been demonstrated that the oxidation is highly pH dependent. In basic solutions, the reaction proceeds quickly, while at acidic conditions it almost stops.

The same general trend with pH was in evidence in this study when ozone was used as the oxidant, although not to the extent of that seen with oxygen under acidic conditions. For example, using the half-order model, the  $k_{1/2}$  [(mg/l)<sup>0.5</sup>/min] values were 0.47 and 0.22 for R-29 and R-39, respectively, while the  $t_{1/2}$  (min) values were 19.9 and 42.4.

Using these kinetic data, the mg UDMH oxidized/mg  $O_3$  applied was 0.26 and 0.73 for R-39 and R-29 to the point of total UDMH oxidation.

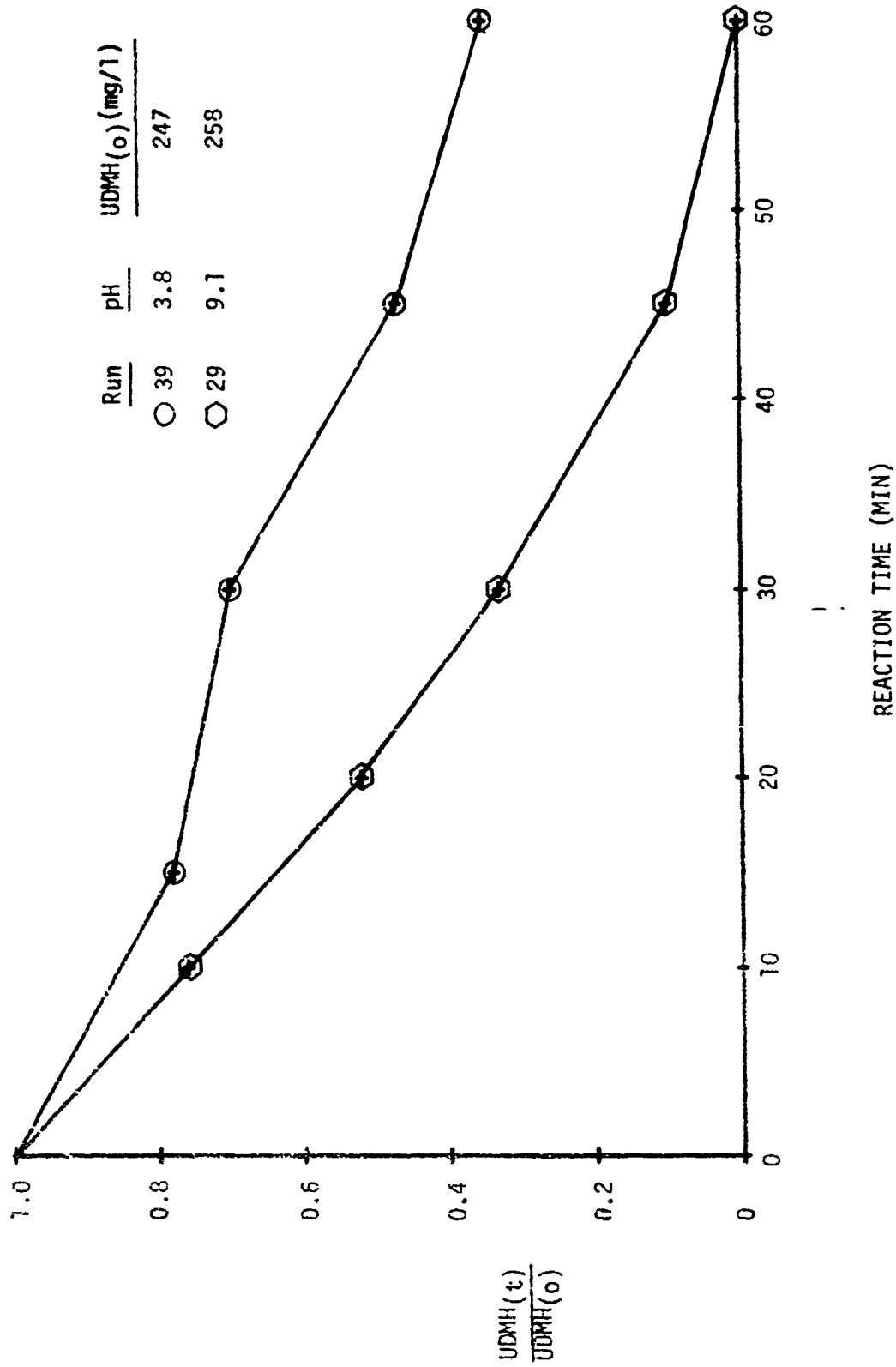


Figure 28. The Effect of pH on the Ozone Oxidation of UDMH

### b. Specie Concentration Effect

The effect of initial concentration on the ozone oxidation of UDMH was studied in four experiments R-27, R-29, R-32 and R-30 where the initial concentration of UDMH was 112, 258, 510 and 953 mg/l. The data are graphed in Figure 29.

Employing the one-half order kinetic model,  $k [(mg/l)^{0.5}/min]$  values of 0.55, 0.47, 0.48 and 0.29 for R-27, R-29, R-32 and R-30 and the  $t_{1/2}$  (min) values were 11.3, 19.9, 27.5 and 62.9, respectively.

Using the half-order model constant values above, the mg UDMH oxidized at that point in the reaction/mg  $O_3$  applied were calculated to be 0.56, 0.70, 1.03, and 0.82 for R-27, R-29, R-32 and R-30.

### c. Ozone Partial Pressure

In R-35, R-29 and R-36 the inlet ozone concentration to the LMTOC was 4.42, 9.83 and 30.1 mg  $O_3$ /l gas. All other operational parameters remained the same for these three runs. The resulting data, graphed in Figure 30, permitted examination of the effect of ozone partial pressure on the reaction rate.

Basically, increasing the inlet ozone concentration yielded progressively higher  $k_{1/2} [(mg/l)^{0.5}/min]$  values of 0.21, 0.47 and 0.77 for R-35, R-29 and R-36. Likewise the  $t_{1/2}$  constants were reduced. In R-35, R-29 and R-36, the  $t_{1/2}$  (min) values were 42.3, 19.9 and 11.3, respectively.

Projecting the time to zero UDMH concentration with the above kinetic data, yielded 0.78, 0.73 and 0.40 mg UDMH oxidized/mg  $O_3$  applied for R-35, R-29 and R-36, respectively. The 0.40 value is low because at the high inlet ozone concentration ozone cannot be transferred sufficiently quickly to the solution and leaves the reactor in the off-gasses. However, as the  $t_{1/2}$  values attest, the amount of hydraulic residence time required is reduced as ozone partial pressure is increased.

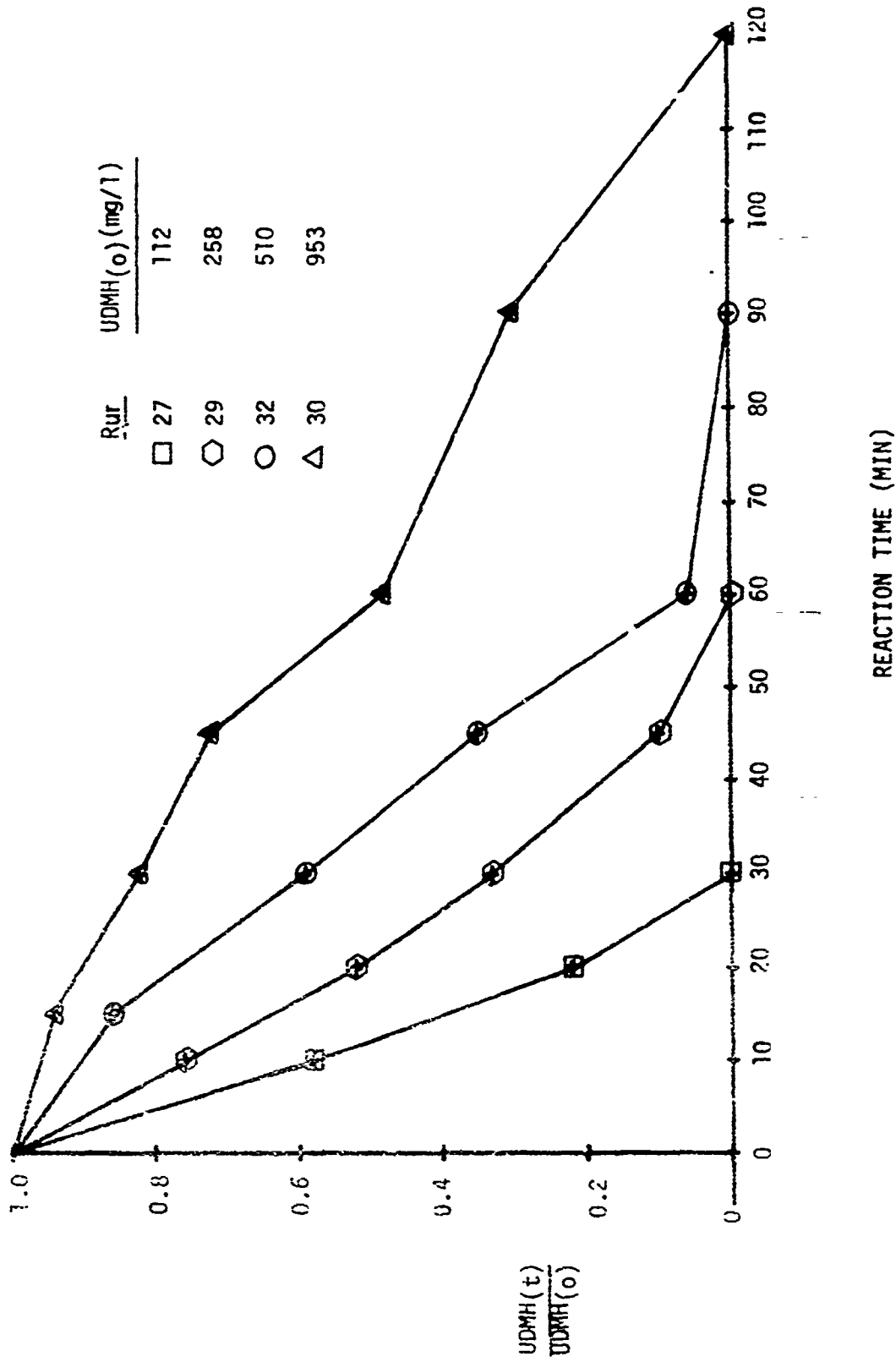


Figure 29. The Effect of Initial Concentration on the Ozone Oxidation of UDMH



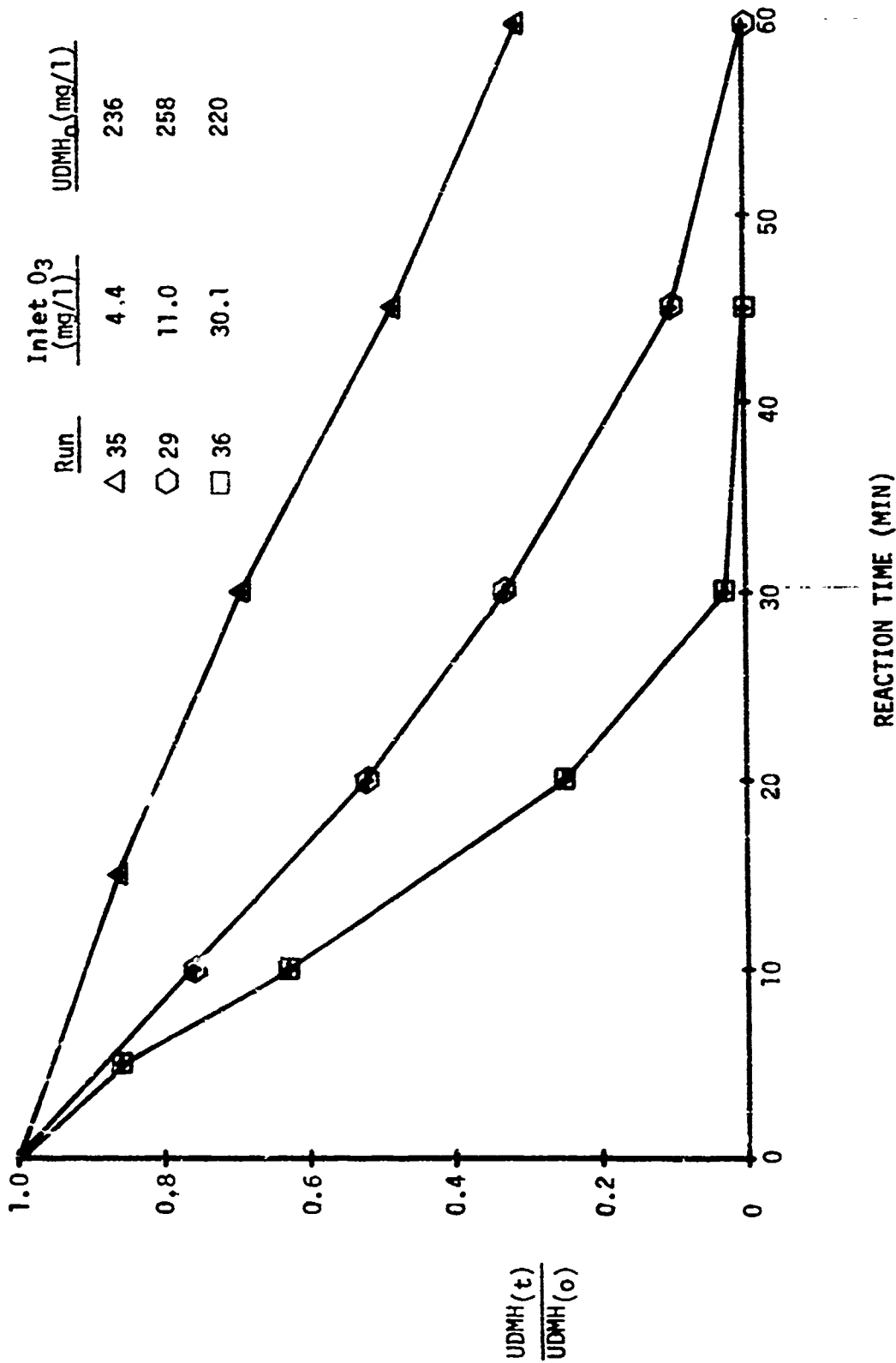


Figure 30. The Effect of Inlet Ozone Gas Concentration on the Ozone Oxidation of UDMH

#### d. Superficial Gas Velocity Effect

The effect of SGV was studied in R-38, R-29 and R-37. For these runs, the SGV values were 0.9, 1.5 and 1.8 cm/sec corresponding to 20, 30 and 40 SCFH of gas flow rate to the LMTOC. UDMH concentration as a function of time is plotted in Figure 31 for each of these runs.

Assuming the half-order kinetic model applies to these data the derived  $k_{1/2}$  values were 0.36, 0.47, 0.31 for R-38, R-29 and R-37, respectively and the  $t_{1/2}$  values were 24.5, 19.9 and 17.3.

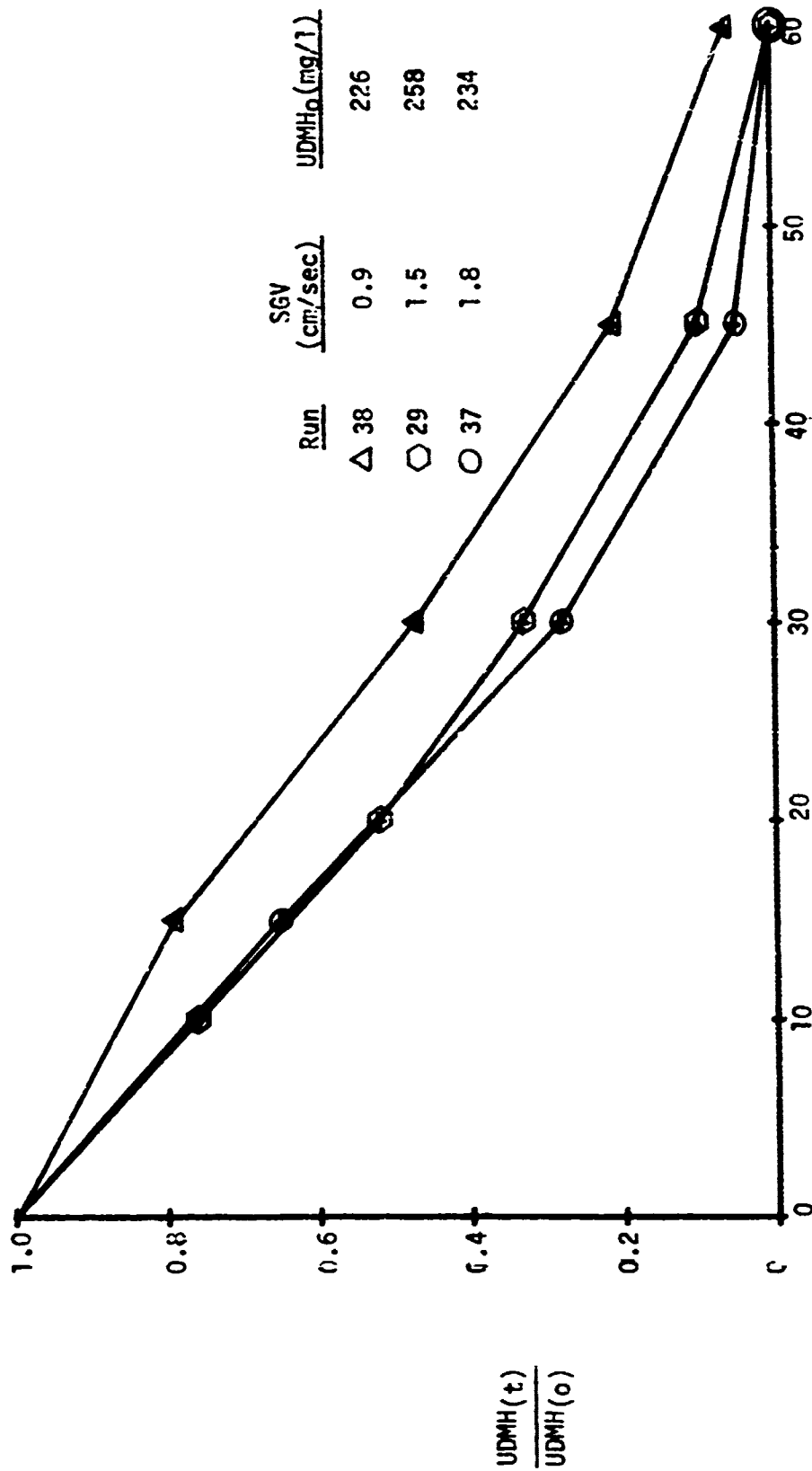
Calculating the mass of UDMH oxidized to zero concentration per mass of ozone applied for R-38, R-29 and R-37 gave 0.75, 0.73 and 0.62, respectively. The relatively good agreement among these values is expected since SGV at constant ozone partial pressure and reactor operating conditions should give the same mg UDMH oxidized/mg  $O_3$  applied data. The discrepancies noted above are the result of deviation from these assumptions.

#### e. Catalysts

The effect of the catalysts UV light and ultrasound were investigated in the LMTOC and the OUR, respectively.

The effect of UV light can be assessed by examining the data, from R-29 (UV light) and R-31 (no UV light), which is graphed in Figure 32. The effect of UV light as a catalyst is positive as seen by the  $k$  [(mg/l)<sup>0.5</sup>/min] values of 0.47 and 0.34 and the  $t_{1/2}$  (min) values of 19.2 and 26.2 for the run with UV light versus the run without UV light.

The mg UDMH oxidized/mg  $O_3$  applied for R-29 and R-31 were 0.73 and 0.46, respectively. These figures were calculated from the kinetic model constants discussed above.



REACTION TIME (MIN)

Figure 31. The Effect of Superficial Gas Velocity on the Ozone Oxidation of UDMH

$$\frac{\text{UDMH}(t)}{\text{UDMH}(o)}$$

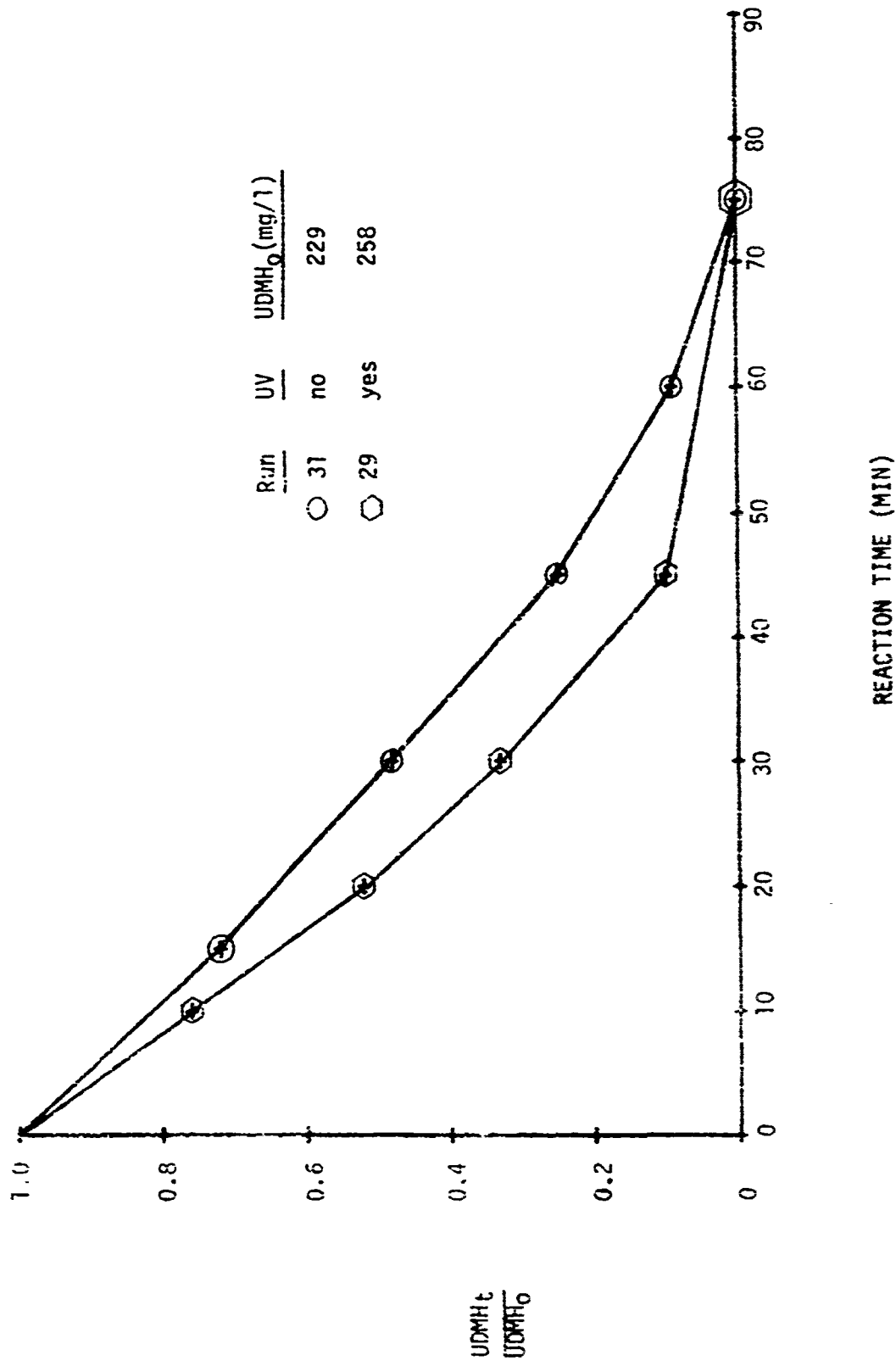


Figure 32. The Effect of Ultraviolet Light on the Ozone Oxidation of UDMH

The effect of ultrasound on the kinetics of ozone oxidation of UDMH was studied in R-33 (ultrasound) and R-34 (no ultrasound). These data, which are plotted in Figure 33, show that ultrasound is not particularly effective as a catalyst.

Assuming one half-order kinetics, the  $k$  [(mg/l)<sup>0.5</sup>/min] values are 1.71 and 1.54 for R-33 and R-34 while the  $t_{1/2}$  values were 7.5 and 8.0 min respectively. Calculating the mg UDMH oxidized/mg O<sub>3</sub> applied to zero UDMH concentration gave 0.62 and 0.48 for R-33 and R-34, respectively. The improved utilization of ozone in the presence of ultrasound is principally due to improved gas mass transfer caused by the action of ultrasonics. These sound waves reduce bubble coalescence and reduce the liquid film resistance which partially explains this benefit.

Since these runs were performed in the OUR, which is constructed of pyrex glass, it was possible to note color changes in the batch as a function of time. The following comments apply equally to R-33 and R-34.

At time zero, the UDMH batch was colorless, however, within 1 min of ozonation the reactor contents changed from colorless to a pink color. During the next minute, the batch assumed a more intense pink color. This condition remained until 17 minutes into the run, when the color began to change to a brownish-pink. At 20 minutes the color of the reactor contents turned to a light brown and simultaneously ozone appeared in the OUR off-gas. At 25 minutes into the experiment, the batch turned a light green. This color became less intense with time as the ozonation proceeded to the termination of the run at 60 minutes.

Two other observations should be made regarding these runs. First, the appearance of ozone in the OUR off-gas coincides with the loss of the pink color and the fact that less than 5% of the initial UDMH concentration remained in solution at that time. In both R-33 and R-34, all UDMH in the batch was oxidized at between 20 and 30 minutes of ozonation. Second, on

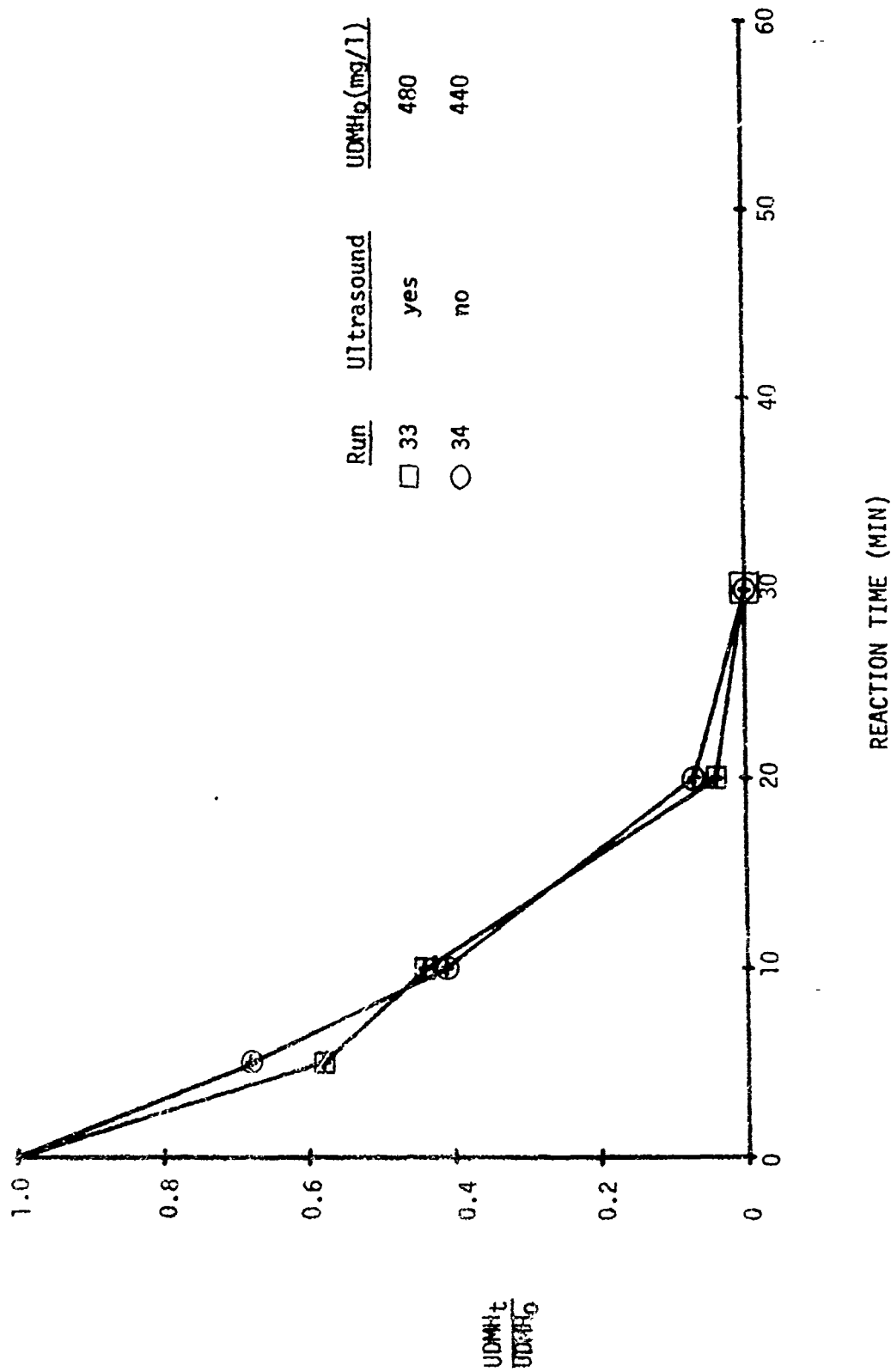


Figure 33. The Effect of Ultrasonics on the Ozone Oxidation of UDMH

standing (less than 2.0 minutes) the samples taken from the OUR lost their color. Finally, during the course of this project, a 100 mg/l batch of UDMH was ozonated in the OUR, but no color changes were noted. Therefore, it appears that to visually observe color change, in the ozone oxidation of UDMH, the initial specie concentration must be between 100 and 440 mg/l (R-34). R-60 was performed with an initial concentration of 5,600 mg/l and samples analyzed by a UV spectrophotometer between 200 and 400 min. These data can be found in Appendix C.

#### f. Characterization Run

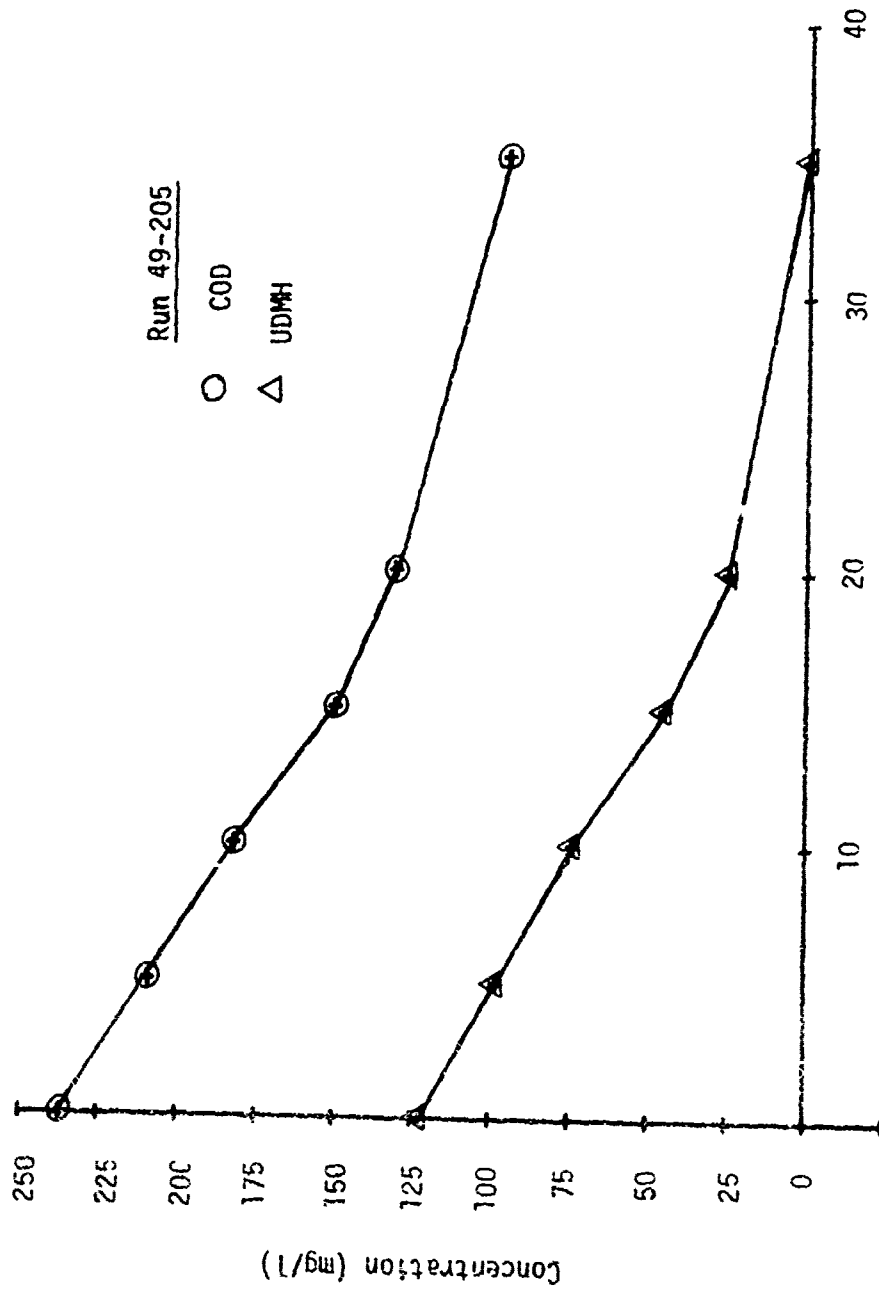
R-49-205 was performed to produce an effluent for aquatic toxicity studies. This batch contained 122 mg/l of UDMH and was ozonated for a period of 35 minutes. At that time, ozone was found in the reactor off-gas and chemical analyses indicated that all UDMH had been oxidized.

Plotted in Figure 34 are the UDMH and COD data for R-49-205. The data indicate that the rate of destruction of COD and UDMH were essentially the same from approximately 0 through 20 minutes of ozonation, then with the buildup of reaction by-products, the rate of COD destruction was reduced. During this run, the batch TOC was reduced from 54 to 37 mg/l and nitrate-N increased from 0 to 7.2 mg/l. Methanol concentration increased continuously but to only 6.0 mg/l after 35 minutes of ozonation.

The  $k$  [(mg/l)<sup>0.5</sup>/min] and  $t_{1/2}$  (min) constants for the zero order kinetics model were 0.63 and 10.2. Using these constants the calculated mg UDMH oxidized/mg O<sub>3</sub> applied was 0.62.

#### g. Air Sparging of Unsymmetrical Dimethylhydrazine

The effect of sparging air through aqueous solutions of UDMH in the presence and absence of UV light was studied in R-41 and R-40. The data are plotted in Figure 35.



REACTION TIME (MIN)

Figure 34. The Destruction of UDMH and COD by Ozone Oxidation



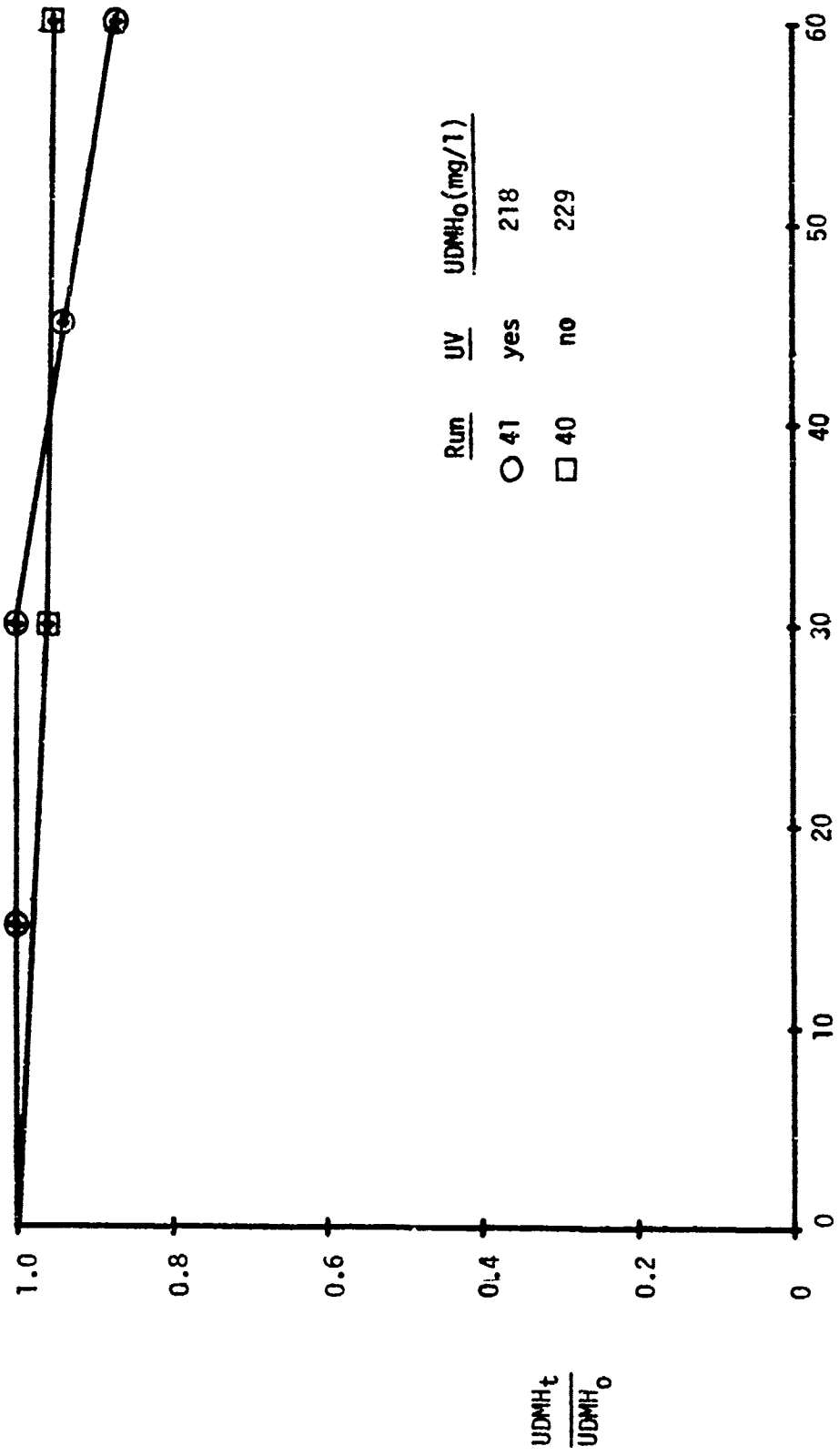


Figure 35. The Effect of Ultraviolet Light on the Air Sparging of UDMH

In the presence of UV light 14% of the UDMH was removed (R-41) while only 5% of the UDMH in R-40 was converted in 60 minutes of sparging. The  $k$  [(mg/l)<sup>0.5</sup>/l) values are 0.023 and 0.014 and  $t_{1/2}$  (min) values of 377 and 630 for R-41 and R-40, respectively.

## SECTION V

### CONCLUSIONS

#### 1. pH

Increasing solution pH increases the rate of ozone oxidation of H, MMH and UDMH. Ozonation of hydrazine at pH 3.1 yielded about twice the amount of Nitrate-N as compared with the 9.1 pH run.

#### 2. Specie Concentration Effect

Increasing specie concentration, at fixed reactor operating conditions of pH, catalyst type, ozone partial pressure and superficial gas velocity, increases the required hydraulic retention time to achieve a desired effluent concentration for all three hydrazine fuels. The amount of methanol produced from the ozone oxidation of MMH is proportional to specie concentration.

#### 3. Ozone Partial Pressure

Increasing ozone partial pressure decreases the  $t_{1/2}$  values for H, MMH and UDMH, but the efficiency of ozone utilization is reduced.

#### 4. Superficial Gas Velocity Effect

Increasing SGV decreases the  $t_{1/2}$  values at constant ozone partial pressures and reactor operating conditions.

## 5. Catalyst

The presence of UV light in the reactor reduces  $t_{1/2}$  values and increases reaction rates for M, MMH and UDMH oxidation by ozone over the corresponding no UV light reaction. This effect is very small with H as the substrate.

Ultrasound as a catalyst when compared with the no sound, under the experimental conditions tested, gave mixed results yet the overall rate of ozone oxidation of hydrazine in the OUR was improved over the LMTOC runs.

## 6. Air Sparging of H, MMH and UDMH

The decomposition of MMH during oxygen or air sparging is dramatically enhanced by the presence of UV light. The same trend occurs with H and UDMH however not to the degree noted with MMH.

## REFERENCES

1. See, G.G., K.K. Kacholia and T.S. Steenson, "Research and Development of an Ozone Contactor for the Oxidation of Refractory Organics," Proc. Forum on Ozone Disinfection, Int. Ozone Institute, Chicago, IL (1976).
2. See, G.G., P.Y. Yang and K.K. Kacholia, "Research and Development of an Ozone Contactor System," Final Report to U.S. Army Research and Development Command, Contract DAMD 17-76-C-6041 (1976).
3. Sierka, R.A., "Mass Transfer and Reaction Rate Studies of Ozonated MUST Wastewaters in the Presence of Sound Waves," U.S. Army Medical Research and Development Command Contract DAMD 17-76-C-6057, Final Report (1976).
4. Standard Methods for the Examination of Water and Wastewater, 14th Ed., American Public Health Association, Washington, DC (1976).
5. Shechter, H., "Spectrophotometric Method for Determination of Ozone in Aqueous Solutions," Water Research, 7, 729 (1973).
6. Watt, G.W. and J.D. Chrisp, "Spectrophotometric Method for the Determination of Hydrazine," Anal. Chem., 24, 2006 (1952).
7. Pinkerton, M.K., J.M. Lauer, P. Diamond and A.A. Tamas, "A Colorimetric Determination for 1,1-Dimethyl-hydrazine (UDMH) in Air, Blood and Water," J. Am. Ind. Hyg. Assoc., 24, 239 (1963).
8. Jirka, A.M. and M.J. Carter, "Micro Semi-Automated Analysis of Surface and Wastewaters for Chemical Oxygen Demand," Anal. Chem., 47, 1397 (1975).
9. Methods for Chemical Analysis of Water and Wastes, U.S. EPA National Environmental Research Center, Cincinnati, Ohio (1974).

10. Hogben, D., S.T. Peavy and R.N. Varner, "Omnitab II User's Reference Manual," NBS Technical Note 552, National Bureau of Standards, Gaithersburg, MD (1971).
11. Gollan, A.Z., K.J. McNulty, R.L. Goldsmith, M.H. Kleper and D.C. Grant, "Evaluation of Membrane Separation Processes, Carbon Adsorption, and Ozonation for Treatment of MUST Hospital Wastes," Final Report on Contract DAMD 17-74-C-4066 to U.S. Army Medical Research and Development Command (1976).
12. McCarthy, J.J., W.F. Cowen, E.S.K. Chian and B.W. Peterman, "Evaluation of an Air Stripping-Ozone Contactor System," U.S. Army Medical Bioengineering Research and Development Laboratory, Technical Report 7707 (1977).
13. Chang, B.J., A Model Study of Ozone-Sparged Vessels for the Removal of Organics from Water and Wastewater, Ph.D. Thesis (Civil Engineering), University of Illinois, Urbana-Champaign (1978).
14. Stumm, W., "Ozone as a Disinfectant for Water and Sewage," J. Boston Soc. Civ. Eng., 45, 68 (1958).
15. Yoshida, F. and K. Akita, "Performance of Gas Bubble Columns: Volumetric Liquid-Phase Mass Transfer Coefficient and Gas Holdup," AICHE J., 11, 9 (1965).
16. Bowen, E.J. and A.W. Birley, "The Vapor Phase Reaction Between Hydrazine and Oxygen," Transactions of the Faraday Society, 47, 580 (1951).
17. Chian, E.S.K. and P.K. Kuo, "Fundamental Study on the Post Treatment of RO Permeates from Army Wastewaters," Second Annual Summary Report to U.S. Army Medical Research and Development Command, Contract DAMD 17-75-C-5006 (1976).

18. Gormley, W.T. and R.E. Ford, "Deoxygenation of Environmental Waters by Hydrazine-Type Fuels," Proc. Ann. Conf. Environ. Toxicol., Fairburn, OH, Oct., 387 (1973).
  
19. Lysenko, T.F., L.F. Atyaksheva, B.V. Strakhov and G.I. Emel'yanova, "Kinetics and Mechanism of the Oxidation by Ozone of 1,1-Dimethylhydrazine in Aqueous Solution," Translation in Russian J. Physical Chemistry, 49, 1849 (1975).

APPENDIX A  
REACTOR OPERATIONAL DATA

Table A-1. Hydrazine Data

Table A-2. Monomethylhydrazine Data

Table A-3. Methanol Concentrations in MMH Ozonations

Table A-4. Unsymmetrical/Dimethylhydrazine Data

Table A-5. Nitrate Concentrations in Hydrazine Ozonations\*

\* For the aquatic toxicity run with hydrazine (R-70) characterization see data in Table A-6.

TABLE A-1. HYDRAZINE DATA

Run #	Initial pH	Reactor	Catalyst	O <sub>3</sub>		SGV cm/sec	Hydrazine Conc. (mg/L)										
				In mg O <sub>3</sub> /l	Out gas		0	5	10	15	20	30	45	60	75	90	
44	9.1	LMTOC	UV	10.8	2.8	1.5	139	106	74	37	<0.05	0.05					
45	9.2	LMTOC	UV	12.6	0.4	1.5	432		384	322	246	172	84				
51	9.1	LMTOC	None	11.0	8.5	1.5	125	93	62	30	<0.05	0.05					
56	3.1	LMTOC	UV	11.6	2.2	1.5	150		137	128	113	98					
54	9.1	LMTOC	UV	-	-	1.5	133		130	120	102	87					
52	9.1	LMTOC	UV	11.0	0.6	0.9	138	114	90	60	9	0.05					
53	9.1	LMTOC	UV	9.7	2.4	1.8	137	94	47	9	<0.05						
49	9.1	LMTOC	UV	4.4	0.2	1.5	138	112	83	54	18	<0.05					
50	9.1	LMTOC	UV	30.0	7.4	1.5	126	87	47	11	<0.05	<0.05					
55	9.2	LMTOC	None	-	-	1.5	132		126	119	112	107					
57	9.4	LMTOC	UV	13.0	0.0	1.5	5600		5400	4900	4750	4200					
46	9.2	LMTOC	UV	13.1	0.0	1.5	785	750	690	630	550	460					
47	9.2	OUR	Ultrasound	9.2	0.7	1.5	705	625	525	270	65	<0.05*					
48	9.2	OUR	None	13.3	1.0		730	600	465	340	200	33	<0.05*				

NOTE: \* Run # 47 is 39 min.  
48 is 38 min.



TABLE A-2. MONOMETHYLHYDRAZINE DATA

Run #	Initial pH	Reactor	Catalyst	In <sup>O3</sup> mg	Out <sup>O3</sup> gas	SGV cm/sec	MMH Conc. (mg/l)										
							0	5	10	15	20	30	45	60	75	90	120
2	9.1	LMTOC	UV	12.1	0.0	1.5	1171	1165	1139	929	837	191	33				
13	9.1	LMTOC	UV	10.1	1.7	1.5	128	63	2	0.4	0.2						
14	9.1	LMTOC	UV	12.3	0.2	1.5	505	288	274	251	36	9	4				
15	9.1	LMTOC	None	11.3	3.1	1.5	117	115	19	3	1	0.2	<0.2				
16	9.1	LMTOC	UV	9.1	1.3	1.5	103	49	2	0.2	<0.2	<0.2	<0.2				
17	9.1	LMTOC	UV	11.5	0.5	1.5	158	100	35	2	0.5						
18	2.6	LMTOC	UV	10.9	1.8	1.5	158	127	100	64	34						
10	9.1	LMTOC	UV	5.2	0.7	1.5	89	76	3	<0.02							
19	9.2	LMTOC	UV	27.7	2.7	1.5	102	5	2	0.8							
20	9.1	OUR	Ultrasound	-	-	1.5	103	91	85	82	80						
23	9.1	OUR	Ultrasound	-	10.1	1.5	100	5	0.7	<0.2	0.2*						
21	9.1	LMTOC	UV	-	-	1.5	83	70*	5	2	0.5						
24	9.1	LMTOC	None	-	-	1.5	103	100	69	102	101	102*					
25	9.2	LMTOC	UV	-	-	1.5	97	71	35	3	0.6						
26	9.1	OUR	None	-	-	1.5	82	90	74	79	71						
42	9.1	LMTOC	UV	10.7	0.4	0.9	120	65	17	1	0.5						
43	9.1	LMTOC	UV	9.4	0.6	1.8	115	58	3	0.5	0.2						

NOTE: \* Run 23 is 40 min., 21 is 8 min., 24 is 42 min.

TABLE A-3. METHANOL CONCENTRATIONS IN MMH OZONATIONS

Run #	Time (Min)										
	0	5	10	15	20	30	45	60	75	90	120
2	16			85		120	154	172		195	210
13	6			17		13	9	5			
14	10			75		67	53	52	52	50	
15	5			18		24	16	12	6	2	
16	4			19		12		6	3		
17	4		17		15	12	8				
18				8		13	28	17			
10	4			15		13	8	7			
19	5	16	16	13	11	7					
20	3			15		13	8	7			
23	5	18	17		10	6	2*				
21			11*			6	4	2			
24	9			14		15	8*				
25	5			13		8	5	4			
26	12			7		3	12	11			
42											
43	1	11	22	27	25	22	17	11			

NOTE: \* Run 23 is 40 min., 21 is 8 min., 24 is 42 min.

TABLE A-4. UNSYMMETRICAL DIMETHYLHYDRAZINE DATA

Run #	Initial pH	Reactor	Catalyst	In O <sub>3</sub> mg O <sub>3</sub> /l gas	Out O <sub>3</sub> mg O <sub>3</sub> /l gas	SGV cm <sup>3</sup> /sec	UDMH Conc. (mg/l)															
							0	5	10	15	20	25	30	35	40	45	50	60	75	90	120	
27	9.1	LMTOC	UV	10.6	0.3	1.5	112	65	25	<0.1	<0.1	<0.1	<0.1	<0.1	<0.1	<0.1	<0.1	<0.1	<0.1	<0.1		
28	9.1	OUR	None	9.4	10.2	1.5	104	<0.1	<0.1	<0.1	<0.1	<0.1	<0.1	<0.1	<0.1	<0.1	<0.1	<0.1	<0.1	<0.1		
29	9.1		UV	11.0	0.1	1.5	258	196	134	86	26	0.1										
30	9.1		UV	11.5	0.2	1.5	953	897	783	687	458										286 <0.1	
31	9.1	LMTOC	None	11.8	0.1	1.5	229	164	109	58	22	<0.1									<0.1	
32	9.1	OUR		11.2	0.02	1.5	510	440	300	180	30	<0.1	<0.1	<0.1	<0.1	<0.1	<0.1	<0.1	<0.1	<0.1	<0.1	
33	9.1	OUR		10.7	10.7	1.5	480 280	210	20	<0.1	<0.1	<0.1	<0.1	<0.1	<0.1	<0.1	<0.1	<0.1	<0.1	<0.1	<0.1	
34	9.1	OUR		12.0	6.9	1.5	440 300	180	30	<0.1	<0.1	<0.1	<0.1	<0.1	<0.1	<0.1	<0.1	<0.1	<0.1	<0.1	<0.1	
35	9.1	LMTOC		4.4	0.0	1.5	236	204	164	113	73											
36	9.1	LMTOC		30.1	1.0	1.5	220 189	138	54	7	<0.1											
37	9.2	LMTOC		9.8	0.3	1.8	234	153	66	11	<0.1											
38	9.1	LMTOC		11.4	0.0	0.9	226	176	106	47	14											
39	3.1			13.9	1.7	1.5	247	193	153	116	87											
40	9.1	LMTOC		-	-	1.5	229	220	218	207	189											
41	9.1	LMTOC		-	-	1.5	218	218	218	207	189											
49-205	9.1	LMTOC		12.0	-	1.5	122 98	74	45	25	0.7*	1760*										
60	-	OUR		-	-	1.5	2651 2252 2202															1065*

NOTE: \* Run # 49 is 35 min., 60 is 55 min., and 70 min.

TABLE A-5. NITRATE CONCENTRATIONS IN HYDRAZINE OZONATIONS\*

Run #	pH	UV	Time (Min.)						
			0	10	15	20	30	45	60
44	9.1	o	0.9	1.3		1.7	2.5	2.7	3.8
51	9.1	no	1.2			3.3	3.9	4.1	4.7
56	3.1	on	0.5		2.0		3.9	5.7	7.8

\*For the aquatic toxicity run with Hydrazine (R-70) characterization data are in Table A-6.

TABLE A-6. CHARACTERIZATION RUN #70 (HYDRAZINE)

Time (Min)	H (mg/l)	COD (mg/l)	Nitrate-N (mg/l)
0	122	102	0.2
5	106	101	0.64
10	90	76	0.52
15	72	71	0.82
20	52	55	1.24
30	17	26	1.62
45	<0.05	<10	2.49

TABLE A-7. CHARACTERIZATION RUN #43 (MONOMETHYL HYDRAZINE)

Time (Min)	MMH (mg/l)	VOC (mg/l)	TOC (mg/l)	COD (mg/l)	Nitrate-N (mg/l)
0	114	17	32	264	0.19
5	109	21	34	238	1.38
10	61	27	36	210	1.48
15	103	30	42	196	1.64
20	58	28	37	167	1.94
30	2.7	27	36	135	2.18
45	0.5	21	31	106	2.52
60	<0.2	16	25	73	2.86

TABLE A-8. CHARACTERIZATION RUN #49-205 (UNSYMMETRICAL DIMETHYLHYDRAZINE)

Time (Min)	UDMH (mg/l)	TOC (mg/l)	COD (mg/l)	Nitrate-N (mg/l)
0	122	54	237	0.03
5	98	41	209	1.10
10	74	40	181	2.11
15	45	38	150	3.34
20	25	38	131	4.40
35	0.7	37	96	7.22

APPENDIX B  
AQUATIC TOXICITY TESTING

1. MATERIALS AND METHODS

a. Fathead Minnow Assays

Static acute toxicity experiments with fathead minnows (Pimephales promelas) were used for evaluating the toxicity of H, MMH, and UDMH before and after ozonation. Range-find bioassays (24-hr) were run with each pure compound to determine the approximate toxicity range. These tests were followed by full scale, 96-hr bioassays to determine a definitive LC50 value.

Range-find tests were conducted in 2 liters of aerated well water (dissolved oxygen >8.0 mg/l) and full scale tests in 14 liters of the same water. The well water had a total hardness of 192 mg/l as CaCO<sub>3</sub>, pH 7.8, and total alkalinity of 138 mg/l as CaCO<sub>3</sub>.

The test organisms were placed into nominal concentrations of the pure test material (obtained from Aldrich Chemical Co. or the US Air Force) and their percent survival was monitored every 24 hours. Dead fish were removed daily. The test solutions, prepared by dilution of stock concentrations, were added directly to the test vessels, stirred gently, and were not renewed during the test. Continuous aeration of the test vessels was required for H, MMH, and UDMH because of the high oxygen demand. Two fish were placed into each range-find vessel with no replication, while 10 fish were used in each full scale test with one replication (i.e., 20 fish per test concentration). Fathead minnows were young-of-the-year fish obtained from Osage Catfisheries, Osage Beach, Missouri, weighing approximately 0.5 g and measuring 3 to 5 cm long. All fish were acclimated to the laboratory before testing. A 16-hr light, 8-hr dark photoperiod was maintained throughout each test and the fish were not fed during the test period. All tests were conducted at 20°±1°C (ambient room temperature), and the dissolved oxygen was measured prior to the addition of the test materials, at intermittent intervals during the tests, and when all of the fish in any test solution were dead.



LC50 values for 96-hr exposures were calculated using the method of Litchfield and Wilcoxon (B-1).

Borate-buffered, ozonated solutions of the hydrazines, were diluted to 2.5-50% by volume, in addition to 100% solution for range-find bioassays with minnows. A control of ozonated sodium borate solution was assayed in the same way. Lack of sufficient sample prevented full scale tests from being performed with these waters. The objective of the tests was to estimate the approximate toxicity levels to minnows before and after ozonation.

b. Daphnia Assays

Daphnia magna were also used in static acute bioassays. The Daphnia were 1st instar (12-24 hr old) specimens reared and tested in a  $18 \pm 1^\circ\text{C}$  environment. Range-find tests with pure hydrazines were set up with two replicates of five concentrations and one water control using five Daphnia per solution. Full scale tests with the hydrazines were run using 10 Daphnia per solution, with four replicates. Mortality was noted at 24 and 48 hours of exposure; no distinction was made between dead and immobilized organisms. The survivors included only those Daphnia that exhibited swimming movement. The EC50 of a full scale test was calculated using the method of Litchfield and Wilcoxon (B-1).

c. Ozonated Hydrazine Solutions

Three ozonation runs, No. 70, 43, and 49-205, were made with H, MMH, and UDMH, respectively, at initial concentrations of approximately 100 mg/l. The ozonations were continued until ozone was detected in the off gas, indicating that the primary ozone demand had been met. After the ozonations, the water was pumped from the LMTOC reactor and stored at  $4^\circ\text{C}$  until assayed. All ozonations were made at pH 9.1 with borate buffer using UV light catalysis. A borate buffer control for fish toxicity testing was prepared by ozonating a solution of sodium borate (approximately 0.01 M) at pH of 9.4, then allowing the ozone to decompose before bioassay, as measured by UV absorbance at

254 nm. Chemical analyses of these runs as a function of time are given in Figures 15, 16, 25, 26 and 34 of the text. Results of organic characterization of ozonation by-products by GC/MS are given in Appendix C.

## 2. RESULTS AND DISCUSSION

Ozonation reduced the toxicity of the solutions containing H, MMH, and UDMH. Prior to ozonation the toxicity ranged from 0.35 mg/l to 4.5 mg/l for fatheads and >0.1 to <10.0 mg/l for daphnids (Table I). After ozonation of 100 mg/l solutions the toxicity values were generally greater than 25% v/v reaction mixture. The toxicity values for the sodium borate controls were similar to those for  $H_2O_3$  to fatheads, indicating that the residual toxicity to this compound may have been due to the borate solution. However, the toxicity of reaction mixtures for all other solutions was greater than for controls, indicating that some toxic reaction product(s) were still present.

Difficulties associated with small volumes of reaction mixtures plus contamination of the well supplying the test waters prevented the performing of full scale tests on reaction mixtures. This in turn prevented the establishment of definitive LC/EC50's for the reaction mixtures. Nevertheless the data are sufficiently consistent to conclude that ozonation does reduce the toxicity of the three compounds in question, but significant toxicity still exists in the reaction mixture.

Characterization of the reaction mixture followed by toxicity testing of pure compounds and possibly some combinations of compounds would be necessary to pinpoint the exact cause(s) of toxicity.

TABLE B-1. AQUATIC TOXICITY RESULTS

Compound	Fathead Minnow		Daphnia	
	pH	LC50	pH	EC50
H	--	4.5 <sup>a</sup> mg/l	8.6	0.1 ≤ x < 1 <sup>b</sup> mg/l
H+O <sub>3</sub>	7.5	50% ≤ x < 100% v/v	7.0	12.5% ≤ x < 25% v/v
MMH	--	1.22 <sup>a</sup> mg/l	7.6	≤ 5.0 <sup>b</sup> mg/l
MMH+O <sub>3</sub>	9.1	25% ≤ x < 50% v/v	8.8	25% ≤ x < 50% v/v
UDMH	--	0.35 <sup>a</sup> mg/l	8.1	5.0 ≤ x < 10.0 mg/l
UDMH+O <sub>3</sub>	9.1	12.5% ≤ x < 25% v/v	7.0	50% v/v
	7.5	40% ≤ x < 50% v/v		
O <sub>3</sub> Sodium Borate	7.5	50% ≤ x < 100% v/v	7.0	25% ≤ x < 50% v/v
O <sub>3</sub> Sodium Borate	9.4	< 50% v/v	--	--

- a. Results of full scale 96-hr bioassays.  
 b. Results of range-find bioassays.

## REFERENCES

- B-1. Litchfield, J.T. and F. Wilcoxon, "A Simplified Method of Evaluating Dose-Effect Experiments," J. Pharmacol. Exp. Ther., 96, 99 (1949).

## APPENDIX C

### CHEMICAL CHARACTERIZATION OF OZONATED HYDRAZINE FUELS

#### 1. MATERIALS AND METHODS

##### a. GC-FID/Hall Detector Analysis

The methods used for these analyses have been given in Section III of the text.

##### b. GC/MS Analyses

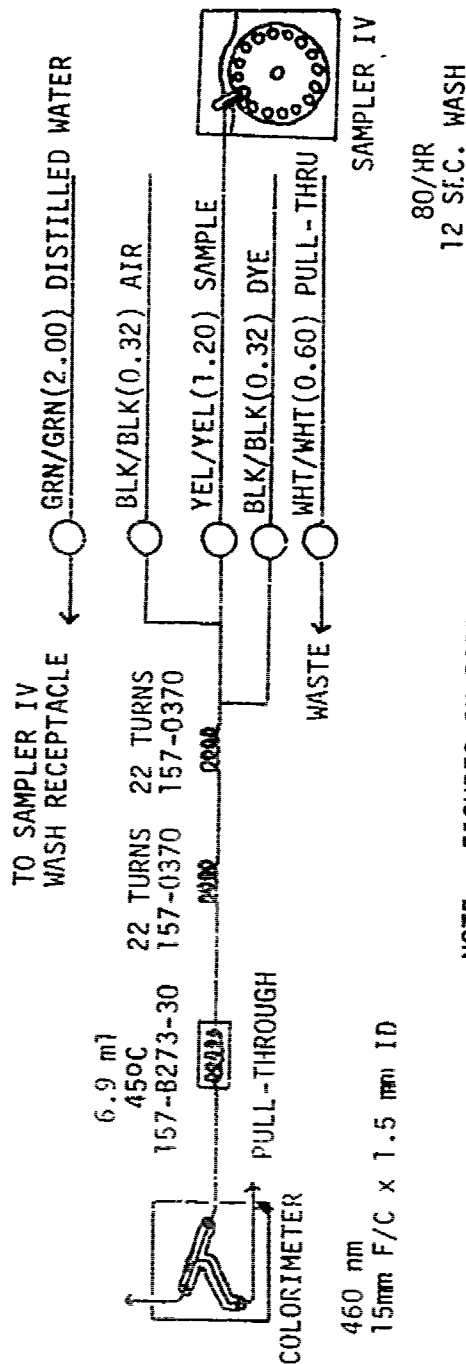
A Finnigan Model 3500 gas chromatograph-mass spectrometer interfaced with a Systems 150 data system was used for acquiring mass scans continuously from 5 to 200 atomic mass units (amu) with 10 msec integration time per amu, starting at 2 min after sample injection onto the GC column. The GC column was 5 ft x 1/4 in OD (2mm ID) glass packed with 60/80 mesh Tenax GC<sup>®</sup>. The column was temperature programmed from 70°C (2min hold) to 250°C at 10°/min for ozonated UDMH solutions and 50°C (2 min hold) to 100°C at 10°/min for the ozonated MMH solution.

##### c. UV Spectra

The methods used for these analyses have been given in Section III of the text.

##### d. Automated Analyses of H and MMH

Figure C-1 shows the AutoAnalyzer<sup>®</sup> module constructed to analyze H and MMH. This module was adapted from Technicon Manifold No. 116-D533-01, primarily by changing the sample and pull-through pump tubes. The dye solution was prepared by dissolving 5 g of p-dimethylaminobenzaldehyde in 100 ml of methanol, then adding 50 ml conc. HCl and diluting to 1 liter with glass distilled water.



NOTE: FIGURES IN PARENTHESES SIGNIFY  
FLOW RATES IN IL/MIN.

Figure C-1. MANIFOLD FOR HYDRAZINE AND MMH

## 2. RESULTS AND DISCUSSION

### a. Residual Levels of Hydrazine Fuels in Ozonated Solution

These data have been presented in the text and are tabulated in Appendix A, for H, MMH, and UDMH.

### b. MMH Ozonations

Preliminary GC/FID surveys from 50<sup>o</sup> to 200<sup>o</sup>C of ozonated MMH solutions from a high initial concentration (1171 mg/l) of MMH indicated the presence of at least four peaks in addition to methanol (Figure C-2). However, problems with the temperature programmer did not allow accurate retention time data to be collected. Analysis of the aquatic bioassay sample of ozonated MMH (R-43) by GC/FID showed only the presence of methanol, perhaps since the initial MMH concentration was lower, only 115 mg/l. Unfortunately, samples from the high concentration ozonation of MMH were not saved for GC/MS analysis. Injection of the R-43 (60 min ozonated) sample onto the GC/MS showed the distribution of m/e 31 (CH<sub>3</sub>O<sup>+</sup>) vs. scan number in Figure C-3. The mass spectrum confirmed the presence of methanol in this peak. More research is required to identify the other four peaks seen in the ozonation of 1171 mg/l of MMH.

### c. UDMH Ozonations

Two UDMH ozonation runs were studied; 1) R-49-205, ozonated for 35 min (C<sub>0</sub> = 122 mg/l UDMH) and 2) R-60, ozonated for 70 min (C<sub>0</sub> > 4508 mg/l).

Figure C-4 shows the GC/FID chromatogram from R-49-205. Two small peaks were seen after the water peaks. When the same sample was chromatographed with a nitrogen-specific Hall detector (Figure C-5), two large peaks were seen after the water peaks. For reference, a water injection is shown in Figure C-6, for the Hall detector. Because of the geometry difference

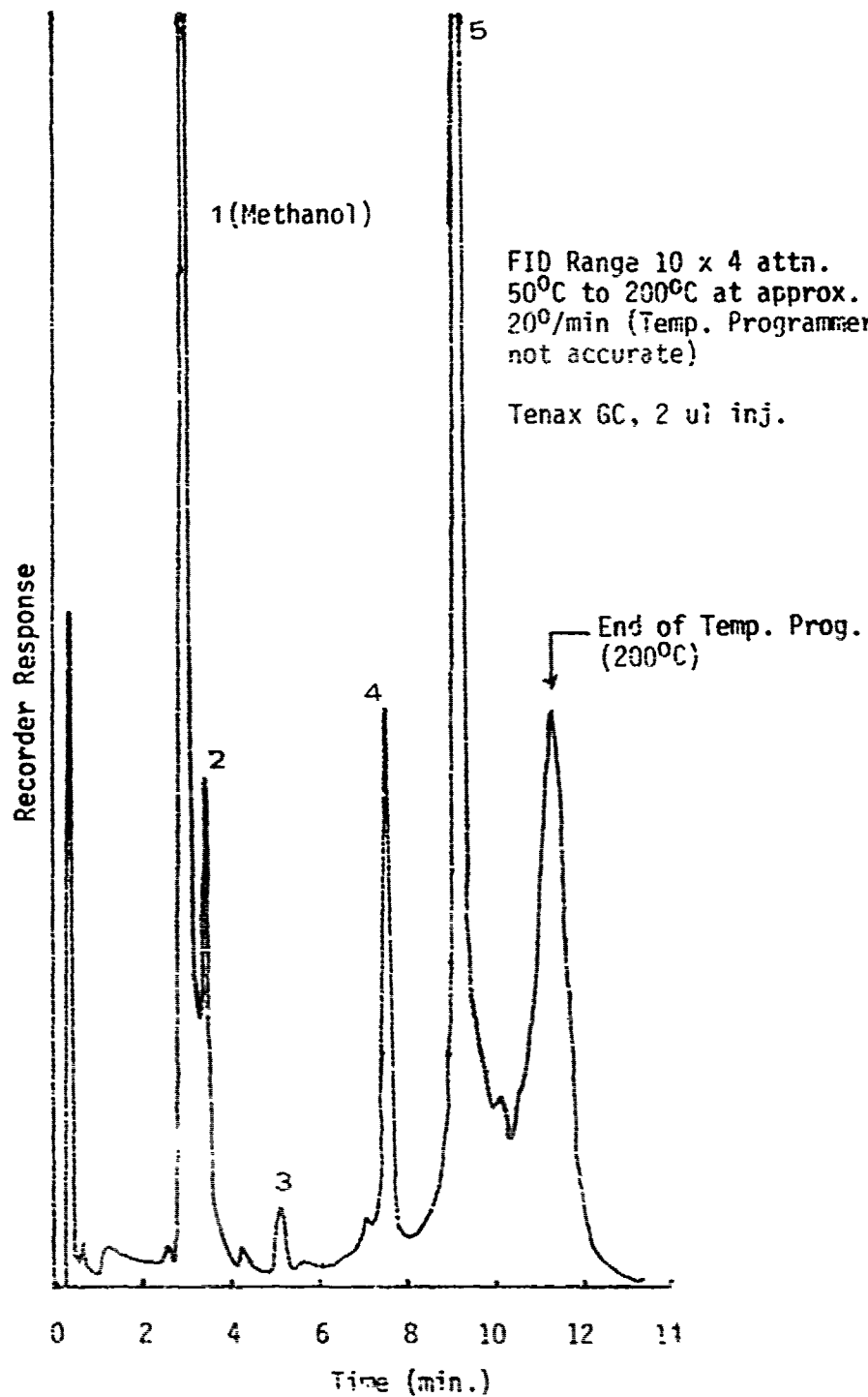


Figure C-2. FID Survey of Products from Ozonation of 1171 mg/l MMH (Run 2, 60 min.)



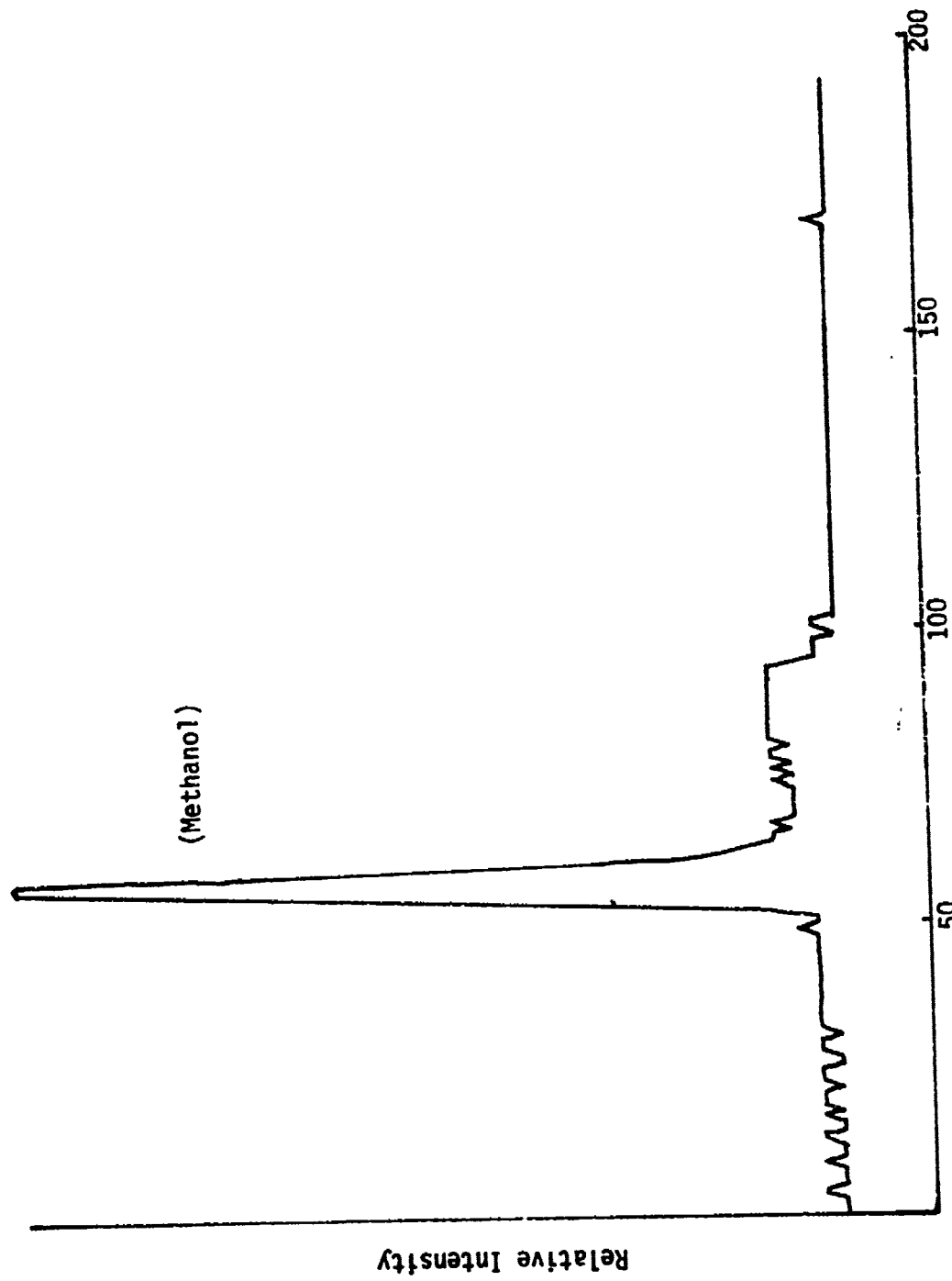


Figure C-3. Distribution of  $m/e$  31 vs. Scan No. for R-43-60 min Ozonated MMH.

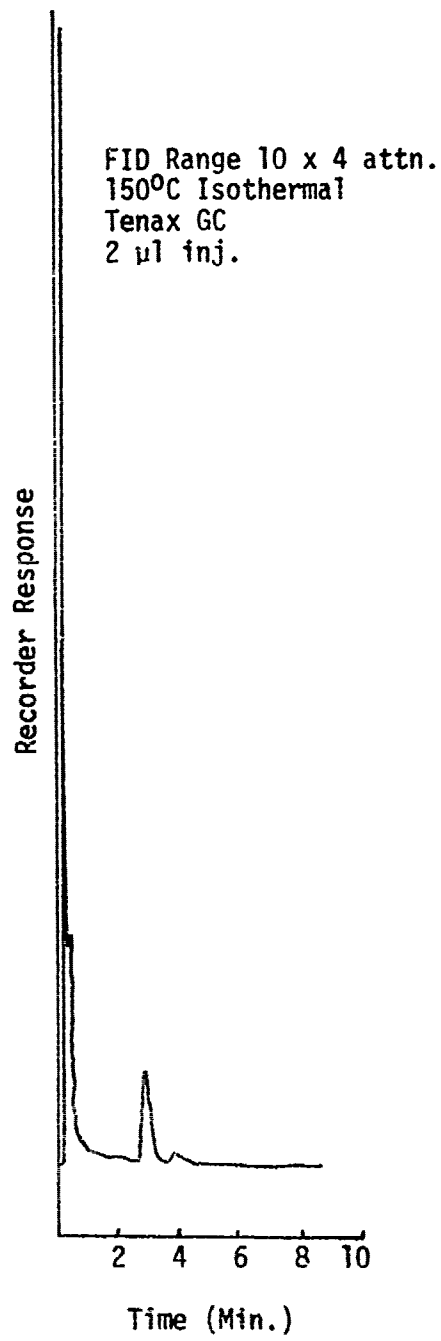
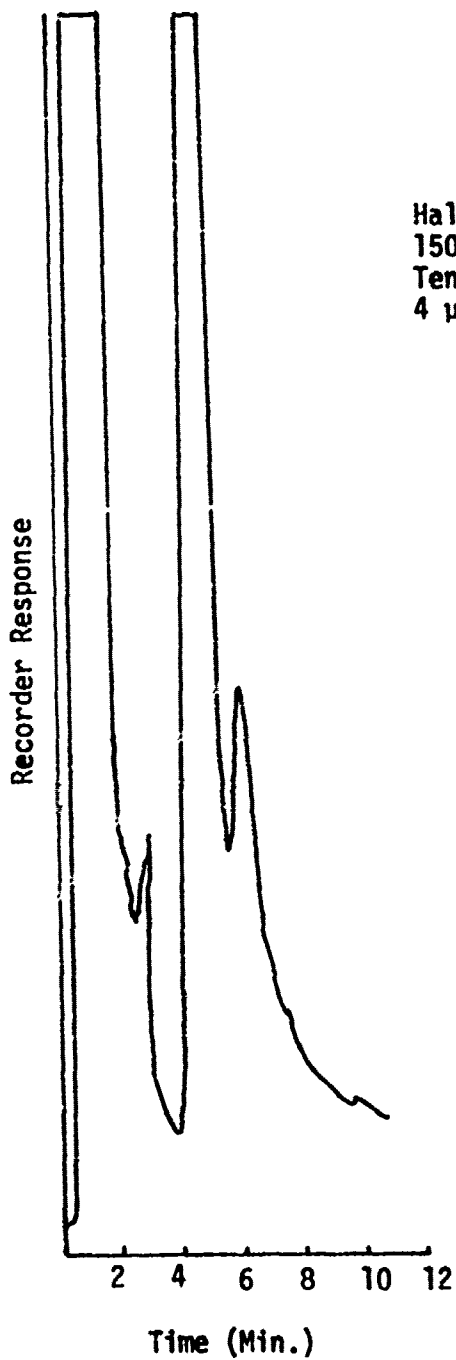


Figure C-4. FID Chromatogram of R-49-205-35 min Ozonated UDMH.



Hall Detector Range 30 x 1 attn.  
150°C Isothermal  
Tenax GC  
4 µl inj.

Figure C-5. Hall Detector Chromatogram of  
R-49-205-35 min Ozonated UDMH.

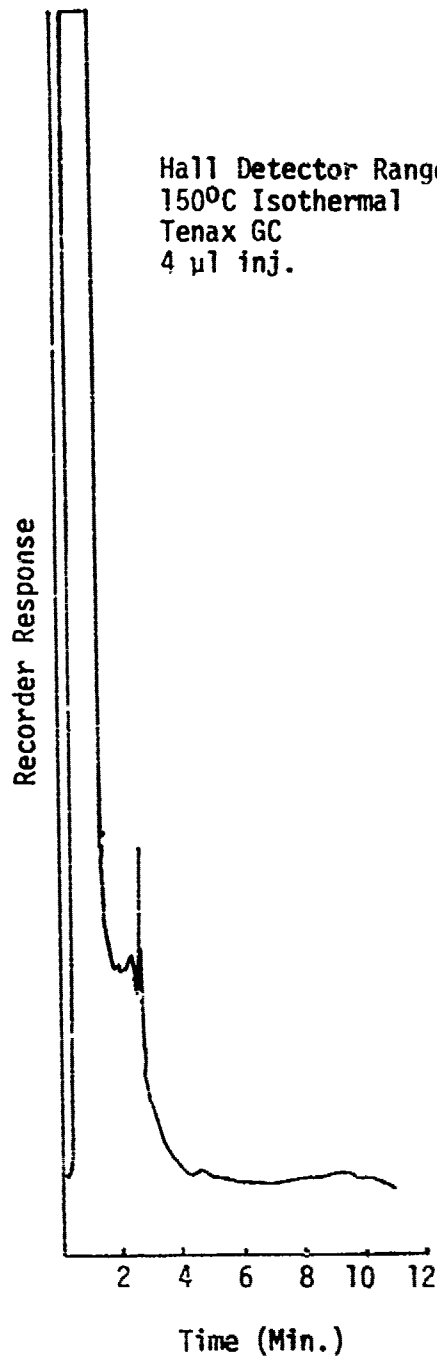
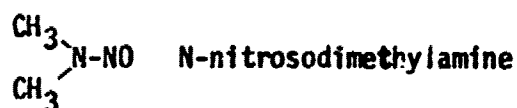


Figure C-6. Hall Detector Response to Water.

between the Hall and FID detectors, the peaks from the Hall detector usually have broader shapes and longer retention times than do the same peaks detected by the FID. Figure C-7 shows the total ionization current (TIC) response of the GC/MS for the same sample from run 49-205. The distribution of m/e 42 is also shown in this figure. Again, two peaks were detected. The mass spectra confirmed the presence of N-nitrosodimethylamine and dimethylformamide.



Isothermal GC/FID analysis of a 70 min ozonated sample from R-60 (Figure C-8) showed several peaks in addition to the two peaks seen in sample R-49-205 (35 min). UDMH was identified by comparison with a standard solution. Approximately the same pattern of peaks showed up on the GC/Hall detector chromatogram (Figure C-9), if allowance is made for the increased retention time of the Hall detector. However, the UDMH peak and its neighbor peak (see Figure C-8) may be combined in Figure C-9. A TIC chromatogram from the GC/MS, with a temperature program from 70° to 250°C showed 15 peaks (Figure C-10). Of these 15, seven peaks were confirmed as the compounds listed in Table C-1, and 13 were due to products of the UDMH ozonation.

UV scans of the R-60 ozonated UDMH solutions as a function of time are shown in Figure C-11. For reference, a pH 9.4 UDMH scan is also shown (dashed line). During ozonation, an absorption band at about 235 was observed to increase with time. This band has also been reported by Loper (C-1) during air oxidation of UDMH. This band corresponded to that of

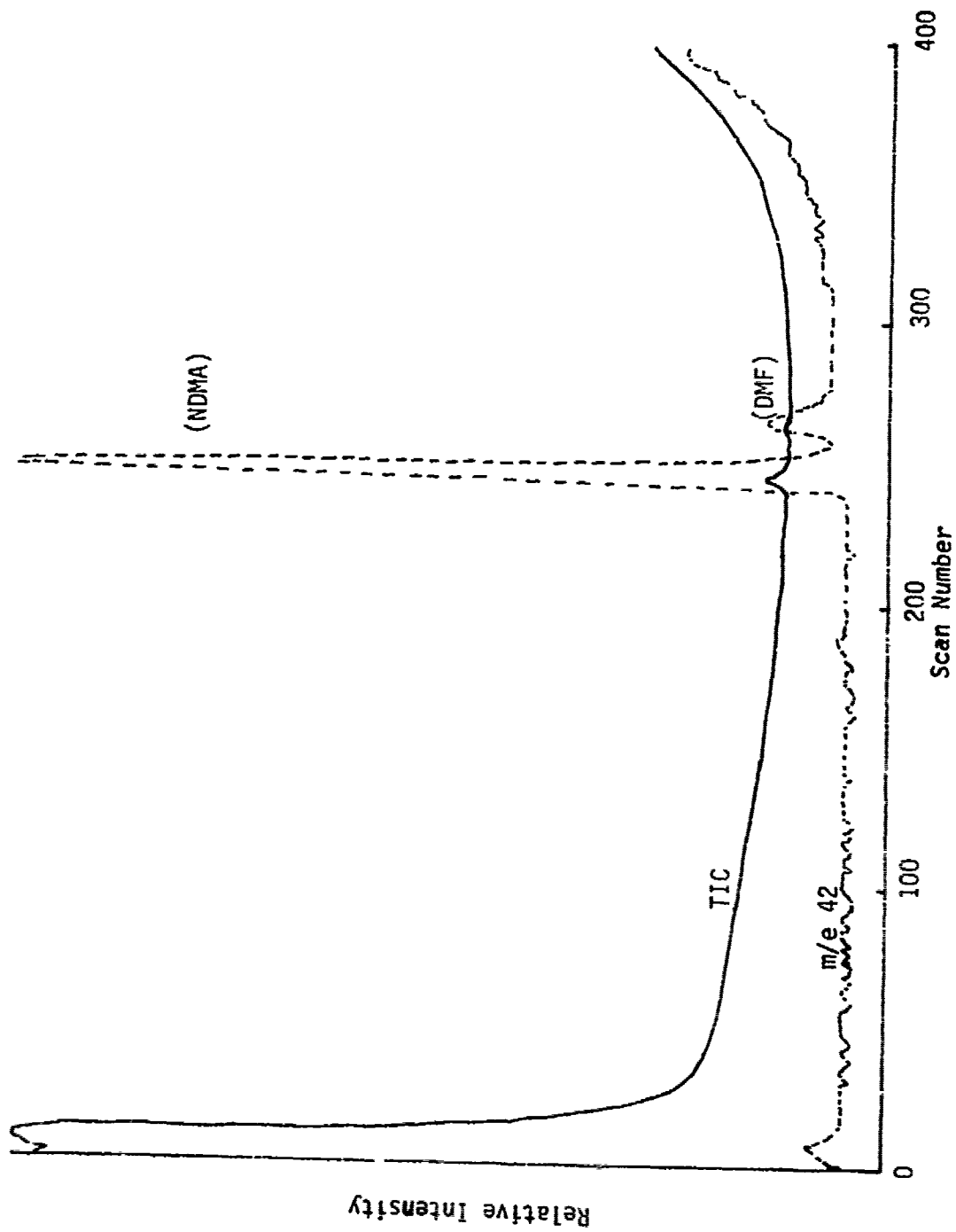


Figure C-7. Total Ionization Current and m/e 42 Chromatograms for R-49-205-35 min. Ozonated UDMH

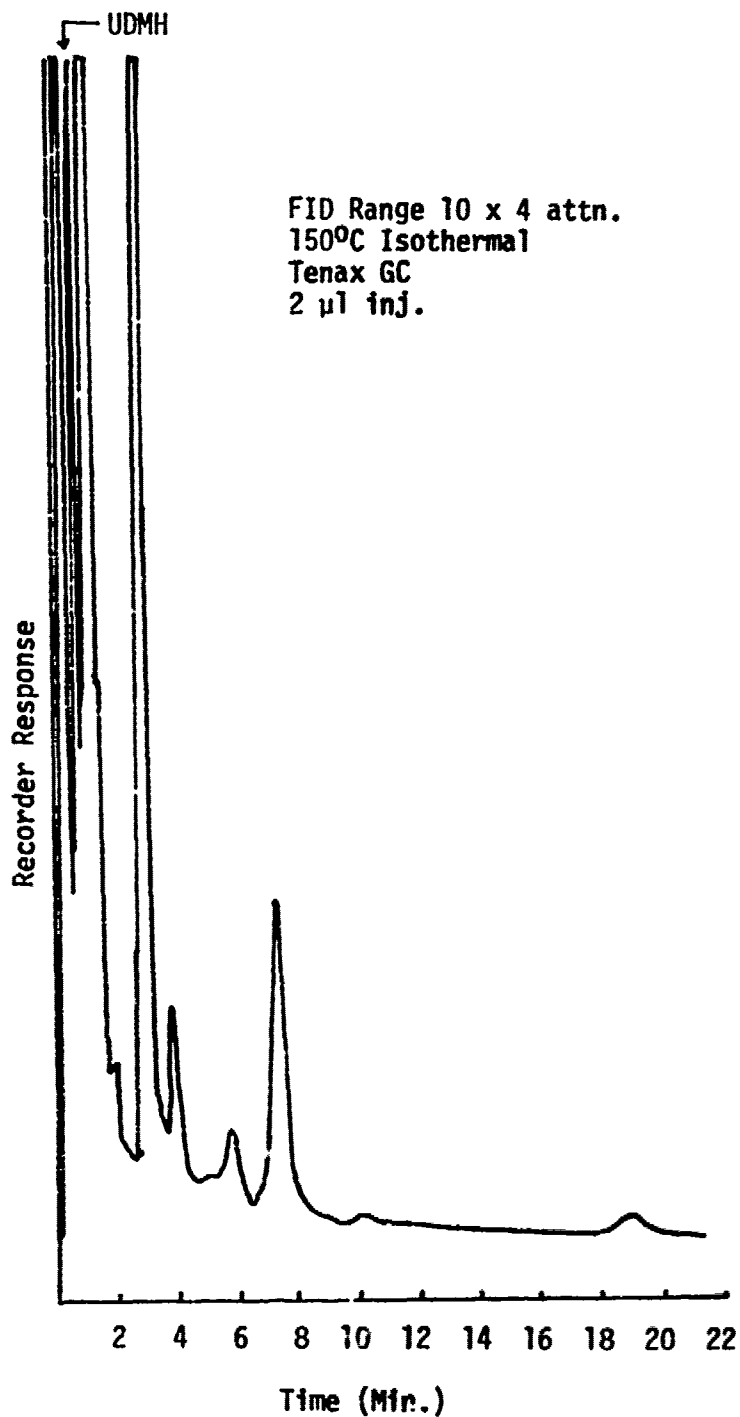


Figure C-8. FID Chromatogram of R-60-70 min. Ozonated UDMH.

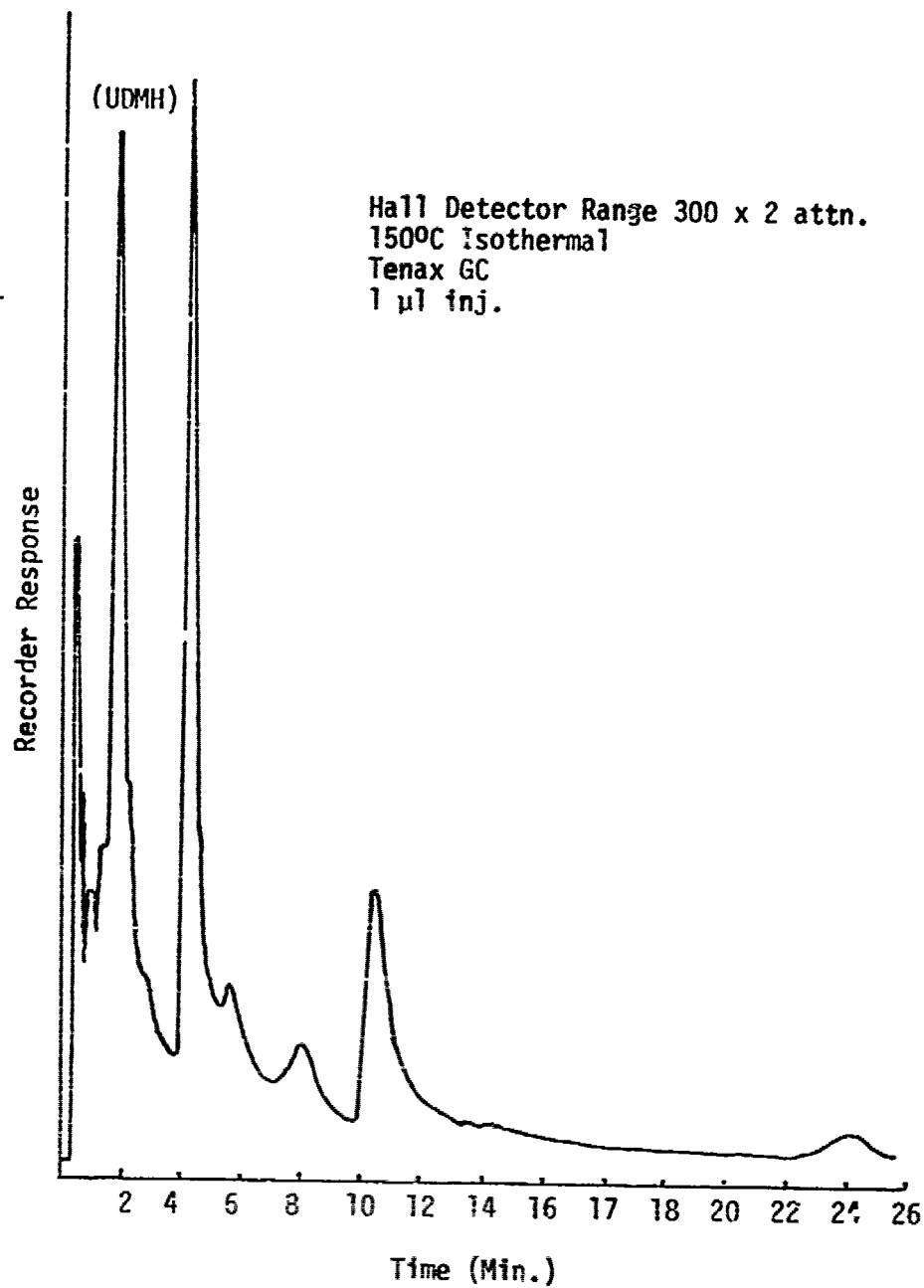


Figure C-9. Hall Detector Chromatogram of R-60-70 min. Ozonated UDMH.



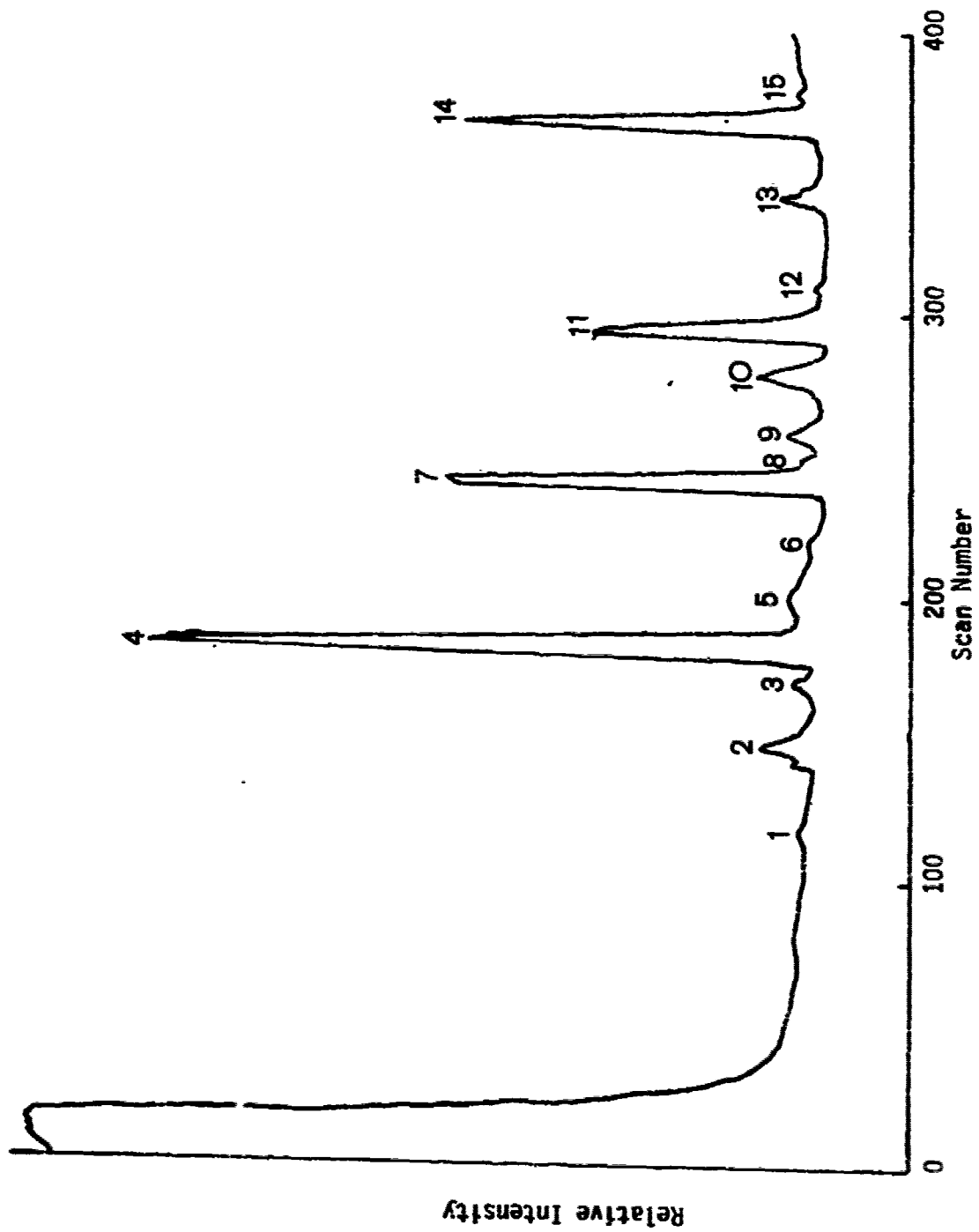


Figure C-10. Total Ionization Current Chromatogram of R-60-70 min Ozonated UDMH.

TABLE C-1. COMPOUNDS IN OZONATED UDMH SOLUTION CONFIRMED BY GC/MS

<u>Peak # (Fig. C-10)</u>	<u>Compound</u>
1	Acetone (Instrument Background)
2	Unsymmetrical Dimethylhydrazine
3	Formaldehyde Monomethylhydrazone <sup>a</sup>
4	Formaldehyde Dimethylhydrazone <sup>b</sup>
7	N-Nitrosodimethylamine
9	Dimethylformamide
10	Tetramethyl Tetrazene <sup>c</sup>

<sup>a</sup>  $\text{CH}_3\text{NHN}=\text{CH}_2$

<sup>b</sup>  $(\text{CH}_3)_2\text{N}-\text{N}=\text{CH}_2$

<sup>c</sup>  $(\text{CH}_3)_2\text{N}-\text{N}=\text{N}-\text{N}(\text{CH}_3)_2$

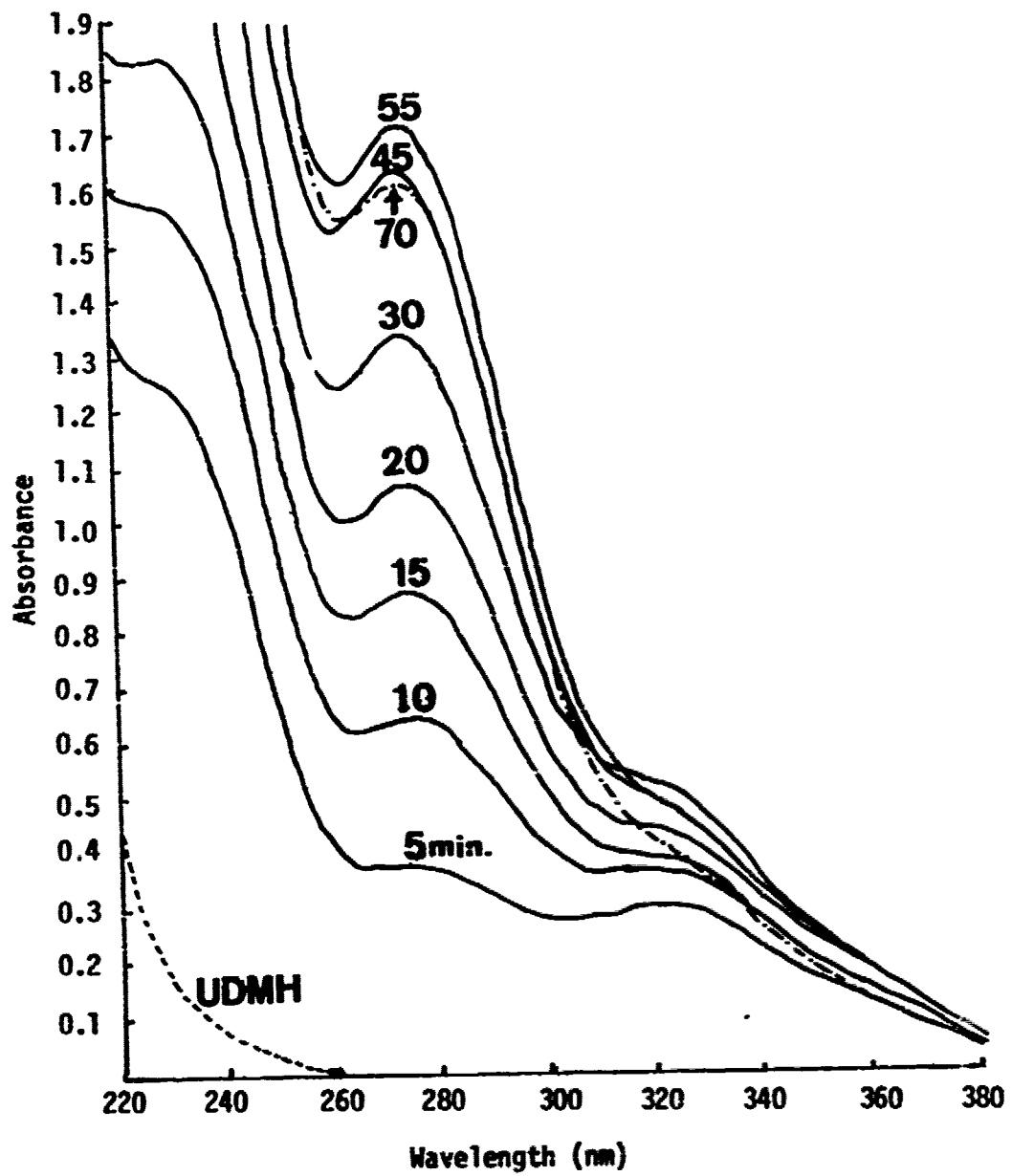


Figure C-11. Ultraviolet Absorption of UDMH and UDMH Ozonated at pH 9.1.

formaldehyde dimethylhydrazone; UDMH had an absorption at 190 nm, below the region scanned in Figure C-11. The 235 nm band was also observed by Lysenko *et al.* (C-2) upon oxidation of UDMH by ozone at pH 9. They attributed this absorption to tetramethyl tetrazene. Banerjee *et al.* (C-3) also reported tetramethyl tetrazene, in UDMH/CuSO<sub>4</sub>-oxygenations at pH 9.12. They also reported increases in absorbance at 326 nm. Figure C-11 shows this band as well as a band at about 275 nm. This latter peak was also observed by Lysenko *et al.*, although they did not attempt to explain it. Most nitrosamines show a strong UV band at about 230 nm and a weak band at a higher (330-350 nm) wavelength, hence there was also evidence of N-nitrosodimethylamine in the UV scans.

It should be noted that methanol was also detected during the R-60 ozonation (Figure C-12), and it appeared to increase in a continuous manner up to 70 minutes. Methanol would elute with the water peak in the chromatogram in Figure C-9, hence was not included in the list of peaks of Table C-1.

### 3. CONCLUSIONS

The ozonation of MMH produces methanol, which would continue to exert a ozone demand in order to meet effluent quality criteria with respect to oxygen demand. In addition, four other compounds are apparently formed from the ozonation of MMH, but have not yet been identified by GC/MS.

Ozonation of UDMH produces at least 13 compounds in addition to methanol. One of the identified compounds is a known animal carcinogen (N-nitrosodimethylamine), and the other identified compounds are formaldehyde monomethylhydrazone, formaldehyde dimethylhydrazone, dimethylformamide, and tetramethyl tetrazene. The health significance of these compounds should be considered before discharge of incompletely ozonated UDMH solutions.

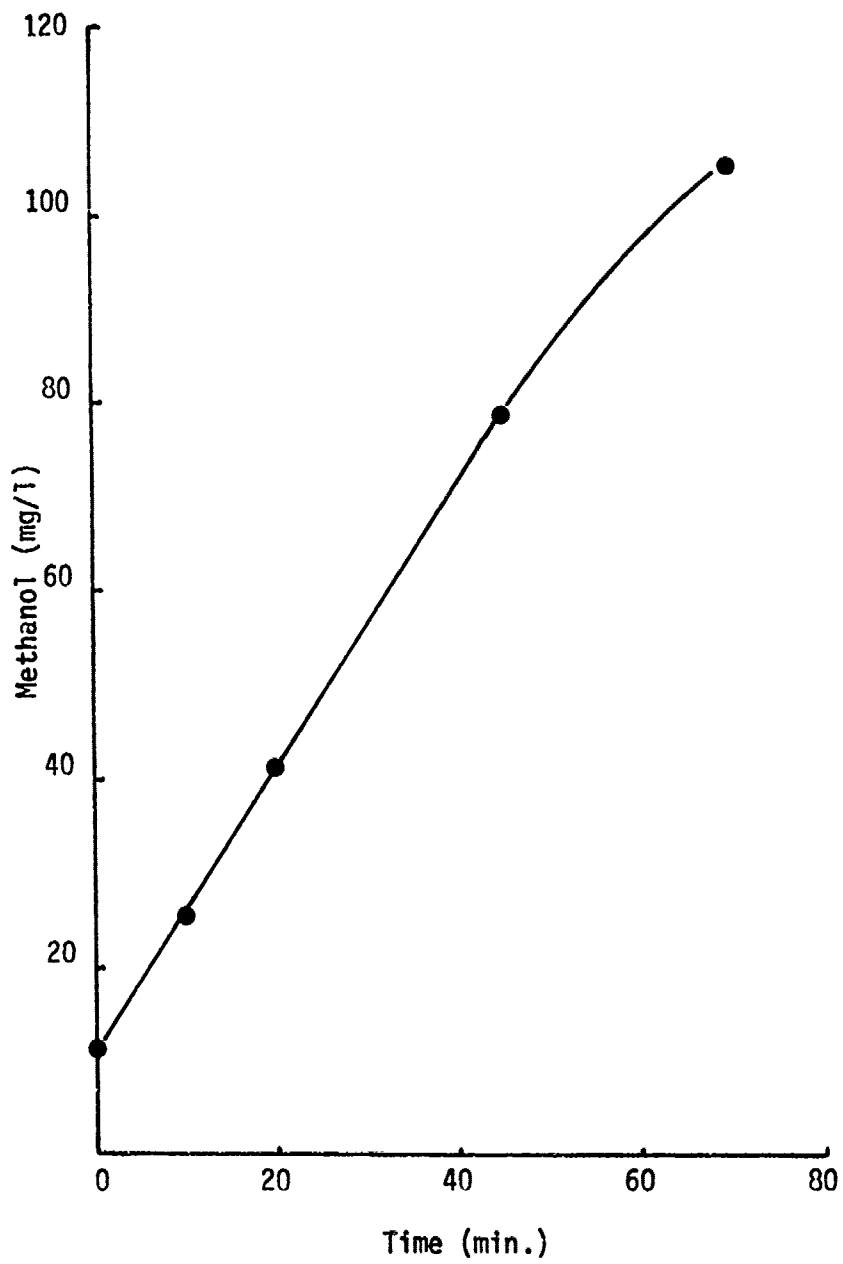


Figure C-12 Production of Methanol During Ozone Oxidation of UDMH (Run 60).

These limited chemical studies have demonstrated that ozonation of MMH and UDMH in alkaline solution results in several intermediate products, which may present discharge problems as a result of organic carbon loading or toxicity.

## REFERENCES

- C-1. Loper, G.L., "Gas Phase Kinetic Study Air Oxidation of UDMH," paper No. 12, in Proceedings of the Conference on Environmental Chemistry of Hydrazine Fuels, Tyndall AFB, 13 Sept. 1977, CEEDO-TR-78-14 (1978).
- C-2. Lysenko, T.F., L.F. Atyaks eva, B.V. Strakhov and G.I. Emel'yanova, "Kinetics and Mechanism of the Oxidation by Ozone of 1,1-Dimethylhydrazine in Aqueous Solution", Translation in Russian J. Physical Chemistry, 49, 1849 (1975).
- C-3. Banerjee, S., H.C. Sikka, and R. Tray, "Environmental Degradation of 1,1-Dimethyl-Hydrazine", paper No. 11, in Proceedings of the Conference on Environmental Chemistry of Hydrazine Fuels, Tyndall AFT, 13 Sept. 1977, CEEDO-TR-78-14 (1978).
- C-4. Sen, N.P., "Final Chromatography and Detection", in Environmental Carcinogens Selected Methods of Analysis, Vol. 1 - Analysis of Volatile Nitrosamines in Food Ed. H. Egan, IARC Scientific Publication No. 18 Lyon, France (1978).

APPENDIX D

KINETIC DATA GENERATED BY OMNITAB COMPUTER PROGRAM

Table D-1. Kinetics of Hydrazine Oxidation

Table D-2. Kinetics of Monomethylhydrazine Oxidation

Table D-3. Kinetics of Unsymmetrical Dimethylhydrazine Oxidation



TABLE D-1. KINETICS OF HYDRAZINE OXIDATION

Run No.	Computer No.	Initial Conc. (mg/l)	Zero Order Model		First Order Model		Second Order Model				
			$k_0$ (mg/l-min)	$t_{1/2}$ (min)	F Ratio (n)	$k_1$ (min) <sup>-1</sup>	$t_{1/2}$ (min)	F Ratio (n)	$k_2$ (1/min-mg)	$t_{1/2}$ (min)	F Ratio (n)
44	101	139	3.35	20.7	7251.469 (4)	$3.93 \times 10^{-2}$	17.6	108.170 (4)	$5.3 \times 10^{-4}$	18.6	27.469 (4)
50	105	126	7.74	8.1	16320.2 (4)	$13.8 \times 10^{-2}$	5.0	50.858 (4)	$4.0 \times 10^{-3}$	2.0	11.068 (4)
51	102	125	2.94	21.3	949.707 (5)	$12.7 \times 10^{-2}$	5.5	13.090 (5)	$4.3 \times 10^{-1}$	54.8	5.804 (5)
56	103	150	0.84	89.8	1399.764 (5)	$0.7 \times 10^{-2}$	105.5	434.721 (5)	$5.2 \times 10^{-5}$	0.0	190.523 (5)
49	104	138	2.71	25.5	7771.56 (5)	$3.8 \times 10^{-2}$	18.0	85.190 (5)	$7.7 \times 10^{-4}$	0.1	16.942 (5)
52	106	138	2.74	25.2	900.575 (5)	$4.7 \times 10^{-2}$	14.8	26.856 (5)	$1.6 \times 10^{-3}$	0.2	8.423 (5)
54	111	133	0.68	97.8	93.309 (5)	$0.6 \times 10^{-2}$	113.8	67.582 (5)	$5.5 \times 10^{-5}$	0.0	49.844 (5)
55	112	132	0.04	177.9	213.797 (5)	$0.3 \times 10^{-2}$	225.6	269.298 (5)	$2.6 \times 10^{-5}$	0.0	341.786 (5)
47	113	705	21.12	16.7	1390.851 (5)	$6.6 \times 10^{-2}$	10.5	53.055 (5)	$3.3 \times 10^{-4}$	0.3	13.738 (5)
46	110	785	5.26	74.5	1897.5 (6)	$0.8 \times 10^{-2}$	84.5	455.541 (6)	$1.3 \times 10^{-5}$	98.0	177.181 (6)
48	114	730	24.64	14.8	1260.95 (6)	$8.2 \times 10^{-2}$	8.4	60.479 (6)	$5.9 \times 10^{-4}$	2.3	10.287 (6)
45	108	432	4.27	50.6	170.209 (7)	$1.7 \times 10^{-2}$	41.0	64.503 (7)	$8.0 \times 10^{-5}$	28.9	21.952 (7)
57	109	5600			64.869 (8)			58.784 (8)			52.745 (8)
53	107	137	4.33	15.8	4773.97 (4)	$7.5 \times 10^{-2}$	9.2	46.410 (4)	$2.3 \times 10^{-3}$	3.1	9.922 (4)

TABLE D-2. KINETICS OF MONOMETHYLHYDRAZINE OXIDATION

Run No.	Computer No.	Initial Conc. (mg/l)	Zero Order Model			First Order Model			Second Order Model		
			$k_0$ (mg/l-min)	$t_{1/2}$ (min)	F Ratio (n)	$k_1$ (min) <sup>-1</sup>	$t_{1/2}$ (min)	F Ratio (n)	$k_2$ (1/min-mg)	$t_{1/2}$ (min)	F Ratio (n)
13	201	128	3.33	19.2	75.282 (4)	$12.4 \times 10^{-2}$	5.6	99.087 (4)	$4.0 \times 10^{-2}$	2.0	10.768 (4)
17	204	120	2.88	20.8	67.647 (4)	$10.8 \times 10^{-2}$	6.4	43.185 (4)	$3.6 \times 10^{-2}$	0.2	12.744 (4)
19	206	102	5.19	9.8	25.435 (4)	$18.4 \times 10^{-2}$	3.8	55.309 (4)	$1.7 \times 10^{-2}$	0.6	36.098 (4)
24	212	103	0.04	9.8	16.09 (4)	$0.4 \times 10^{-2}$	177.7	16.009 (4)	$3.8 \times 10^{-6}$	2559	15.926 (4)
20	213	100	5.94	8.4	32.725 (4)	$25.1 \times 10^{-2}$	2.8	113.851 (4)	$5.8 \times 10^{-2}$	0.2	17.509 (4)
15	202	117	2.23	26.2	54.647 (5)	$50.7 \times 10^{-2}$	1.4	96.658 (5)	$1.1 \times 10^{-2}$	7.7	13.619 (5)
18	203	158	2.06	38.4	7056.69 (5)	$2.2 \times 10^{-2}$	31.2	123.851 (5)	$2.9 \times 10^{-4}$	22.1	27.961 (5)
42	207	120	2.43	24.7	78.770 (5)	$9.0 \times 10^{-2}$	7.7	144.477 (5)	$2.4 \times 10^{-2}$	0.3	16.705 (5)
43	208	115	2.37	19.3	163.660 (7)	$10.3 \times 10^{-2}$	6.6	55.467 (7)	$2.7 \times 10^{-2}$	0.3	12.937 (7)
14	209	505	6.45	39.1	167.835 (7)	$4.7 \times 10^{-2}$	14.9	80.748 (7)	$1.6 \times 10^{-3}$	1.3	13.044 (7)
2	210	975	6.37	76.5	17.726 (7)	$1.9 \times 10^{-2}$	36.5	17.700 (7)	$1.3 \times 10^{-3}$	0.8	8.764 (7)
10	205	89	0.93	47.7	0.0 (2)	$1.1 \times 10^{-2}$	60.8	0.0 (2)	$1.4 \times 10^{-4}$	80.9	0.0 (2)

TABLE D-3. KINETICS OF UNSYMMETRICAL DIMETHYLHYDRAZINE OXIDATION

Run No.	Computer No.	Initial Conc. (mg/l)	Zero Order Model			First Order Model			Second Order Model		
			$k_0$ (mg/l-min)	$t_{1/2}$ (min)	F Ratio (n)	$k_1$ (min) <sup>-1</sup>	$t_{1/2}$ (min)	F Ratio (n)	$k_2$ (l/min-mg)	$t_{1/2}$ (min)	F Ratio (n)
37	306	226	5.9	21.7	894.330 (4)	$5.8 \times 10^{-2}$	11.9	50.557 (4)	$1.4 \times 10^{-3}$	3.2	9.179 (4)
33	313	479	24.56	9.6	125.827 (4)	$14.2 \times 10^{-2}$	4.8	63.401 (4)	$1.9 \times 10^{-3}$	1.1	13.081 (4)
27	308	112	4.42	12.7	3009.3 (3)	$7.1 \times 10^{-2}$	9.7	131.01 (3)	$1.4 \times 10^{-3}$	6.4	26.96 (3)
40	311	229	0.21	544.0	38.525 (3)	$0.94 \times 10^{-3}$	736.5	39.326 (3)	$4.2 \times 10^{-6}$	1090.0	40.165 (3)
31	301	229	3.67	31.2	896.847 (5)	$3.4 \times 10^{-2}$	20.3	134.317 (5)	$4.8 \times 10^{-3}$	0.9	17.060 (5)
29	302	258	5.47	52.3	806.874 (5)	$4.5 \times 10^{-2}$	15.5	116.25 (3)	$5.6 \times 10^{-4}$	6.9	16.355 (5)
39	303	247	2.83	43.6	636.512 (5)	$1.7 \times 10^{-2}$	41.0	5193.285 (5)	$1.1 \times 10^{-4}$	36.8	187.515 (5)
35	304	236	2.68	44.2	1495.37 (5)	$1.7 \times 10^{-2}$	39.8	145.726 (5)	$1.3 \times 10^{-4}$	32.6	42.734 (5)
36	305	220	7.49	14.7	657.730 (5)	$9.5 \times 10^{-2}$	7.3	56.645 (5)	$3.0 \times 10^{-3}$	1.5	10.473 (5)
38	307	225	3.71	30.3	581.881 (5)	$3.9 \times 10^{-2}$	17.9	83.121 (5)	$7.1 \times 10^{-4}$	6.3	12.698 (5)
32	310	510	7.56	33.7	520.66 (5)	$3.5 \times 10^{-2}$	19.9	26.278 (5)	$3.1 \times 10^{-4}$	6.3	7.307 (5)
41	312	218	0.33	332.4	13.210 (5)	$1.6 \times 10^{-3}$	433.1	12.732 (5)	$8.0 \times 10^{-6}$	573.3	12.262 (5)
30	309	953	7.25	65.7	313.027 (6)	$1.1 \times 10^{-2}$	59.2	101.192 (6)	$2.0 \times 10^{-5}$	52.5	39.531 (6)
34	314	440	21.91	10.0	227.119 (4)	$12.3 \times 10^{-2}$	5.6	106.703 (4)	$1.3 \times 10^{-3}$	1.8	16.574 (4)

TABLE D-3. Continued

Run No.	Computer No.	Initial Conc. (mg/l)	One-Half Order Model		
			$k_{1/2}$ (mg/l) <sup>0.5</sup> /min	$t_{1/2}$ (min)	F Ratio (n)
37	306	226	0.508	17.3	485.397 (4)
33	313	479	1.710	7.49	509.475 (4)
27	308	112	0.555	11.3	932.029 (3)
40	311	229	0.014	629.8	38.94 (3)
31	301	229	0.338	26.158	2515.299 (5)
29	302	258	0.472	19.92	2018.017 (5)
39	303	247	0.218	42.4	4335.246 (5)
35	304	236	0.212	42.3	373.136 (5)
36	305	220	0.772	11.26	493.222 (5)
38	307	225	0.358	24.53	564.853 (5)
32	310	510	0.480	27.52	87.216 (5)
41	312	218	0.0228	377.2	12.970 (5)
30	309	953	0.288	62.9	178.715 (6)
34	314	440	1.540	7.98	11492.11 (4)

INITIAL DISTRIBUTION

DDC/TCA	2
AUL/LSE	1
Det 1 AFESC/PRT	1
Det 1 AFESC/ECW	10
Det 1 AFESC/ECC	3
SAMSO/LV-1	2
SAMSO/LUV	2
USAF Hosp Vandenburg/SGPB	2
6595 ASTW/SZA	1
6595 ASTW/SZM	1
NASA-SP-FGS-2	1
NASA - DF	1
NASA - DD-MED-41	1
NASA - SA - RTP	1
USAMBRDL	50
NEPSS	1
NCEL Code L54	1
OEHL/CC	1